

# **ASTRA**



## **A Space Charge Tracking Algorithm**

**Version 3.2**  
**March 2017**

Author: Klaus Floettmann  
DESY  
Notkestr.85  
22603 Hamburg  
Germany  
Klaus.Floettmann@DESY.De

Copyright © DESY, Hamburg 1997 – Copyright and any other appropriate legal protection of the computer program ASTRA and associated documentation reserved in all countries of the world.

The ASTRA program package can be downloaded free of charge for non-commercial and non-military use. Dissemination to third parties is illegal. DESY reserves copyrights and all rights for commercial use for the program package ASTRA, parts of the program package and of procedures developed for the program package.

DESY undertakes no obligation for the maintenance of the program, nor responsibility for its correctness, and accepts no liability whatsoever resulting from its use.

## Table of Contents

1. Introduction.....	1
2. Definition of the initial particle distribution .....	2
3. The program <i>generator</i> .....	4
4. The program <i>Astra</i> .....	6
4.1. Namelist structure of Version 3 .....	6
4.2. Example input file without space charge .....	6
4.3. Space Charge Calculation .....	8
4.4. Calculation of the space charge field with the cylindrical grid algorithm.....	8
4.4.1 Set up of the grid.....	9
4.4.2 Merging longitudinal grid cells.....	9
4.4.3 Time step control .....	10
4.4.4 The emission of particles from a cathode .....	10
4.4.5 Correction of the mirror charge for the case of a non-planar cathode .....	11
4.4.6 Minimum time step without emission process.....	11
4.4.7 Scaling of the space charge field .....	12
4.4.8 The Mélange option .....	13
4.5. Calculation of the space charge field with the 3D FFT algorithm.....	15
4.5.1 Restrictions of the 3D FFT algorithm.....	15
4.5.2 Estimation of the average number of particles per cell.....	15
4.5.3 Scaling of the space charge field and time step control.....	15
4.6. Automatic transition from 2D to 3D calculation .....	16
4.7. Emission process.....	16
4.8. The Auto_phase option .....	17
4.9. Scanning and optimizing beam parameters .....	18
4.10. Definition of Modules.....	20
4.11. Apertures and Secondary Electron Emission in <i>Astra</i> .....	21
4.11.1 Secondary electron emission.....	21
4.12. Data output and organization of output files.....	24
4.13. Emittance calculation.....	28
4.13.1 Influence of solenoid fields.....	28
4.13.2 Correction of a transverse beam tilt .....	28
4.13.3 Calculation of the projected emittance .....	29
4.13.4 Calculation of the Trace Space emittance.....	29
4.13.5 Calculation of the core emittance .....	30
4.13.6 Calculation of the ‘reduced emittance’ .....	30
4.13.7 Calculation of the emittance excluding cross over particles.....	31
4.13.8 Emittance calculation of a sub-ensemble of particles.....	31
4.13.9 General redirection of the emittance calculation .....	31
5. Graphics programs .....	33
5.1. Running the graphics programs on Windows PC systems .....	33
5.2. Running the graphics programs on Linux/UNIX systems.....	33
5.3. The win_config.dat file .....	33
5.4. The namelist WIN_CONFIG .....	34
5.5. The program <i>lineplot</i> .....	35
5.5.1 Menu 1 of 4 .....	35
5.5.2 Menu 2 of 4 .....	37
5.5.3 Menu 3 of 4 .....	38
5.5.4 Menu 4 of 4 .....	38

5.6. The program <i>postpro</i> .....	39
5.6.1 Menu 1 of 2.....	41
5.6.2 Menu 2 of 2.....	42
5.6.3 Sub menu ‘Slice Emittance’.....	42
5.6.4 Sub menu ‘Phase Space Manipulations’.....	43
5.7. The program <i>fieldplot</i> .....	45
5.7.1 Menu 1 of 2.....	45
5.7.2 Menu 2 of 2.....	46
5.7.3 Sub Menu ‘Space Charge Fields’.....	46
6. Input namelists for <i>Astra</i> .....	49
6.1. The namelist NEWRUN.....	49
6.2. The namelist OUTPUT.....	52
6.3. The namelist SCAN.....	55
6.4. The namelist MODULES.....	58
6.5. The namelist ERROR.....	59
6.6. The namelist CHARGE.....	63
6.7. The namelist APERTURE.....	66
6.8. The namelist WAKE.....	68
6.9. The namelist CAVITY.....	70
6.10. The namelist SOLENOID.....	79
6.11. The namelist QUADRUPOLE.....	81
6.13. The namelist DIPOLE.....	84
6.14. The namelist LASER.....	87
7. Input namelist for <i>generator</i> .....	93
7.1. The namelist INPUT.....	93
7.2. 1D distributions.....	98
7.2.1 uniform distribution.....	98
7.2.2 plateau distribution.....	98
7.2.3 inverted parabola (longitudinal).....	100
7.2.4 Gaussian distribution.....	100
7.2.5 truncated Gaussian distribution.....	101
7.3. 2D distributions.....	102
7.3.1 radial uniform distribution.....	102
7.3.2 (truncated) 2D-Gaussian distribution.....	102
7.4. 3D distributions.....	103
7.4.1 isotropic momentum distribution.....	103
7.4.2 photo emission from a Fermi-Dirac distribution.....	104
7.4.3 uniformly filled ellipsoid.....	105
7.5. Miscellaneous options.....	106
7.5.1 ring type distributions.....	106
7.5.2 emission from a curved cathode.....	106
8. Appendix I: Field expansion formulas.....	107
9. Appendix II: Representation of a travelling wave by two standing waves.....	110
10. Appendix III: Rotation of Elements in <i>Astra</i> .....	111
11. Selected references.....	112

## List of Tables

Table 1: Structure of particle distribution files. ....	2
Table 2: Definition of important status flags. ....	3
Table 3: Generic file names, logical switches and scales for the data output with <i>Astra</i> . ....	25
Table 4: Data structure of output files. ....	27
Table 5: Core emittance values of a double gaussian particle distribution. ....	30
Table 6: Color and symbol code for <i>postpro</i> plots. ....	40

## 1. Introduction

The Astra (**A** Space Charge **T**racking **A**lgorithm) program package consists of the four parts:

1. The program *generator* which may be used to generate an initial particle distribution.
2. The program *Astra* which tracks the particles under the influence of external and internal fields.
3. The graphic program *fieldplot* which is used to display electromagnetic fields of beam line elements and space charge fields of particle distributions.
4. The graphic program *postpro* which is used to display phase space plots of particle distributions and allows a detailed analysis of the phase space distribution.
5. The graphic program *lineplot*, which is used to display the beam size, emittance, bunch length etc. versus the longitudinal beam line position or versus a scanned parameter, respectively.

*Astra* is written in Fortran 90 and runs on different platforms. The main development platforms are LINUX and Windows. Executables for other platforms are updated less frequently.

The menu controlled graphic programs are based on the subroutine package PGPLOT<sup>1</sup>.

They are basically self-explanatory, but some more details will be given in chapter 5.

The input files for the programs *generator* and *Astra* are organized in form of Fortran 90 namelists. Each namelist starts with an ampersand (&) followed by the name of the namelist and ends with a slash (/). Note that the slash has to be followed by a line feed, even in the last line of the input deck.

Version 1 and 2 of Astra required that an input deck contained all valid namelists in a fixed order. This restriction does not apply for Version 3, i.e. only those namelist which are required need to be specified and they can appear in arbitrary order. The minimal form of a namelist is:

```
&NAME  
/
```

Within a namelist parameters are specified in the form: 'name = Value'. The order of the parameters within a namelist is free and only those parameters which are relevant have to be specified. Specifications are separated by a comma or a line feed, with an arbitrary number of blanks or blank lines in between. Character input (keywords and file names) has in general to be enclosed by quotation marks ('...'). On some platforms this is not mandatory, it is still recommended to ease exchange between platforms. The input of keywords is not case sensitive. In general only the first character(s) are significant. Significant characters are indicated by **bold letters** in this manual. Most, but not all compilers allow to include comments in the input file behind an exclamation mark.

---

<sup>1</sup> PGPLOT is a graphics subroutine library freely available for non-commercial use. For downloading and further information see: <http://astro.caltech.edu/~tjp/pgplot> .

## 2. Definition of the initial particle distribution

Rather than generating the initial particle distribution internally, the tracking program *Astra* reads the initial particle coordinates from a file. This file may be generated by the program *generator* or by a user written program. However, also any output distribution of the *Astra* code, which has not been generated with the `Local_emit = T` option, can be used as input distribution, thus supporting the piecewise tracking of a long beam line. In order to be compatible with the graphic program *postpro* the input distribution file name should end with the extension '.ini' or with '.zpos.run', where *zpos* is a four digit number specifying the longitudinal beam position and *run* is a three digit number specifying the run number (see chapter 5.6). Table 1 lists the structure of particle distribution files. The Fortran format depends on user settings and is: 1P,8E12.4, 2I4 (default) or 1P,8E20.12,2I4 if `High_res = T` or binary if `binary = T`. The same settings are valid for *generator* and *Astra*.

	1	2	3	4	5	6	7	8	9	10
Parameter	x	y	z	px	py	pz	clock	macro charge	particle index	status flag
Unit	m	m	m	eV/c	eV/c	eV/c	ns	nC		

Table 1: Structure of particle distribution files.

The first line of the file defines the coordinates of the reference particle in absolute coordinates. It is recommended to refer it to the bunch center. **Longitudinal particle coordinates, i.e. z, pz and t are given relative to the reference particle.** (If the reference particle is lost the average position of the particle position will be saved with status flag = -99. Coordinates are relative to the average position in this case.) If the particles shall be emitted from a cathode they have to be generated with the same longitudinal position, e.g.  $z = 0.0$  and with an appropriate spread in time, i.e. clock values in nanoseconds. In addition the status flag has to be set accordingly (see Table 2).

The macro charge of the particle is given in nano Coulomb. It is possible to specify each particle with a different charge; the emittance calculation will be done with the appropriate weighting.

The particle index specifies the kind of particle to be tracked:

- Index 1 refers to electrons,
- 2 to positrons,
- 3 to protons and
- 4 to hydrogen ions.

Index 5 – 14 refer to particles with user defined ratio of mass to charge state.

The sign of the charge specified in the column 8 is not relevant. It is possible to mix different kinds of particles as an initial particle distribution.

The status flag contains information of the particle status as listed in Table 2. Particles with a negative status flag are either lost by some mechanism or not yet started. (The output files list the coordinates of all particles even of those that have been lost. The order of the particles does not change; hence it is easily possible to follow the development of individual particles.) Passive particles are tracked as normal particles but they are not taken into account in the calculation of the beam emittance etc. and they are not taken into account when the space charge field is calculated. They will, however, be tracked taken the action of the space charge field onto them into account. They are typically used to cut off beam tails or halo particles. The trajectories of 'probe particles' and the space charge fields acting onto these particles will be found in an output file for later analysis.

Status flag	Comment	Status
-99 <sup>1</sup>	average position of distribution	will not be tracked
-95	ref. particle only; $Z_0 > Z_{Stop}$	lost
-94	ref. particle only; more than Max_Step steps	lost
-92 <sup>2</sup>	probe rejected by space charge at the cathode	lost
-91 <sup>2</sup>	rejected by space charge at the cathode	lost
-90	probe particle before $Z_{min}$	lost
-89	particle before $Z_{min}$	lost
-86 <sup>3</sup>	probe particle traveling backwards	lost
-85 <sup>3</sup>	particle traveling backwards	lost
-31	particle discarded by user	lost
-30	particle preliminary discarded by user	lost
-22	probe secondary electron, lost on aperture	lost
-21	secondary electron, lost on aperture	lost
-20	passive probe particle, lost on aperture	lost
-19	passive particle, lost on aperture	lost
-17	trajectory probe particle, lost on aperture	lost
-15	standard particle, lost on aperture	lost
-6	passive probe particle, at the cathode	not yet started
-5	passive particle, at the cathode	not yet started
-4	secondary particle	not yet started
-3	trajectory probe particle at the cathode	not yet started
-1	standard particle, at the cathode	not yet started
0	passive probe particle	tracking <sup>4</sup>
1	passive particle	tracking <sup>4</sup>
3	trajectory probe particle	tracking
4	cross over particle <sup>5</sup>	tracking
5	standard particle	tracking
6, 9...33	probe secondary electrons of generation 1, 2...10 or higher	tracking
8, 11...35	secondary electrons of generation 1, 2...10 or higher	tracking

- 1 if the reference particle is lost the average position of the distribution will be saved with index -99
- 2 only if Schottky parametrs are specified.
- 3 only active, if L\_rm\_back = T is set.
- 4 passive particles are not taken into account for the set-up of the space charge grid, the calculation of space charge fields and for the calculation of internal beam parameters. If the 2D space charge routine is active the particles are still tracked under the influence of space charge fields, while in case of the 3D routines the space charge field is zero for these particles.
- 5 only if cross\_start  $\neq$  cross\_end. See section 4.13.7.

Table 2: Definition of important status flags.

### 3. The program *generator*

The program *generator* generates an initial particle distribution file according to the previously described specifications.

The input file for *generator* has to have the extension '.in'. The default file name is 'generator.in'. The input file consists of a single namelist named INPUT. A tabulated listing of all possible input parameters is given in chapter 7. The below listed input file gives a simple example for the generation of a Gaussian particle distribution:

```
&INPUT
  FNAME = 'Example.ini'
  Add=FALSE,      N_add=0,
  IPart=500,      Species='electrons'
  Probe=True,     Noise_reduc=T,          Cathode=F
  Q_total=1.0E0

  Ref_zpos=0.0E0, Ref_Ekin=2.0E0

  Dist_z='gauss', sig_z=1.0E0,          C_sig_z=2.0
  Dist_pz='g',     sig_Ekin=1.5,        cor_Ekin=0.0E0

  Dist_x='gauss',  sig_x=0.75E0,
  Dist_px='g',     Nemit_x=1.0E0,       cor_px=0.0E0
  Dist_y='g',      sig_y=0.75E0,
  Dist_py='g',     Nemit_y=1.0E0,       cor_py=0.0E0
/
```

Running *generator* with this input file will result in the generation of the file 'Example.ini' containing the coordinates of 500 electrons with a total charge of 1 nC. Since 'Cathode = F(alse)' the particles are not emitted from a cathode and a longitudinal extension of the bunch has to be specified rather than a time spread. 'Probe = True' will result in the specification of six probe particles at the positions:

$$0.5 \sigma_x, 0.5 \sigma_z; \quad 1.0 \sigma_x, 1.0 \sigma_z; \quad 1.5 \sigma_x, 1.5 \sigma_z;$$
$$0.5 \sigma_y, -0.5 \sigma_z; \quad 1.0 \sigma_y, -1.0 \sigma_z; \quad 1.5 \sigma_y, -1.5 \sigma_z.$$

The trajectories of these particles and the space charge fields acting onto these particles will be saved if 'TrackS = True' is set.

The specification 'Noise\_reduc = T(rue)' forces the program to distribute the particles not randomly but quasi-randomly following a so-called Hammersley sequence. As a result statistical fluctuations are reduced, while at the same time artificial correlations are avoided which would be generated by a set up on a grid.

The longitudinal position of the bunch is at 0.0 m and the kinetic energy is 2.0 MeV. The longitudinal distribution is Gaussian with an rms width of 1mm and a cut at 2 sigma. The distribution of the longitudinal momenta is uniform with an rms width of 1.5 keV. Alternatively it would be possible to specify a longitudinal emittance rather than the energy spread. No correlated energy spread is introduced.

The transverse distribution is Gaussian in x and y with an rms width of 0.75 mm. The distribution of the transverse momenta is also Gaussian and is set up in a way that the beam emittance will be  $1 \pi$  mrad mm. No correlated beam divergence is introduced.

Besides the complete listing of all possible input parameters in chapter 7, a collection of the properties of different distributions can be found in chapters 7.2 to 7.4.

In order to assemble more complicated distributions it is possible to add up several distributions into a common file. In this case 'Add = True' and 'N\_add = n' has to be specified, where n is the number of distributions to be added. Than the namelist INPUT has to be specified n times with different parameters. (FNAME, Add and

N\_add might be specified only once in the first namelist.) The reference particle of the combined distribution will be the reference particle defined in the first namelist.

If a dispersion is specified an energy correlated transverse offset will be added in a final step. The calculated emittance will hence be larger than specified in the input file.

After running *generator* the result can be visualized by calling *postpro* with the appropriate input argument, e.g. 'postpro Example.ini'. See chapter 5.6.

Besides the file Example.ini the file NORRAN will be created by *generator*. It contains a new seed value for the random generator and will be updated every time *generator* is used.

## 4. The program *Astra*

The program *Astra* tracks particles through user defined external fields taking into account the space charge field of the particle cloud. The tracking is based on a non-adaptive Runge-Kutta integration of 4<sup>th</sup> order.

The beam line elements are set up w.r.t. a global coordinate system in *Astra*. The axis of the (preferred) motion of the bunch is the z-axis (longitudinal axis). The horizontal plane is related to the x-axis, and the vertical plane is defined via the y-axis.

All calculations in *Astra* are done with double precision, while output and input may be in single precision.

The input file for *Astra* has to have the extension '.in'. The default file name is 'rfgun.in'. The input of each class of beam line element is organized in a separated namelist. Besides the namelists for the beam line elements the namelist NEWRUN contains general instructions for the tracking, CHARGE contains the settings for the space charge calculation and SCAN contains instructions for the scanning routine. In the following an example input file without space charge will be discussed. In a second step the calculation of space charge fields will be included before finally the scanning routine will be described.

### 4.1. Namelist structure of Version 3

Version 1 and 2 of *Astra* required that an input deck contained all valid namelists in a fixed order. This restriction does not apply for Version 3, i.e. only those namelist which are required need to be specified and they can appear in arbitrary order.

### 4.2. Example input file without space charge

```
&NEWRUN
  Head=' Example of ASTRA users manual'
  RUN=1
  Distribution = 'Example.ini',      Xoff=0.0,   Yoff=0.0,
  TRACK_ALL=T,      Auto_phase=T

  H_max=0.001,      H_min=0.00

&OUTPUT
  ZSTART=0.0,      ZSTOP=1.5
  Zemit=500,      Zphase=1
  RefS=T
  EmitS=T,      PhaseS=T
/

&CHARGE
  LSPCH=F
  Nrad=10, Cell_var=2.0, Nlong_in=10
  min_grid=0.0
  Max_Scale=0.05
/

&CAVITY
  LEField=T,
  File_Efield(1)='3_cell_L-Band.dat', C_pos(1)=0.3
  Nue(1)=1.3,      MaxE(1)=40.0,      Phi(1)=0.0,
/
```

```
&SOLENOID
  LBField=T,
  File_Bfield(1)='Solenoid.dat', S_pos(1)=1,2
  MaxB(1)=0.35, S_smooth(1)=10
/
```

NEWRUN starts with a header string and a run number, which should be used to protocol different parameter settings. The run number will be found as an extension of all output files generated by *Astra*. The input particle distribution has been previously generated with *generator*. It is used without a transverse offset, i.e. on-axis. After the phasing of the cavity ('Auto\_phase = T', see chapter 4.8) the reference particle, i.e. the first particle in the input distribution file, will be tracked through the beam line to check the beam line settings<sup>1</sup>. In a second step the reference particle will be tracked again, starting with an offset at  $x = x_{rms}$  and  $y = y_{rms}$ . If 'TRACK\_ALL = False' is set the tracking will stop here. The maximum time step for the Runge-Kutta integrator is defined with the parameter H\_max, while H\_min is only active if the space charge fields are taken into account (see section 4.4.3).

The second namelist OUTPUT is devoted to the generation of output<sup>2</sup>. While the tracking starts at any position where the initial particle distribution is launched, output will be generated between ZStart and ZStop. The tracking will stop when the bunch position, i.e. the average position of all active particles is larger than ZStop.

The names of all files generated by *Astra* start with the project name, i.e. with the name of the input file and end with the run number. In between, separated by dots a type dependent name is given to the files. Table 3 gives a complete listing of all output files generated by *Astra* including the logical switches to start or suppress the generation of output.

*Astra* generates output on different length scales of the beam line. 'RefS = True' generates output of the off-axis reference trajectory, energy gain etc. at each Runge-Kutta time step.

Output of the beam emittance and other statistical beam parameters is generated if 'EmitS = True'. For the calculation of statistical bunch parameters the distance ZStop-ZStart is divided into Zemit intervals. Note, that the Runge-Kutta time step is adjusted, i.e. reduced if necessary, in order to interrupt the tracking close to the specified locations. (The beam position refers to the average longitudinal beam position.) This might lead to a reduction of each time step, i.e. to an increased accuracy of the calculation, if the intervals are shorter than the bunch motion in one time step. A warning is given in this case because the result of the calculation might depend on an output parameter if H\_max is too big!

The complete particle distribution is saved at Zphase different locations if 'PhaseS = True'. The distance ZStop-ZStart is divided into Zphase intervals and the nearest location defined by means of Zemit is chosen. Therefore it is recommended to set  $Zemit = n \cdot Zphase$ ,  $n \in \mathbb{N}$ . The approximate position is indicated in the file name as a four digit number, which corresponds in general to the rounded beam position in cm. If necessary the units for the file name definition is changed (if the distance of the output positions is too small, or if the last output position is too big). If required the naming convention is changed to a relative position (i.e. output position minus start position) which is indicated by a warning message.

All namelists but NEWRUN start with a logical switch, which allows to deactivate all

<sup>1</sup> If 'Track\_On\_Axis=True' is set tracking will stop here.

<sup>2</sup> Many but not all of the parameters in OUTPUT were in the namelist NEWRUN in previous versions of ASTRA and are still accepted in this namelist.

elements in that list, without changing other parameters. Hence, with ‘LSPCH = False’, the calculation of space charge forces is deactivated.

The namelist CAVITY allows to include rotational symmetric fields of standing wave cavities, as well as of traveling wave structures and electrostatic fields. The dependence of the longitudinal electric field component on the longitudinal position on the symmetry axis of the field has to be given in form of a table in case of standing wave structures and electrostatic fields. The radial and magnetic field components are deduced from the derivative of the longitudinal field w.r.t. the longitudinal position. File\_Efield(n) contains the name of the file where this table can be found, for the n<sup>th</sup> cavity. Nue(n) states the frequency, MaxE(n) the **maximum** amplitude of the field and Phi(n) the phase of the wave. By default the energy gain of each cavity is scanned prior to the tracking of the reference particle in *Astra*. The user-defined phase refers than to the phase of the maximum energy gain in a cosine-like manner. Note, that the phase of the wave  $\omega \cdot t + \phi$  is increasing with time, i.e. the tail of the bunch ‘sees’ a higher phase than the head. Thus, in order to give the tail a higher energy than the head, one has to go to negative phases Phi(n). The phase, denoted by the program as a result of the auto-phasing procedure, is the number used internally. It refers to the phase of the wave at the time stamp of the reference particle when it is starting to be tracked. The auto-phasing can be switched off by setting ‘Auto\_Phase = False’ in NEWRUN.

The namelist SOLENOID contains information about solenoid fields. Like in case of cavity fields a table of the longitudinal field component along the symmetry axis is required. Besides the file name of the table, only the **maximum** amplitude of the field has to be specified. (The scaling of the field to the defined amplitude might also be switched off by setting ‘S\_noscale = True’.) In the example some smoothing is applied to the field table.

No other elements are used in this example.

### 4.3. Space Charge Calculation

*Astra* offers cylindrical symmetric and fully 3D options for the space charge calculation. In terms of computing time the algorithms themselves are of comparable performance, however, 3D space charge calculations require, due to the larger number of grid cells, a much larger number of macro particles in order to avoid statistical problems. Moreover in case of the 3D algorithm only a linear interpolation within the grid cells applied, while a cubic spline interpolation is employed within the cylindrical grid algorithm. Therefore a finer grid resolution might be required in the case of the 3D algorithm.

### 4.4. Calculation of the space charge field with the cylindrical grid algorithm

For the calculation of the space charge field a cylindrical grid (r,  $\phi$ , z coordinates), consisting of rings in the radial direction and slices in the longitudinal direction, is set up over the extension of the bunch. The grid is Lorentz transformed into the average rest system of the bunch, where the motion of the particles is to good approximation non relativistic and a static field calculation can be performed by integrating numerically over the rings thereby assuming a constant charge density inside a ring. The field contributions of the individual rings at the center points of the grid cells are added up and transformed back into the laboratory system. Here the field at any given point between the grid center points is calculated by means of a cubic spline

interpolation, so that the field and the first derivatives w. r. t. the space coordinates are continuous functions. Outside of the grid a  $1/r$  extrapolation is applied, so that the space charge field is defined (with reduced accuracy) over the whole space. For the tracking the space charge field is treated like the external field, i.e. an Runge-Kutta integration is performed based on the sum of all external and internal forces. It would, however, be too time consuming (and useless) to calculate the space charge field on the grid center points again at every Runge-Kutta time step. Therefore an automatic procedure has been implemented which scales the space charge field and the grid dimensions with the variation of the beam size, the beam energy etc. A new calculation of the field on the grid center points is initiated every time the scaling factor of the field exceeds a user-defined limit.

#### 4.4.1 Set up of the grid

The space charge fields are calculated on a cylindrical grid, consisting of rings in the radial direction and of slices in the longitudinal direction. The grid is set up dynamically, i.e. the grid dimensions are based on the actual dimensions of the bunch. The user has to define the number of slices (parameter `Nlong_in`) and rings (parameter `Nrad`) that shall match exactly the dimensions of the bunch. For the calculation two more rings and four more slices are added outside of the bunch.

The total number of particles inside a ring scales, for a distribution with uniform charge density, linearly with the radius in the outside region of the bunch but more quadratically at the innermost region. As an example consider the case of 5000 particles uniformly distributed in a grid of 10 rings of equal thickness. In the innermost ring only about 50 particles will be located, while in the outermost ring about 950 particles will be counted. When these particles are additionally distributed into 100 longitudinal slices, half of the innermost rings will be empty, which causes statistical fluctuations in the field description. Furthermore one has to take into account, that the field of a charge ring acts predominantly to the outside of the ring. Thus the field in the outside region of the bunch is composed by more or less all particles while this is not the case in the central region of the bunch. To counteract this unfavorable situation it is possible to vary the radial grid height over the bunch radius by means of the parameter `Cell_var` in *Astra*. If for example '`Cell_var = 2`' is chosen, the innermost ring will be twice as high as the outermost ring. In order to get a sufficient statistical accuracy it is nevertheless necessary to choose a small number of grid cells or a high number of particles, respectively. The description of the fields will, however, have a better resolution than suggested by the grid size due to the smooth interpolation algorithm.

The space charge fields generated by a particle distribution can be visualized with the program *fieldplot*. (See chapter 5.7.) Here also the number of grid cells and the cell variation may be changed and optimized.

#### 4.4.2 Merging longitudinal grid cells

In order to vary the longitudinal grid size within the bunch neighboring cells can be merged together. If, for example, the bunch consists out of a short spike and a long tail the parameter `N_long_in` is specified so that the spike can be resolved. In order to improve the statistical properties in the rarely populated tail cells can be merged with the statements '`Merge_1 = i, j, k`' to '`Merge_10 = i, j, k`', where  $i$  is the starting cell,  $j$  is the end cell and  $k$  is the number of cells to be merged. For example with `Merge_1 = 1,50,10` cells number 1 to 50 are merged into 5 new cells each consisting

out of 10 original cells. Note that  $\frac{j-i+1}{k}$  has to be an integer. Use *fieldplot* to visualize and optimize the longitudinal grid. An example application of this option is described in [1].

#### 4.4.3 Time step control

For an accurate simulation the time steps of the Runge-Kutta integrator shall not be too large. The required time steps may differ strongly in different parts of a beam line, depending on the relative contribution of space charge and external fields. Time steps are adjusted automatically within user defined limits in *Astra*. The maximum time step, often limited by external fields (RF fields, fringe fields), is determined by the parameter *H\_max*. The convergence of the simulation results for decreasing *H\_max* should be checked. Separate tracking of different sections of the beam line allows to optimize *H\_max* for each section.

The minimum time step is given by the parameter *H\_min*. Criteria to set *H\_min* are discussed in the next two chapters. The scaling of the space charge field (section 4.4.7) is used to estimate the maximum allowable time step. Thus *Astra* performs time steps between *H\_max* and *H\_min*. Even shorter time steps are made in order to reach a certain position e.g. to generate output. The development of the average step size is stored in a file when the option 'TcheckS = True' is set.

#### 4.4.4 The emission of particles from a cathode

In order to simulate the emission of particles from a (plane) cathode the particles are started from the cathode according to the timing spread of the initial particle distribution. The particles are ordered according to their emission time and the space charge field is scaled for the increased charge after the emission of each particle. Thus a smoothly rising space charge field is obtained. The time step of each particle is adjusted according to its emission time, and a complete recalculation of the space charge field is performed after each user-defined step size *H\_min*. No scaling of the field other than the scaling with the charge within the time step is applied.

If during the emission the space charge field shall be updated *n* times, *H\_min* has to be *T/n* where *T* is the total emission time. In general *H\_min* is an uncritical parameter if *n* is reasonably high. It is however useless to set *n* very high if the number of particles is not very high.

Alternatively, the average number of particles to be emitted during each emission step can be specified with the parameter *N\_min*. To activate this option *H\_min* should be specified as zero. Then it is set according to:

$$H\_min = T \frac{N\_min}{Npart} \quad (4.1)$$

with *Npart* being the total number of particles in the bunch.

Since the number of particles is small during the first steps of the emission process the number of longitudinal slices shall be reduced during the emission by means of the parameter *min\_grid*, which defines the minimal grid size in longitudinal direction. Whenever the bunch length is so small, that the grid size would be below *min\_grid*, the number of slices is reduced accordingly. The bunch length *s\_min* after the first time step, *t* = *H\_min* has been performed can be estimated as:

$$s_{min} = \frac{eE}{2m} t^2 \quad (4.2)$$

where *E* is the accelerating field strength and *m* is the rest mass of the particles in the bunch.

If `min_grid` is set to this value the number of slices increases smoothly as the bunch length and the number of particles during the emission process.

If `min_grid` is specified as zero, it is set automatically according to Eq. (4.2). For this the mass of the reference particle is used, (important only in case of a particle mixture.)

For setting up the grid also particles which are not emitted yet are taken into account for the radial direction, in order to avoid too small radii during the first steps of the process.

By default the mirror charge of the bunch at the cathode plane is taken into account if the bunch is emitted from the cathode. The fields of the 'mirror bunch' are calculated in the rest system of the mirror bunch at the Lorentz transformed distance between bunch and mirror bunch, transformed back into the laboratory system and added to the field of the bunch. The calculation of the mirror charge is switched off when the contribution of the mirror bunch field at two positions of the bunch (in the center and in the tail of the bunch) is below 1% of the bunch field. For the calculation of the mirror charge the grid is modified in a way that the field is calculated directly in the cathode plane, rather than in the center of a cell.

When the bunch is emitted from a cathode, the longitudinal position of the cathode is set to the minimal particle position by default. When the bunch is not emitted from the cathode but shall be started in front of the cathode the cathode position has to be explicitly specified with the parameter `Z_Cathode`.

The calculation of the mirror charge can be suppressed by setting '`Lmirror = False`'. Retarded time effects and radiation effects are not taken into account.

#### 4.4.5 Correction of the mirror charge for the case of a non-planar cathode

In order to correct the mirror charge contribution in the case of a non-planar cathode the cathode surface has to be described by means of a table. The table contains in the first two columns the longitudinal and radial position of a number of points describing the contour of the cathode. The third and fourth column of the table contains the components of the tangential unit vector of the cathode at the same points. For each point of the table a charge ring will be located slightly behind the cathode surface. The rings carry charges such, that the electric field vector of the combined space charge field is perpendicular to the cathode surface. In order to determine the charges a system of equations with  $n$  unknowns has to be solved for  $n$  points in the input table. In addition to the table the curvature of the cathode on the axis has to be specified in the input deck. Special care is required in case of a field description by means of a 3D field map because the map is defined on a rectangular grid and cannot follow the cathode contour. By adjusting the field values on the grid positions behind the cathode a correct field description is still possible.

The cathode contour incl. the position of the charge rings behind the cathode and the field on the cathode surface can be visualized with `fieldplot`. See also section 7.5.2. This procedure has been worked out by D. Janssen and V. Volkov. An example application of this option is described in [2].

#### 4.4.6 Minimum time step without emission process

When the simulation starts without emission from a cathode the parameter `H_min` is in general uncritical. By default it is reset to `H_max/100` if it is set to zero in the input deck.

In cases of extreme space charge forces the following criterion becomes, however, significant: In a real beam all particles move simultaneously, while in a simulation

particles move one after the other in small steps. In order to avoid that particles move a significant fraction of a grid cell within one time step, which would lead to an unphysical variation of the space charge field, the bunch dimension should change by an amount which is small compared to a grid cell within a single time step. In cases of extreme space charge fields this criterion might be violated. Hence *Astra* controls this criterion and reduces the time steps if required. The user defined parameter *Exp\_control* specifies the maximum tolerable variation of the bunch extensions relative to the grid cell size within one time step. *Exp\_control* = 0.1 specifies, that the bunch is allowed to expand by only 10% of the minimal grid size within a time step. While the control of this criterion may lead to very small step sizes it does often not increase the overall CPU time by a significant amount, because the efficiency of the scaling procedure of the space charge field improves.

#### 4.4.7 Scaling of the space charge field

The space charge field of the bunch is (at least at sufficient high energies) a slowly with time varying function. Hence, instead of calculating new field coefficients at every time step, it is justified to scale the field coefficients according to:

$$E_r \propto \frac{Q}{Q_0} \times \left( \frac{\sigma_{r_0}}{\sigma_r} \right)^{nr(r)} \times \left( \frac{\sigma_{z_0}}{\sigma_z} \right)^{nr(z)} \times \left( \frac{\gamma}{\gamma_0} \right)^{nr(\gamma)}$$

$$E_z \propto \frac{Q}{Q_0} \times \left( \frac{\sigma_{r_0}}{\sigma_r} \right)^{nz(r)} \times \left( \frac{\sigma_{z_0} \gamma_0}{\sigma_z \gamma} \right)^{nz(z,\gamma)}$$

$$B_\phi \propto Er \frac{\beta}{\beta_0}$$

where  $Q/Q_0$ ,  $\sigma_r/\sigma_{r_0}$ ,  $\sigma_z/\sigma_{z_0}$ ,  $\gamma/\gamma_0$  and  $\beta/\beta_0$  denote the relative variation of the bunch charge, the bunch radius, length, energy and velocity, respectively.

At the same time the grid has to be scaled with the variation of the radial bunch size and the bunch length.

$nr(r)$ ,  $nr(z)$ ,  $nr(\gamma)$ ,  $nz(r)$  and  $nz(\gamma z)$  are functions that depend on the aspect ratio  $A = \sigma_z \frac{\gamma}{\sigma_r}$  of the bunch in the rest system. They are constant for  $A \gg 1$ .

In case of a pancake like bunch the fields are proportional to:

$$E_r \propto \frac{Q}{Q_0} \times \left( \frac{\sigma_{r_0}}{\sigma_r} \right)^2 \times \frac{\gamma}{\gamma_0}$$

$$E_z \propto \frac{Q}{Q_0} \times \left( \frac{\sigma_{r_0}}{\sigma_r} \right)^2 \times \frac{\sigma_{z_0} \gamma_0}{\sigma_z \gamma}$$

while a cigar like bunch scales like:

$$E_r \propto \frac{Q}{Q_0} \times \frac{\sigma_{r_0}}{\sigma_r} \times \frac{\sigma_{z_0}}{\sigma_z}$$

$$E_z \propto \frac{Q}{Q_0} \times \left( \frac{\sigma_{z_0} \gamma_0}{\sigma_z \gamma} \right)^2$$

The functions used in *Astra* are only approximate functions that fit roughly numerical

results for a number of bunch dimensions with uniform longitudinal and radial distribution. However, the scaling is in any case better than assuming a constant field.

If the scaling factor for the radial or longitudinal electric field exceeds a user-defined limit a new space charge calculation is initiated. The parameter `Max_scale` defines this limit; if for example '`Max_scale = 0.05`' the scaling factor has to be between 1.05 and 0.95, respectively.

An extrapolation of the time depended scaling factors is used to determine the maximum allowable next step size. If the next step size would be below `H_min` a new calculation of the space charge field is initiated. Therefore the space charge field is not only updated more frequently in regions of strongly varying space charge fields, also the average step size is reduced.

Strong changes of the particle distribution, without variation of the bunch dimensions, cannot be taken into account by the scaling routine and have to be treated separately. This effect is observed during the compensation process of space charge induced emittance growth close to the emittance minimum, when the particles in the bunch center move outwards, while the particles in the head and the tail of the bunch are still moving inward. In order to limit the number of scaling steps in this case, the parameter `Max_count` can be set.

As long as particles are emitted from a cathode the scaling procedure is not active. Instead the space charge fields are updated after each time step `H_min`.

The effectiveness of the scaling and the setting of `Max_scale` can be controlled by setting '`TrackS = True`'. A file will be logged that contains the trajectories of particles marked as probe particles and the space charge fields acting onto these particles. Both can be displayed with the program *lineplot*. (While *Astra* can deal with any number of probe particles, *lineplot* will support the display of only up to one hundred particles.) Since the data are logged at each Runge-Kutta time step the generated files tend to be large. Therefore one might consider using this option only for short critical sections and not for long beam lines. Additional information about the scaling procedure can be gained if the option '`TcheckS = True`' is set. A file will be logged that contains the scaling factors at each time step separated into the contributions

$$\left( \frac{\sigma_{r_0}}{\sigma_r} \right)^{nr(r)}, \quad \left( \frac{\sigma_{z_0}}{\sigma_z} \right)^{nr(z)}, \quad \left( \frac{\gamma}{\gamma_0} \right)^{nr(\gamma)} \quad \text{etc.,}$$

which allows to identify the driving force of the space charge field development. Also the scaling counter, which counts how often the field is scaled before it is updated and the time between updates of the space charge fields is saved. The later one is used to calculate the average Runge-Kutta time step. See the description of *lineplot* section 5.5.2 for displaying results.

#### 4.4.8 The Mélange option

With the Mélange option it is possible to define a particle distribution consisting of groups of particles which will be treated separately in the space charge calculation. These groups may have a different energy or may be different particle types. The standard scaling of the time steps might not work in all cases as stable as usual in this case, because it can react only on the average development of all particles. (In detail it depends on how different the distributions are.) Careful convergence checks for the space charge calculation parameters are recommended. Some parameters might need a more strict definition and as a result the calculation might slow down. First tests should be done on a short section.

The Mélange option works only with the 2D space charge routine, relative transverse

offsets of the particle groups are hence not possible.

The Mélange option is controlled with the parameter Melange in the namelist Charge. Melange = 2 means that 2 different distributions are mixed together. Note that the calculation takes place on a common grid, i.e. if the distributions are longitudinally separated by a large distance a much larger grid will be set up and more grid cells are needed.

To mark the two groups first a mixed distribution is created, e.g. with generator using the 'add' command. This distribution needs to be modified externally: while the first group of particles keeps the status flag 5 as usual, the second group gets the flag 7, a third group would get flag 10 and for every further group the flag number would be increased by 3 (10, 13, ...).

Astra will calculate beam parameters for the mixed distribution with standard settings, but can also be forced to take only one group into account, see section 4.13.9 of the manual. Also the color settings in postpro can be redefined in a similar way, see section 5.6.

### References

- [1] C. Limborg-Depry, P. Emma, Z. Huang, J. Wu 'Computation of the longitudinal space charge effect in photoinjectors' EPAC 2004.  
<http://accelconf.web.cern.ch/AccelConf/e04/PAPERS/TUPLT162.PDF>
- [2] V. Vlokov, K. Floettmann, D. Janssen, 'Superconducting RF Gun Cavities for large Bunch Charges' PAC 2007.  
<http://accelconf.web.cern.ch/AccelConf/p07/PAPERS/FRPMN063.PDF>

## 4.5. Calculation of the space charge field with the 3D FFT algorithm

To activate the 3D space charge calculation the parameter 'Lspch3D = t' has to be set in addition to 'Lspch = t'. For the 3D algorithm a Cartesian grid is used. The number of grid lines is specified with the parameters Nxf, Nyf and Nzf for the x-, y- and z-direction, respectively. Since the algorithm is based on a fast Fourier transform the number of grid lines in each direction has to be equal to  $2^n$ ,  $n \in \mathbb{N}$ . *Astra* will give a warning and reset the grid cell specification to the nearest possible value in case of an invalid input. The number of grid cells in each direction is equal to the number of grid lines minus one. With the parameters Nx0, Ny0 and Nz0 the number of empty boundary cells can be specified, which allows a finer tradeoff of computation time and statistical noise in the computation (see section 4.5.2.). The space charge calculation takes place as electro static calculation in the average rest frame of the bunch. A constant charge density inside the cell is assumed. The potential of the space charge field is derived by a convolution of the charge density of the grid with the analytically calculated Green's function as described in [1]. The derivatives of the electrostatic potential yield then the components of the space charge field which is transformed back into the laboratory frame. In order to suppress noise the potential may be smoothed with a soft iterative procedure. The parameters Smooth\_x, Smooth\_y and Smooth\_z can be used to specify the number of iterations to be applied for each direction. The setup of the grid and the effect of the smoothing should be checked with *fieldplot*.

### 4.5.1 Restrictions of the 3D FFT algorithm

The 3D algorithm doesn't provide special features for the emission of particles from the cathode in its present form. Image charge forces cannot be included. During the emission the complete grid is set up already after the first time step.

The field description is restricted to the grid; hence the optional use of passive particles, which may travel outside of the grid, is limited.

### 4.5.2 Estimation of the average number of particles per cell

The Cartesian grid forms a cuboid around the bunch which leads necessarily to a number of empty cells since a bunch is in general not cuboid. An adjustable number of additional empty cells can be included in the boundaries in order to allow a finer adjustment of grid resolution and required number of particles. Assuming a uniformly filled cylindrical bunch with ellipsoidal transverse cross section the average number of particles per grid cell  $N_{cell}$  can be estimated as:

$$N_{cell} = \frac{4}{\pi} \frac{N_{tot}}{(Nxf - 1 - 2Nx0)(Nyf - 1 - 2Ny0)(Nzf - 1 - 2Nz0)}$$

And for the case of a uniformly filled ellipsoid as:

$$N_{cell} = \frac{6}{\pi} \frac{N_{tot}}{(Nxf - 1 - 2Nx0)(Nyf - 1 - 2Ny0)(Nzf - 1 - 2Nz0)}$$

### 4.5.3 Scaling of the space charge field and time step control

The scaling of the space charge field and the setup of the time steps follows the same procedures and formulas as described above for the 2D algorithm. Instead of the radial field both transverse components are treated separately, so that the procedure works also in case of varying transverse aspect ratio.

## 4.6. Automatic transition from 2D to 3D calculation

It is possible to switch between 2D and 3D space charge calculation within a tracking calculation. For this the switch `L2D_3D` is set to true and the position at which the transition should be made is specified with the parameter `z_trans`. When the bunch passes `z_trans` the results of a 3D space charge calculation are applied to all particles beyond `z_trans`, while a 2D calculation is made for particles before the specified position. The number of longitudinal cells of the 2D grid has to be reduced as more and more particles passing `z_trans`. Thus a minimal grid length has to be specified with the parameter `min_grid_trans` equivalently to the minimal grid length defined for the emission process.

## 4.7. Emission process

Important aspects of the simulation of the emission process in *Astra* are described in section 4.4.4.

Particle distributions which can be generated with *generator* are described in chapter 7 and following. Besides this it is possible to load particle distributions from other programs if they are compatible to the file structure described in chapter 2.

Within *Astra* it is possible to rescale a number of parameters of the particle distribution (e.g. the bunch size, the charge etc., see chapter 6.1) and to define offsets, which allows doing parameter scans as described in chapter 4.8.

Additionally it is possible to modify the emission form a cathode by specifying a delay time and parameters to model the Schottky effect, respectively.

If the delay time *Tau* is not zero in the input deck an exponential delay will be applied to the emission of the particles. Thus, if for example the input distribution represents an incoming photon bunch, it is possible to model a delay of the photo emission process of the cathode. The delay time is randomly chosen and added to the predefined emission time. Note, that statistical noise might be increased if the initial distribution is quasi-random.

The Schottky effect describes the lowering of the work function or electron affinity of a material by an external electric field, which leads to an increased electron emission from a cathode [2]. In *Astra* the charge of a particle is determined at the time of its emission as:

$$Q = Q_0 + Srt\_Q\_Schottky \sqrt{E} + Q\_Schottky E$$

where *E* is the combined (external plus space charge ) longitudinal electric field in the center of the cathode.

The charge *Q<sub>0</sub>* is the charge of the particle as defined in the input distribution (eventually rescaled according to the parameter *Qbunch*) and *Srt\_Q\_Schottky* and *Q\_Schottky* describe the field dependent emission process. For an exemplary discussion of the Schottky and related effects see [3] and references therein.

To visualize the development of the space charge field on the cathode and important beam parameters during the emission process set ‘CathodeS = True’. See Table 3 and Table 4 and section 5.5.4.

## References

- [1] Ji Qiang et al. ,Erratum: Three-dimensional quasistatic model for high brightness beam dynamics simulation' PRST-AB 10,129901 2007.  
<http://prst-ab.aps.org/abstract/PRSTAB/v10/i12/e129901>  
 see also:  
<http://prst-ab.aps.org/abstract/PRSTAB/v9/i4/e044204>
- [2] W. Schottky 'Über kalte und warme Elektronenentladungen' Zeitschrift für Physik, Vol. 14, pp. 63-106, 1923.
- [3] J. H. Han et al. 'Emission mechanisms in a photocathode RF gun' PAC 2005.  
<http://accelconf.web.cern.ch/AccelConf/p05/PAPERS/WPAP003.PDF>

### 4.8. The Auto\_phase option

By default the energy gain of each cavity representing an accelerating RF mode is scanned prior to the tracking of the reference particle in *Astra*. The user-defined input phases refer to the phases of the maximum energy gain in a cosine-like manner. Note, that the phase of the wave  $\omega \cdot t + \phi$  is increasing with time, i.e. the tail of the bunch 'sees' a higher phase than the head. Thus, in order to give the tail a higher energy than the head, one has to go to negative phases. The auto-phasing procedure can be switched off by setting 'Auto\_Phase = False' in NEWRUN, in which case absolute phases are requested. Absolute phases refer to the phase of the wave at the time stamp at which the tracking is started. The results of the auto-phasing procedure (max. energy gain and phases) are printed onto the screen. The phases may hence be used as offset phases when the auto-phasing procedure is going to be switched off in subsequent runs.

The Auto\_phase option acts only on accelerating RF modes, i.e. DC fields, TE modes and dipole modes are rejected from the scan.

In the auto-phasing procedure the reference particle is tracked through the consecutive cavities. For each cavity the phase is scanned several times with decreasing phase steps around the phase of maximum energy gain. Once the phase of maximum energy gain has been determined with high accuracy the particle is finally tracked at the user defined phase through the cavity and up to the entrance of the subsequent cavity. Note, that the optimum phase of the complete particle distribution coincides only with the optimum phase of the reference particle if it is located at the weighted average longitudinal or temporal position of the distribution, respectively.

In the case of overlapping modes the order of the phasing procedure is determined by the order of the start positions of the cavities or in the case of equal start positions, by the order in which the modes appear in the input deck. If the particle velocity is changing inside the cavity, the phases of overlapping modes are, however, not independent of each other. It is recommended to use the auto-phasing option for each mode separately and then use absolute phases in this case.

In long cavity sections a small discrepancy between the phases determined by the auto-phasing procedure and the phases which minimize the energy spread of the beam (without space charge fields) can be observed in some cases. Different factors contribute to this discrepancy, one is, that the reference particle is due to statistical fluctuations in general not exactly in the center of the particle distribution another one are numerical inaccuracies.

The phasing of the cavities is related to the internal clock of the tracking program. The starting time of the tracking program is determined via the input distribution, see Table 1. The starting time can also be changed with the parameter Toff in the namelist NEWRUN. If the RF structures described in the input deck have all the same

frequency a modification of Toff is equivalent to a phase shift of all cavities with the parameter  $\phi(0)$ .

In general the starting time is an arbitrary value. In some cases, if for example a timing jitter of the particle source shall be investigated a defined variation of the starting time is necessary. (See the output parameters of the scanning routine in chapter 6.3.) Note, however, that a modification of the starting time will be compensated by a phase shift if 'Auto\_Phase = True' is set.

#### 4.9. Scanning and optimizing beam parameters

*Astra* offers different options to perform parameter scans and optimizations. A simple, predefined scan based on a single particle tracking (the reference particle) is performed by setting 'PHASE\_SCAN = True' in NEWRUN. The energy gain as function of the cavity phase is stored as well as the bunch compression factor, i.e. the ratio of the bunch length at the exit of the cavity to the bunch length at the entrance of the cavity. From the derivative of the energy gain w.r.t. the cavity phase a quantity is derived which is proportional to the RF induced energy spread. (See section 5.5.2.) When the scan for one cavity is finished, the reference particle will be tracked through the cavity on the user-defined phase up to the entrance of the next cavity. Thus, for low energy beams ( $\beta < 1$ ), the result of the scan for downstream cavities depends on the user-defined phase.

User defined scans can be performed with the scanning procedure defined in the namelist SCAN. The following example shows a setting for a scan of the cavity gradient of cavity number one:

```
&SCAN
  LScan=T
  Scan_para='MaxE(1)'
  S_min=10.0,      S_max=50.0, S_num=5
  FOM(1)='hor. Emittance'
  FOM(2)='long. Emittance'
  FOM(3)='bunch length'
/
```

All valid scanning parameters are written in italic letters in the namelist tables of chapter 6. Besides the minimum and maximum set point of the scanning parameter, *S\_min* and *S\_max*, the total number of set points *S\_num* has to be specified. The user also has to define which beam parameters shall be stored. Up to 10 different output parameters can be specified (FOM(1) to FOM(10)). See chapter 6.3 for a listing of valid keywords. The standard output generation (emittance vs. z etc.) is suppressed when a scan is performed. Setting 'LExtend = True' allows to increase the scanning range without losing data from a previously performed scan with the same run number.

While with the specifications discussed above all parameters, as defined with FOM(1) to FOM(10), are saved at the end of the beam line, it is also possible to look for a minimum or maximum within a predefined longitudinal range with the scanning routine. In this case 'L\_min = True' or 'L\_max = True' has to be specified. The minimum or maximum value of FOM(1) within the longitudinal interval *S\_zmin* to *S\_zmax* will be saved. The interval is divided into *S\_dz* subintervals. At the end of each subinterval the emittance etc. is calculated and the value of FOM(1) is updated accordingly. The values of FOM(2) to FOM(10) will be saved at the position of the minimum/maximum of FOM(1). The position of the minimum/maximum will also be

saved.

Automatically searching for a setting where the parameter FOM(1) reaches a minimum, a maximum or a predefined value (match\_value) by refined scans in smaller intervals around the optimum is activated by setting O\_min, O\_max or O\_match true. The parameter O\_depth defines the number of refined scans to be performed. The total number of runs in this case is about S\_numb · O\_depth. If the optimum is outside the initial interval (S\_min – S\_max) the interval is increased in direction of the optimum by at most 10 steps.

The options O\_min, O\_max etc. and L\_min, L\_max etc. can be combined. With the setting:

```
&SCAN
  LScan=T
  Scan_para='MaxB(1)'
  S_min=0.1,      S_max=0.2,      S_numb=5
  O_min=.TRUE.,  O_depth=3
  L_max=.TRUE.,  S_zmin=1.0,      S_zmax=1.5,  S_dz=10
  FOM(1)='hor. spot size'
/
```

the maximum of the horizontal beam size between 1 and 1.5 m will be minimized.

Another possibility for parameter scans is given with the looping option. All namelists start with the parameters LOOP. If 'LOOP = True' is set, the parameter NLoop in the namelist NEWRUN has to be set to a positive integer value. The complete namelist for which the looping has been activated has to be specified NLoop times with varying parameters. (With the exception of the namelist ERROR, see chapter 6.5.) *Astra* will perform NLoop complete tracking calculations, working successively through the specified namelists and incrementing the run number automatically. It is possible to specify 'NLoop = True' simultaneously in more than one namelist. With the following settings two runs will be performed with two different solenoid field maps:

```
&NEWRUN
  Loop=.FALSE.
  ...
  ...
  NLoop=2
  ...
/

...
...

&SOLENOID
  Loop=True
  File_Bfield(1)='Solenoid_1'
  ...
  ...
/

&SOLENOID
  Loop=True
  File_Bfield(1)='Solenoid_2'
  ...
  ...
/
```

## 4.10. Definition of Modules

The namelist MODULES (chapter 6.4) allows to combine elements from other namelists to modules. Modules can be used to do parameter scans or to introduce correlated errors, e.g. for a number of magnetic elements which are powered by a common power supply, a number of RF structures which are driven by the same klystron or elements which are mounted on a common girder. Module definitions don't substitute the individual definitions in the respective namelists but act in addition onto the elements. In the following example:

```
&MODULES
  LModule=t
  Module(1,1)='cavity(2)'
  Module(1,2)='cavity(3)'

  Module(2,1)='quadrupole(1)'
  Module(2,2)='quadrupole(2)'
  Module(2,3)='cavity(3)'

  Mod_Efield(1)=0.9
  Mod_Phase(1)=-2.0

  Mod_zpos(2)=1.5
  Mod_xoff(2)=1.0e-3
  Mod_xrot(2)=1.5e-3
  Mod_Bfield(2)=1.15
/
```

elements 2 and 3 of the namelist cavity are combined to module 1 and elements 1 and 2 of the namelist quadrupole form together with element 3 of the namelist cavity module number 2.

The strength of the RF elements of module 1 is scaled to 90% of their individual settings and the phase is shifted (in addition to the individual settings) by -2.0 degree.

The strength of magnetic elements of module 2 is increased by 15 %. Module number 2 has an offset and is rotated in the x-z plane. The rotation of the module leads to an additional offset and a rotation of the module elements depending on their individual positions and the longitudinal pivot point of the module Mod\_zpos. Individual offsets and rotation angles can still be specified for each element in the respective namelist.

The program would accept also to scale the strength of RF elements of module number 2 or to apply offsets to module number 1. Since element 3 of the namelist cavity is an element of module 1 and module 2 this doesn't make sense, however, the user has to take care of this kind of conflicts.

### 4.11. Apertures and Secondary Electron Emission in *Astra*

The namelist APERTURE (chapter 6.7) allows to include apertures and to define material properties for secondary electron emission. Circular apertures can be defined either by a table containing the z-position and the corresponding aperture radius or internally by keywords for the case of a simple collimating hole or cylinder. Planar apertures can be defined internally by keywords only.

The boundaries of apertures defined by keywords are either parallel or perpendicular to the z-axis.

The z-positions in an aperture table have to be in increasing order with a minimum step size of 0, i.e. it is not allowed to step back and create nose-like structures.

The thickness  $s$  of a collimating wall has to be larger than a single particle step i.e.:

$$s \geq v \cdot H_{\max}$$

with  $v$  being the particle velocity, so that a particle can't pass through the wall in one step. Especially when secondary emission is active this applies also for the case of a closed structure (radius = 0), so that particles get lost with the condition  $r > r_{\max}$  and not with e.g.  $z < z_{\min}$ . The aperture sketched on the left side of Fig. 1 does not ensure this, while the aperture on the right side does.

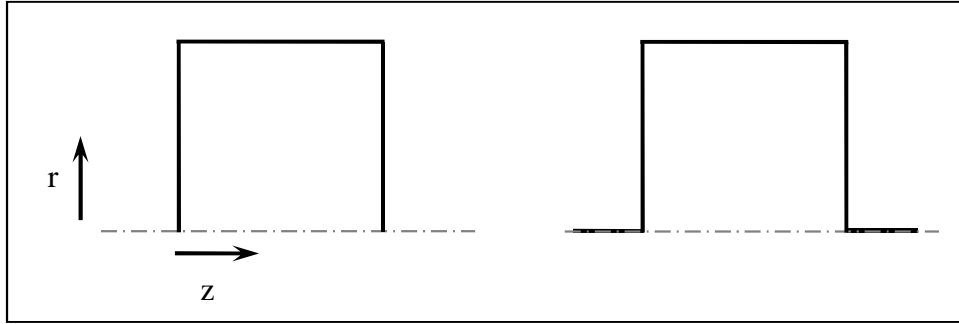


Fig. 1 Sketch of closed apertures. The aperture on the left does not ensure that particles are lost with the condition  $r > r_{\max}$  since the closing walls have zero wall thickness.

#### 4.11.1 Secondary electron emission

Secondary emission of electrons from limiting apertures can be included in the namelist APERTURE.

The Secondary Electron Yield (SEY) is modeled in *Astra* according to the following function [1]:

$$SEY(E_{kin}) = SE\_d0 \frac{E_{kin}}{SE\_Epm} \frac{SE\_fs}{SE\_fs - 1 + \left( \frac{E_{kin}}{SE\_Epm} \right)^{SE\_fs}}$$

$$SE\_fs \geq 1$$

Here  $E_{kin}$  is the kinetic energy of the impact electron and  $SE\_d0$ ,  $SE\_Epm$  and  $SE\_fs$  are the user defined input parameters to describe the material properties. Fig. 2 displays the secondary yield for various values of  $SE\_fs$ . While this parameter describes the functional dependence of the secondary electron yield on the impact energy,  $SE\_d0$  and  $SE\_Epm$  are scaling parameters which determine the maximum yield and the impact energy which gives the maximum yield.

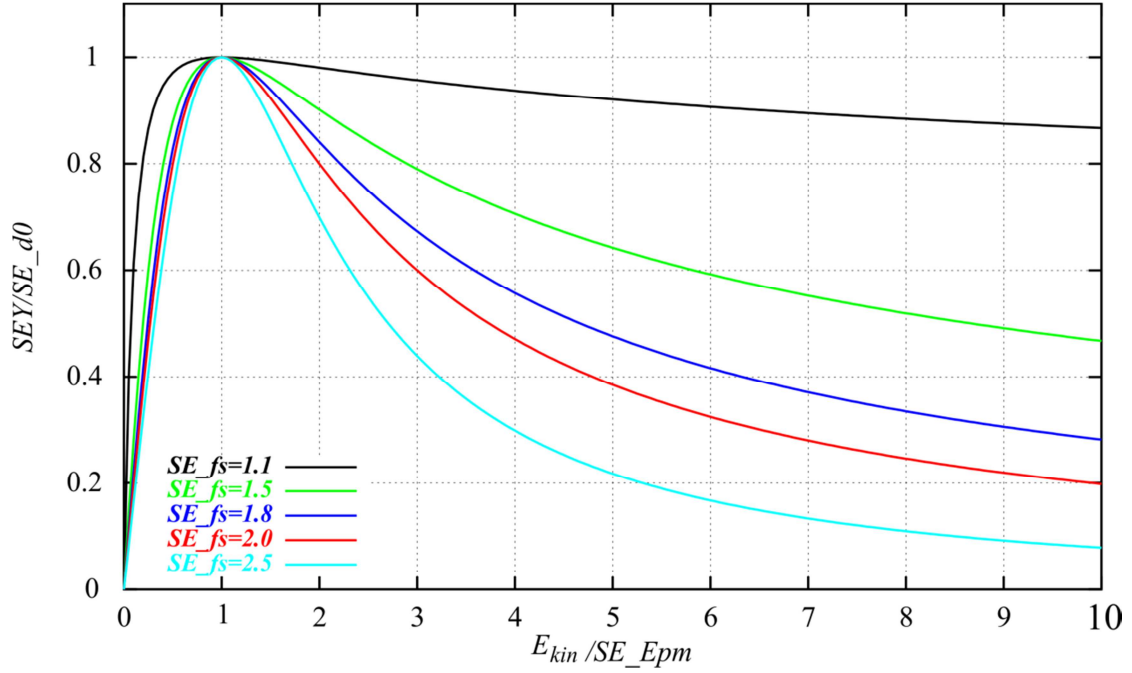


Fig. 2 Secondary Electron Yield for various parameters  $SE_{fs}$ .

When an electron hits an aperture *Astra* generates a random integer number of secondaries according to this model function using a Poisson generator. The macro charge of the secondaries corresponds to the macro charge of the primary electron. The initial kinetic energy of the secondaries is user defined. If the sum of the kinetic energies of all secondaries produced in one event exceeds the kinetic energy of the primary electron the kinetic energy of the secondaries is reduced accordingly. The secondary electrons are emitted isotropically into the half space over the material boundary equivalently to the distribution described in section 7.4.1. An exponential delay time for the particle emission can be included.

While without secondary emission particles are lost somewhat inside the material of an aperture, the entrance position and hence the emission position of the secondary electrons is corrected to the surface boundary if secondary emission is active.

If an external electric field is applied the secondary electron yield can be increased by a field enhancement factor  $R$  as:

$$R = \exp\left( SE_{ff1} \cdot \exp\left( -\frac{SE_{ff2}}{E} \right) \left( 1 + \frac{SE_{ff2}}{2E} \right) \right)$$

where  $SE_{ff1}$  and  $SE_{ff2}$  are user defined parameters and  $E$  is the absolute value of the externally applied field at the position and time of the emission process [4]. Fig. 3 shows  $R$  versus  $SE_{ff1}$  for various values of  $SE_{ff2}$ . The factor  $R$  is not applied when the field is directed into the material.

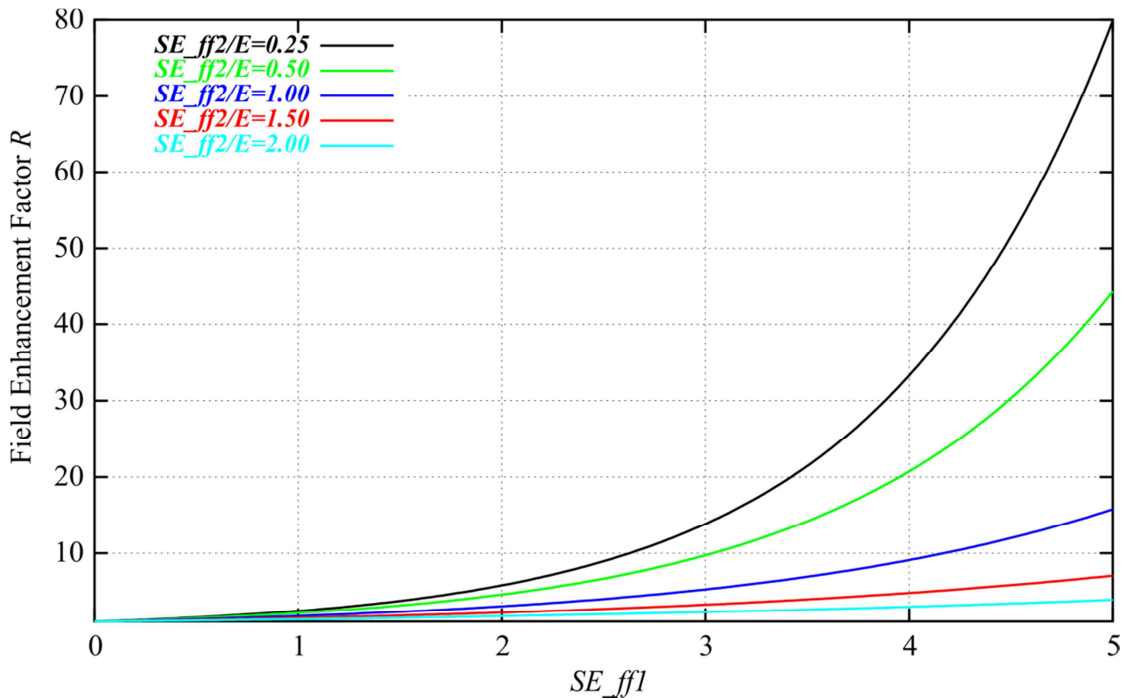


Fig. 3 Field Enhancement Factor  $R$  as function of parameter  $SE\_ff1$  for various ratios of  $SE\_ff2$  to the applied gradient  $E$ .

Examples of *Astra* simulations including secondary emission can be found in references [5]-[7].

### References

- [1] M. A. Furmann, M. T. F. Pivi 'Probabilistic model for the simulation of secondary electron emission', PRST-AB 5, 124404, 2002.  
<http://prst-ab.aps.org/pdf/PRSTAB/v5/i12/e124404>
- [4] H. Jacobs, J. Freely, F. A. Brand 'The Mechanism of Field Dependent Secondary Emission', Phys Rev 88, 1952.  
[http://prola.aps.org/abstract/PR/v88/i3/p492\\_1](http://prola.aps.org/abstract/PR/v88/i3/p492_1)
- [5] J. H. Han, K. Floettmann, M. Krasilnikov 'Secondary Electron Emission in a Photocathode Gun', PRST-AB 8, 03350, 2005.  
<http://prst-ab.aps.org/abstract/PRSTAB/v8/i3/e033501>
- [6] J. H. Han 'Dynamics of Electron Beam and Dark Current in Photocathode RF Guns', DESY-THESIS-2005-045, 2005.  
<http://www-library.desy.de/cgi-bin/showprep.pl?thesis05-045>
- [7] J. H. Han, K. Floettmann, W. Hartung 'Single-side electron multipacting at the photocathode in rf guns', PRST-AB 11, 013501  
<http://prst-ab.aps.org/abstract/PRSTAB/v11/i1/e013501>

## 4.12. Data output and organization of output files

Output of the beam emittance and other statistical beam parameters is generated if 'EmitS = True'. For the calculation of statistical bunch parameters the distance ZStop-ZStart is divided into Zemit intervals. Note that the Runge-Kutta time step is adjusted, i.e. reduced if necessary, in order to interrupt the tracking close to the specified locations. (The beam position refers to the average longitudinal beam position.) This might lead to a reduction of each time step, i.e. to an increased accuracy of the calculation, if the intervals are shorter than the bunch motion in one time step. A warning is given in this case because the result of the calculation might depend on a parameter for the output generation if H\_max is too big.

The complete particle distribution is saved at Zphase different locations if 'PhaseS = True'. The distance ZStop-ZStart is divided into Zphase intervals and the nearest location defined by means of Zemit is chosen. It is recommended to set  $Zemit = n \cdot Zphase$ ,  $n \in \mathbb{N}$ . Additional output positions can be specified by specifying screen locations (see chapter 6.2). The approximate longitudinal position of a saved particle distribution is indicated in the file name as a four digit number, which corresponds in general to the rounded beam position in cm. If necessary the units for the file name definition is changed (if the distance of the output positions is too small, or if the last output position is too big). If required the naming convention is changed to a relative position (i.e. output position minus start position) which is indicated by a warning message.

In some cases it is desirable to generate output based on time steps rather than on locations. For this purpose the switch T\_PhaseS can be set true. A complete particle distribution is saved in time intervals defined by  $Step\_width \cdot H$ , where Step\_width is a user defined integer number and H is the Runge-Kutta time step which is automatically adjusted (between H\_min and H\_max). In order to limit the generation of output with this option the parameter Step\_max can be set to  $n \cdot Step\_width$ , where n is the number of particle distributions to be saved. The T\_PhaseS option can be combined with the PhaseS option.

A log file is generated for each run. In the first section of the log file all namelists of the input deck containing user specified or default values of all possible parameters are stored. The output is generated in a system dependent format; hence this file can in general not be transformed to a different system without problems. While this section is somewhat difficult to read, the way the output is generated allows printout also in cases of serious errors. In the second part of the log file a listing of the names and z-locations or times of saved phase space distributions is stored which is required by the graphic program *postrpo*. The third column of the listing contains the solenoid field value at the location of the saved phase space distribution.

*Astra* produces output on different length scales, time scales or scales for the variation of a parameter, respectively. Table 3 lists generic file names, logical switches and the scale on which data are stored.

Table 4 lists the output file data structure, i.e. the parameters that can be found in the different files, their units and the format of the files. Note, that the generation of output increases the computation time, especially when it is created on short time scales like tcheck and track files. Hence no superfluous output should be generated when computation time is an issue.

generic name	logical switch	approx. scale
project.ref.run	RefS	Runge-Kutta time step $H_{\max}$
project.track.run	TrackS	Runge-Kutta time step H
project.Cathode.run	CathodeS	Runge-Kutta time step H
project.Fields.run	automatic <sup>1</sup>	Runge-Kutta time step H
project.tcheck.run	TcheckS	Runge-Kutta time step H
project.Xemit.run project.Yemit.run project.Zemit.run	EmitS	$(Z_{\text{Stop}}-Z_{\text{Start}})/Z_{\text{emit}}^2$
project.Xemit2.run project.Yemit2.run	Lsub_cor	$(Z_{\text{Stop}}-Z_{\text{Start}})/Z_{\text{emit}}^2$
project.TRemit.run	TR_emitS	$(Z_{\text{Stop}}-Z_{\text{Start}})/Z_{\text{emit}}^2$
project.Cr_emit.run	Cross_start $\neq$ Cross_end	$(Z_{\text{Stop}}-Z_{\text{Start}})/Z_{\text{emit}}^2$
project.Sub_emit.run	Sub_EmitS	$(Z_{\text{Stop}}-Z_{\text{Start}})/Z_{\text{emit}}^2$
project.Cemit.run	C_EmitS	$(Z_{\text{Stop}}-Z_{\text{Start}})/Z_{\text{emit}}^2$
project.C99emit.run	C99_EmitS	$(Z_{\text{Stop}}-Z_{\text{Start}})/Z_{\text{emit}}^2$
project.Larmor.run	LarmorS	$(Z_{\text{Stop}}-Z_{\text{Start}})/Z_{\text{emit}}^2$
project.Sigma.run	SigmaS	$(Z_{\text{Stop}}-Z_{\text{Start}})/Z_{\text{emit}}^2$
project.Density.run	DensityS	$(Z_{\text{Stop}}-Z_{\text{Start}})/Z_{\text{emit}}^2$
project.zpos.run	PhaseS	$(Z_{\text{Stop}}-Z_{\text{Start}})/Z_{\text{phase}}$ , Screen & Wake positions
project.tstep.run	T_PhaseS	Step_width·Runge-Kutta time step
project.Lost_Part.run	LClean_Stack	Runge-Kutta time step H
project.Log.run	PhaseS	Start of the run and $(Z_{\text{Stop}}-Z_{\text{Start}})/Z_{\text{phase}}$ and Screen positions or Step_width·Runge-Kutta time step
project_E.Log.run	Log_Error	Start of the run
project.LandF.run	LandFS	$(Z_{\text{Stop}}-Z_{\text{Start}})/Z_{\text{phase}}$ and Screen positions
project.PScan.run	Phase_scan	1 degree of the RF phase of each cavity
project.Scan.run	LScan	$(S_{\max}-S_{\min})/S_{\text{numb}}$
project.lab.run	LScan	
project.Error.run	ErrorS	run end

run = run number, zpos = z-position, tstep = time step

1 cavity fields are saved when beam loading or time depending field options are used.

2 output is generated in addition at Screen positions and Step\_width·Runge-Kutta time step.

Table 3: Generic file names, logical switches and scales for the data output with *Astra*.

Name	1	2	3	4	5	6	7	8	9	Format	
ref	z m	t ns	pz MeV/c	$dE/dz$ MeV/m	Larmor angle rad	X <sub>off</sub> mm	Y <sub>off</sub> mm	px eV/c	py eV/c	1P,9E12.4 1P,9E20.12	
track	seq. numb	stat. flag	z m	x mm	y mm	Ez V/m	Er, or Ex V/m	0.0, or Ey V/m		2I5,1P,6E12.4	
Cathode	z m	t ns	long. sp. ch. field on cathode V/m	acc. field on cathode V/m	charge nC	min. grid position m	max grid position m	emission flag		1P,7E12.4,L3	
Fields	z m	t ns	Cavity gradient (i) (i = 1...number of cavities N <sub>C</sub> ) MV/m								1P,N <sub>C</sub> E12.4
tcheck	z m	t ns	$\frac{\sigma_{r0}^{nr(r)}}{\sigma_r}$	$\frac{\sigma_{z0}^{nr(z)}}{\sigma_z}$	$\frac{\gamma^{nr(\gamma)}}{\gamma_0}$	$\frac{\sigma_{r0}^{nz(r)}}{\sigma_r}$	$\frac{\sigma_{z0} \gamma_0^{nz(\gamma z)}}{\sigma_z \gamma}$	scaling counter		1P,7E12.4,I10	
Xemit	z m	t ns	X <sub>avr</sub> mm	X <sub>rms</sub> mm	X' <sub>rms</sub> mrad	$\epsilon_{x,norm}$ $\pi$ mrad mm	X·X' <sub>avr</sub> mrad			1P,7E12.4	
Yemit	z m	t ns	Y <sub>avr</sub> mm	Y <sub>rms</sub> mm	Y' <sub>rms</sub> mrad	$\epsilon_{y,norm}$ $\pi$ mrad mm	Y·Y' <sub>avr</sub> mrad			1P,7E12.4	
Zemit	z m	t ns	E <sub>kin</sub> Mev	Z <sub>rms</sub> mm	$\Delta E_{rms}$ kev	$\epsilon_{z,norm}$ $\pi$ keV mm	Z·E' <sub>avr</sub> keV			1P,7E12.4	
Xemit2	z m	$K_{2,Z}^x$ $\pi$ rad m	$K_{3,Z}^x$ $\pi$ rad m	$\mathcal{E}_{x,rms}^{reduced z}$ $\pi$ mrad mm	$K_{2,E}^x$ $\pi$ rad m	$K_{3,E}^x$ $\pi$ rad m	$\mathcal{E}_{x,rms}^{reduced z \& E}$ $\pi$ mrad mm			1P,7E12.4	
Yemit2	z m	$K_{2,Z}^y$ $\pi$ rad m	$K_{3,Z}^y$ $\pi$ rad m	$\mathcal{E}_{y,rms}^{reduced z}$ $\pi$ mrad mm	$K_{2,E}^y$ $\pi$ rad m	$K_{3,E}^y$ $\pi$ rad m	$\mathcal{E}_{y,rms}^{reduced z \& E}$ $\pi$ mrad mm			1P,7E12.4	
TRemit	z m	t ns	$\mathcal{E}_{x,rms}^{trace space}$ $\pi$ mrad mm	$\mathcal{E}_{y,rms}^{trace space}$ $\pi$ mrad mm	$\mathcal{E}_{z,rms}^{trace space}$ $\pi$ $\mu$ m					1P,5E12.4	
Cr_emit	z m	t ns	X <sub>rms</sub> mm	Y <sub>rms</sub> mm	$\epsilon_{x,rms}$ $\pi$ mrad mm	$\epsilon_{y,rms}$ $\pi$ mrad mm	rest charge nC	cross over charge nC		1P,8E12.4	
Sub_emit	z m	t ns	X <sub>rms</sub> mm	Y <sub>rms</sub> mm	$\epsilon_{x,rms}$ $\pi$ mrad mm	$\epsilon_{y,rms}$ $\pi$ mrad mm	charge of sub- ensemble nC	active rest charge nC		1P,8E12.4	

Cemit	z m	$\epsilon_{x,norm.}$ , Cx_95, Cx_90, Cx_80 $\pi$ mrad mm	$\epsilon_{x,norm.}$ , Cy_95, Cy_90, Cy_80 $\pi$ mrad mm	$\epsilon_{x,norm.}$ , Cz_95, Cz_90, Cz_80 $\pi$ keV mm					1P,13E12.4
C99emit	z m	$\epsilon_{x,norm.}$ , Cx_99.99, Cx_99.9, Cx_99 $\pi$ mrad mm	$\epsilon_{x,norm.}$ , Cy_99.99, Cy_99.9, Cy_99 $\pi$ mrad mm	$\epsilon_{x,norm.}$ , Cz_99.99, Cz_99.9, Cz_99 $\pi$ keV mm					1P,13E12.4
Larmor	z m	t ns	avr. Larmor angle rad	rms Larmor angle rad					1P,4E12.4
Sigma	z m	$E_{kin}$ MeV	sig <sub>ij</sub> (i = 1..6, j = i..6)						1P,23E14.6
Density	z m	t ns	Number of particles (i), Particle density (i) (i = 1..5)						1P,12E12.4
zpos <sup>1</sup>									1P,8E12.4,2I4
tstep <sup>1</sup>									1P,8E20.12,2I4
Lost_Part <sup>1</sup>									binary
Log	file name	z m	Bz T						A50,2D12.4
LandF	z m	Npart <sup>2</sup>	Q nC	number of lost particles <sup>3</sup>	deposited energy <sup>3</sup> J	tot. energy exchange with fields <sup>3</sup> J			1P,6E12.4
PScan	phase deg	$E_{kin}$ MeV	compression factor	$\beta / \beta_0$					1P,4E12.4
Scan	Scan_ para	z m	FOM(1) – FOM(10)						1P,12E17.8
lab	Label for scan and error plots: X-axis, Y-axis, title								A80
Error	Run #	z m	FOM(1) – FOM(10)						1P,12E17.8

- 1 zpos = z-position, tstep = time step; zpos, tstep and Lost\_Part files have the same structure as input distribution files, the format depends on user settings.
- 2 Npart = number of active particles.
- 3 within the previous z-interval.

Table 4: Data structure of output files.

### 4.13. Emittance calculation

The standard emittance calculation in *Astra* is based on canonical variables, i.e.:

$$x, \tilde{p}_x \quad \tilde{p}_x = p_x + \frac{eB_z}{2} y$$

$$y, \tilde{p}_y \quad \tilde{p}_y = p_y - \frac{eB_z}{2} x$$

$$z, E_{kin}$$

where  $x, y, z$  are the particle coordinates,  $p_x, p_y$  are the transverse particle momenta,  $B_z$  is the solenoid field at the particle position and  $E_{kin}$  is the kinetic particle energy. For the solenoid a constant field over the length of the bunch is assumed, i.e. the solenoid field value at the center of the bunch is taken for all particles in the bunch.

All particles with status flag > 1 are taken into account for the emittance calculation (see Table 2).

A number of options are provided in order to modify the emittance calculation (and hereby the calculation of spot sizes etc.), which will be discussed below. For the definition of the statistical emittance, relations to optical functions etc. see Ref. [1].

#### 4.13.1 Influence of solenoid fields

Solenoid fields may introduce an angular momentum to a beam, which can appear as correlated emittance contribution. Since the angular momentum introduced at the entrance of a solenoid cancels exactly with the angular momentum generated in the exit field of the solenoid, this emittance contribution should in general be suppressed in the emittance calculation, otherwise it might cover smaller emittance diluting effects inside the solenoid. For the case of a beam, which is generated in a solenoid field free region, this is achieved by the canonical momenta used in the standard settings of *Astra*. (The emittance exchange between the transverse planes due to coupling in case of a non-rotational symmetric beam in  $x, y$  or  $p_x, p_y$  will of course still be seen.)

This approach fails, if the beam is generated in a solenoid field (i.e. from an immersed cathode) and stays inside a solenoid up to the point of interest, because the beam is inside a solenoid but has no angular momentum (which is sometimes called a magnetized beam). The option 'Lmagnetized = True' can be used in order to base the transverse emittance calculation on ordinary rather than on canonical momenta. Each variation of the beam size or the solenoid field strength, which leads to a rotation of the beam, will however still lead to an emittance contribution.

A different approach is realized when the option Lsub\_rot is set true. In this case the angular momentum of the beam is calculated from a correlation in the  $x, p_y$  and  $y, p_x$  phase space and subtracted prior to the emittance calculations.

Even though the net angular momentum is zero when a beam travels through a complete solenoid field, there remains a rotation of the coordinate system of the outgoing beam relative to the incoming beam. This rotation of the transverse coordinate system of the beam is taken into account when the switch Lsub\_Larmor is set true. The effect is a rotation of the output coordinate system only, i.e. the angular momentum is not corrected. The switch is useful when the bunch is asymmetric or imaging problems are to be investigated.

#### 4.13.2 Correction of a transverse beam tilt

In order to correct the influence of a beam tilt in the x-y plane on the calculated

emittance the switch `Lsub_coup` can be set true. A simple rotation of the transverse plane is applied in this case. If no rotation angle is specified an optimized rotation angle is taken. This is however not necessarily constant when parameters change.

#### 4.13.3 Calculation of the projected emittance

The tracking in *Astra* is based on time steps, i.e. the emittance is calculated at a certain time step with the particles being at different longitudinal coordinates (non-local emittance). This leads to a correlated emittance growth when external fields act onto the bunch (Ref. [1]). The emittance of a parallel beam entering for example a quadrupole increases, because the transverse moment of the head of the bunch, which is given by the integral of the field gradient over the path length, is larger than the transverse moment of the tail of the bunch, because the head has traveled a somewhat longer path in the field of the quadrupole. Thus a fan-like structure opens up in phase space. Even when the beam is leaving the quadrupole a small emittance contribution remains, because the head of the bunch has a somewhat different transverse size than the tail, while the transverse momenta are the same. The phase space may again be described by a fan-like structure. This behavior is related to the way the emittance is calculated and describes well-known effects as the luminosity loss due to the so-called hourglass effect. Most transverse emittance diagnostics however measure the emittance at a certain position (= monitor position), thus recording the particle positions when they pass this position, which means at different times. In this way the discussed correlated emittance contributions vanish.

*Astra* offers two options for the calculation of the emittance at a fixed position of all particles (local emittance). For the first option the logical switch `Lproject_emit` is set true in `OUTPUT`. With this option the coordinates of all particles are projected onto the average longitudinal beam position prior to the calculation of the emittance, which gives proper results in field free regions, but still has correlated contributions inside external fields. The second option is activated by setting the logical switch '`Local_emit = True`' in `OUTPUT`. In this case the particle coordinates are stored when passing the monitor position and the emittance is calculated when the complete bunch has passed the monitor. While this option avoids all correlated emittance contributions discussed above, it also has some drawbacks. For the calculation of the longitudinal emittance the longitudinal coordinates are estimated from the time the particle has passed the monitor position and its velocity. Also saved phase space distributions represent transverse coordinates of the particles when they passed the monitor position (i.e. like one would measure it for example on a screen in a real machine) and estimated longitudinal coordinates. Therefore these distributions should no be used as input distributions for further tracking. Finally the distance between monitor positions has to be larger than the bunch length when this option is active. Monitors at shorter distance will be skipped.

#### 4.13.4 Calculation of the Trace Space emittance

In addition to the standard emittance calculation which is based on canonical coordinates the so-called Trace Space emittance is calculated when the option `Tr_emitS` is set true. The Trace Space emittance is based on geometrical parameters, i.e.  $x$  and  $x'$ ,  $y$  and  $y'$  or  $z$  and  $z'$ . Emittance measurements yield in general the Trace Space emittance, since the beam divergence rather than the transverse momenta are measured. The transverse Trace Space emittance differs from the canonical emittance only in case of a beam with large energy spread and large beam divergence. See Ref. [1] for a detailed discussion.

#### 4.13.5 Calculation of the core emittance

Halo particles may have a significant contribution to the beam emittance. In order to evaluate the emittance of the core of the beam the option ‘C\_EmitS = True’ (‘C99\_EmitS = True’) might be set. Based on an rms emittance calculation a single particle emittance can be defined as:

$$\varepsilon_{rms} = \sum \varepsilon_i$$

For the calculation of the core emittance the individual contributions of all particles to the rms emittance are calculated and sorted in ascending order. While *Postpro* allows to plot the emittance as function of the percentage of particles taken into account, *Astra* stores the core emittance for 95 %, 90 % and 80 % (99.99 %, 99.90 % and 90.00 %) of all particles along the beam line, respectively. Table 5 shows the core emittance of a double Gaussian particle distribution as an example and for comparison.

percentage of particles	rms emittance [arb. units]
100%	1.00
95%	0.80
90%	0.67
80%	0.48

Table 5: Core emittance values of a double Gaussian particle distribution.

#### 4.13.6 Calculation of the ‘reduced emittance’

Space charge and RF fields can introduce correlated emittance contributions. Here the transverse momenta  $p_{s,i}$  of the particles are correlated with the longitudinal position within the bunch. The correlations can be removed to a large extent and the so-called reduced emittance, i.e. an emittance without these correlated emittance contributions can be calculated by replacing  $p_{s,i}$  by:

$$\tilde{p}_{s,i} = p_{s,i} - (C_0 + C_1 s_i + C_2 s_i z_i + C_3 s_i z_i^2) \quad (4.3)$$

prior to the emittance calculation.  $s$  can be either of the transverse coordinates  $x$  and  $y$  and  $z$  is the relative longitudinal particle position within the bunch. The term in brackets with the fit coefficients  $C_0 - C_3$  describes a curved plane in the  $x - p_s - z$  space.  $C_0$  is just the average transverse momentum and  $C_1$  describes the correlated beam divergence as in the standard emittance calculation.  $C_2$  describes a linear correlation of the linearly correlated beam divergence to the longitudinal position in the bunch and  $C_3$  describes a quadratic correlation of the linearly correlated beam divergence to the longitudinal position in the bunch.  $C_2$  is for example introduced by the time dependence of RF fields but also in beam line elements if a non-local emittance is calculated (see section 4.13.3), while  $C_3$  approximates correlations as they are introduced by space charge fields.

The same formalism can be applied to correlations with the other longitudinal phase space coordinate, i.e. the kinetic energy.

When in *Astra* the option `Lsub_cor` is set true the reduced emittance is calculated in addition to the standard emittance and saved into separate files. First the correlations with the longitudinal position are taken into account; in a second step the correlations

with the kinetic energy are subtracted. In addition the following terms are calculated and stored:

$$\begin{aligned}
 K_{2,Z}^s &= 0.5 C_{2,Z} s_{rms}^2 z_{rms} \\
 K_{3,Z}^s &= 0.5 C_{3,Z} s_{rms}^2 z_{rms}^2 \\
 K_{2,E}^s &= 0.5 C_{2,E} s_{rms}^2 E_{rms} \\
 K_{3,E}^s &= 0.5 C_{3,E} s_{rms}^2 E_{rms}^2
 \end{aligned}
 \tag{4.4}$$

The difference between standard emittance and reduced emittance can in most cases be approximated by the sum of the absolute values of the terms in Eq. (4.4). Thus the terms display the approximate contributions of the different correlations to the emittance.

For the longitudinal coordinate 2<sup>nd</sup> and 3<sup>rd</sup> order polynomial correlations are subtracted for the reduced emittance.

#### 4.13.7 Calculation of the emittance excluding cross over particles

Particles going through a cross over can increase the emittance substantially. Astra checks the crossover of particles within the user defined beam line section from 'cross\_start' to 'cross\_end'. The particles status flag is set to 4 and a separate file containing the emittance of the particle ensemble excluding particles marked as cross over particles and the charge carried by the excluded particles is generated. The algorithm checks whether particles move diagonally from one quadrant of a Cartesian coordinate system into another. It should not be active within solenoid fields. For this option the parameter Sub\_EmitS has to false.

#### 4.13.8 Emittance calculation of a sub-ensemble of particles

In order to calculate the emittance of a sub-ensemble of particles (e.g. all particles in a slice) the status flag of all particles except those of the subensemble has to be set to 4 (-2 if starting at a cathode) and the option Sub\_EmitS has to be set true in the namelist OUTPUT. A file containing the emittance of the sub-ensemble and the charge contained in the sub-ensemble is created in addition to the file containing the standard emittance calculation of all particles.

#### 4.13.9 General redirection of the emittance calculation

For the emittance calculation all particles with status flags > 1 are taken into account with standard settings. In order to redirect the emittance calculation to a certain subset of particles a file named 'Astra\_steering.par' has to be created. The file should contain the namelist 'Steering\_parameters', in which the logical array Stat(2,-100:100) can be redefined. The first index of the Stat array is always 2 (index 1 = 1 is for internal use only). The second index numbers of the Stat array correspond to the status flags as defined in Table 2. Particles with status flags to which the corresponding Stat array entry is true will be taken into account in the emittance calculation. Hence, for the standard settings Stat(2,I) is false for  $I \leq 1$  and true for  $I > 1$ . If necessary it is possible to use free status flags in order to mark a subset of particles (e.g. flag -2 and 4) and redirect the emittance calculation to this subset.

## References

- [1] K. Floettmann, 'Some basic features of the beam emittance', PRST-AB 6, 034202, 2005.

<http://prst-ab.aps.org/abstract/PRSTAB/v6/i3/e034202>

## 5. Graphics programs

While the programs *lineplot* and *postpro* allow to visualize output produced by *Astra* and *generator* the program *fieldplot* allows to visualize electric and magnetic fields of beam line elements as they are used in *Astra*. *Fieldplot* uses the same subroutines as *Astra* and is hence a tool to control the correct setup of the input deck and the correctness of field maps and field tables. Furthermore it is possible to view space charge fields of any particle distribution with *fieldplot* and to control the setup of the space charge grid. It is highly recommended to download the graphics programs, especially *fieldplot*, and to make use of these options.

The graphics programs are based on the subroutine package PGPLOT<sup>1</sup>. In general it is, however, not necessary to install the PGPLOT subroutine library.

### 5.1. Running the graphics programs on Windows PC systems

The programs run on all windows systems from Windows 95 to Windows XP with standard settings.

The position and size of the graphics windows can be changed with the mouse. The last settings will be automatically stored in the `win_config.dat` file and used as input the next time a graphics program is started. The `win_config.dat` file should not be copied between PC's with different screen size (e.g. Laptop and Desktop PC). Delete the `win_config.dat` file in case of problems.

### 5.2. Running the graphics programs on Linux/UNIX systems

Besides the graphics programs the font file 'grfont.dat' and the PGPLOT windows server (pgxwinserver) have to be downloaded and the path names have to be set accordingly. In case of problems it is advisable to download and install the PGPLOT subroutine package.

The size and position of the two graphics windows can be predefined in the `.Xresources` file. The windows have the numbers 101 and 102. Position and resize the windows with the mouse and extract the geometry information with the command 'xwininfo'. The entry in the `.Xresources` may then look like:

```

.
.
.
pgxwin.win101.geometry: 274x660-18+10
pgxwin.win102.geometry: 274x660-18+10
pgxwin.server.visible: False
.
.
.

```

The last entry suppresses an icon for the `pgxwinserver`.

### 5.3. The win\_config.dat file

The `win_config.dat` file is created by the graphics programs on first use. It contains some basic settings for the graphics routines in the namelist `WIN_CONFIG` and the position and the size of the graphic windows for Windows PCs.

The settings in the namelist `WIN_CONFIG` may be changed by the user.

---

<sup>1</sup> PGPLOT is a graphics subroutine library freely available for non-commercial use. For downloading and further information see: <http://astro.caltech.edu/~tjp/pgplot> .

## 5.4. The namelist WIN\_CONFIG

Parameter	Specification	Unit	Default Value
<b>Fixed</b>	Logical		FALSE
only for Windows PC version. If true, actual window size and position settings will not be stored.			
<b>Line_width</b>	Integer		2
scaling factor for the line width of the plots.			
<b>Character_height</b>	Real		1.2
scaling factor for the character height of plots.			
<b>Color_mode</b>	Integer		2
defines the color scheme for color maps. Color maps are used by default in <i>postpro</i> if the particle number is larger than 10000 and in some parts of <i>fieldplot</i> . (The color schemes are copied from PGPLOT demo 4.) color_mode = 1 gray scale color_mode = 2 rainbow color_mode = 3 heat			
<b>Contrast</b>	Real		1.0
contrast of color maps. <sup>1</sup>			
<b>Brightness</b>	Real		0.5
brightness of color maps. <sup>1</sup>			
<b>Plot_mode</b>	Integer		0
defines whether particle distributions shall be plotted with symbols or as color maps in <i>postpro</i> : Plot_mode = 0 color maps if more than 10000 particles, symbols else Plot_mode = 1 symbols Plot_mode = 2 color maps			
<b>Win101_Scale</b>	Real		1.0
only for Windows PC version. Scaling factor for window 101.			
<b>Win102_Scale</b>	Real		1.0
only for Windows PC version. Scaling factor for window 102.			

<sup>1</sup> To reverse the sense of a color scheme, reverse the sign of Contrast and set Brightness to 1 – Brightness.

## 5.5. The program *lineplot*

The program *lineplot* allows to display a number of beam parameters as the beam emittance, the bunch length etc. versus the longitudinal beam position or versus a scanned parameter. Start the program with 'lineplot [project name],[run number]'. The project name is the name of the *Astra* input file. If no project name is specified the default name 'rfgun' is assumed. The run number has to be separated from the project name by a comma without blanks. (Preceding zeros can be omitted.) If no run number is specified run number 1 is assumed. When starting the code two windows, one for displaying and one for selecting from the menu, will open. The menu contains only 'dishes' of which parameter files exist, i.e. if 'EmitS = False' has been chosen in the *Astra* input file no emittance plot will be offered. By clicking with the left mouse button onto the circles different parameters can be displayed. By clicking onto the word 'menu' different menus will be shown. Note, that additional text information will be displayed in the window from which *lineplot* was started or in a third window in the Windows version. Here also input might be requested.

### 5.5.1 Menu 1 of 4

*1 Trans. Emittance:* Displays the horizontal (black) and vertical (red) rms emittance of the beam along the z-axis. See chapter 4.13 for details on the emittance calculation.

*2 rms Beam Size:* Displays the horizontal (black) and vertical (red) rms beam size of the beam along the z-axis.

*3 rms Beam Divergence:* Displays the horizontal (black) and vertical (red) rms divergence of the beam along the z-axis.

*4 Long. Emittance:* Displays the longitudinal rms emittance of the beam along the z-axis. The calculation is based on a statistical approach equivalent to the transverse case.

*5 rms Bunch Length:* Displays rms bunch length of the beam along the z-axis.

*6 rms Energy Spread:* Displays the rms energy spread of the beam along the z-axis.

*7 cor. Energy Spread:* Displays the correlated part of the energy spread of the beam along the z-axis.

*8 average Energy:* Displays the average energy of the beam along the z-axis.

*9 Particle velocity:* Displays the average velocity of the beam along the z-axis, **assuming electrons**.

*10 Reference particle momentum:* Displays the momentum of the reference particle along the z-axis. The data are based on the first, single particle tracking in *Astra*.

*11 dp/dz:* Displays the momentum gain of the reference particle along the z-axis, i.e. it reproduces the accelerating field as seen by the particle. The data are based on the first, single particle tracking in *Astra*.

*12 Ref. particle trajectory:* Displays the off-axis trajectory of the reference particle along the z-axis. The data are based on the first, single particle tracking in *Astra*, i.e. without space charge.

*13 Larmor angle:* Displays the Larmor angle of the off-axis tracking of the reference particle. Plots for the average Larmor angle and the rms Larmor angle (see Table 4) are not provided.

*14 Trajectories x vs. z; y vs. z:* Displays the trajectories of the probe particles along the z-axis in cartesian coordinates. At maximum 100 trajectories can be displayed.

*15 Trajectories r vs. z; x vs. y:* Displays the trajectories of the probe particles along the z-axis in cylindrical coordinates. At maximum 100 trajectories can be displayed.

*16 Space charge fields:* Displays the space charge fields ( $E_r$  and  $E_z$  for 2D calculations,  $E_x$  and  $E_y$  for 3D calculations) acting onto the probe particles along the z-axis. At maximum the fields of 100 particles can be displayed.

*18 include geometry:* Allows to include a sketch of the beam line aperture into any plot. A file in accordance to an aperture file (see chapter 4.11) is required.

*19 ZOOM:* Allows to zoom into all plots. Coordinates of the abscissa are requested.

*20 fit, save & read:* Opens the sub menu ‘fit, save & read’, which allows to fit a number of analytical functions to the presently displayed data. The data may also be saved to a reference file or read from a reference file for comparison, respectively. The fit, save & read menu is not accessible from all plots.

*21 to file:* Generates a post script file of the present plot.

*22 overview to file:* Generates a post script file which contains the first 9 plots of the menu on one page. Uses default names for the files.

*23 next run:* Increases the run number by one.

*24 previous run:* Decreases the run number by one.

*25 Exit:* Exits *lineplot*.

### 5.5.2 Menu 2 of 4

1 *Energy vs. Phase*: Displays the energy gain versus the RF phase for all cavities in one plot. See chapter 4.8.

2 *dE/dz vs. Phase*: Displays the derivative of the energy gain versus the RF phase, which is proportional to the correlated energy spread, for all cavities. See chapter 4.8.

3 *Compression factor (z)*: Displays the ratio of the final bunch length, i.e. at the exit of the cavity to the initial bunch length, i.e. at the entrance of the cavity for all cavities. In case of a gun cavity, the initial bunch length is replaced by the emission time times the velocity of light. See chapter 4.8.

4 *Compression factor (time)*: Displays the ratio of the final bunch length to the initial bunch length times the inverse ratio of the particle velocities for all cavities. In case of a gun cavity, the initial bunch length is replaced by the emission time. See chapter 4.8.

5 *Particle loss*: Displays the number of lost particles per meter along the z-axis. The intervals are determined by the parameter Zphase.

6 *Energy deposition*: Displays the energy deposited in the surrounding structure by lost particles per meter along the z-axis. The intervals are determined by the parameter Zphase.

7 *Beam loading*: Displays the total energy exchange of the bunch with external fields per meter along the z-axis. The intervals are determined by the parameter Zphase.

9 *Sp. ch. scaling factors*: Displays the space charge scaling factors as described in section 4.4.7.

10 *Sp. ch. scaling counter*: Displays the space charge scaling counter as described in section 4.4.7.

11 *Average time step*: Displays the average Runge-Kutta time step between updates of the space charge fields.

12  *$\beta$ -function*: Displays the optical beta functions, **assuming electrons**, determined

as: 
$$\beta_x = \frac{x_{rms}^2}{\mathcal{E}_{x,rms}}$$

13  *$\alpha$ -function*: Displays the optical alpha functions, **assuming electrons**, determined

as: 
$$\alpha_x = -\frac{x x'_{avr}}{x_{rms}} \cdot \beta_x$$

14 *phase advance*: Displays the phase advance, **assuming electrons**, determined as:

$$\theta = \int \frac{1}{\beta}$$

*15 coherence length*: Displays the coherence length of **electrons**, determined as:

$$L_c = \frac{\hbar\sigma_x}{m_0c \mathcal{E}_{n,rms}}$$

*18 – 25*: See section 5.5.1.

### 5.5.3 Menu 3 of 4

*1 - 10 left FOM(1) to FOM(10)*: Displays the result of a scanning procedure according to the *Astra* input deck. See chapter 6.3.

*1 - 10 right Err. FOM(1) to Err. FOM(10)*: Histograms of error scans according to the *Astra* input deck. See chapter 6.5.

*11 left position*: Displays the longitudinal position at which the values of FOM(1) to FOM(10) were saved.

*11 right Err. position*: Displays the longitudinal position at which the values of Err. FOM(1) to Err. FOM(10) were saved. It should be a constant, if the beam was not lost during the runs.

*15 change number of bins*: Allows to change the number of the bins in the histograms of error scans.

*16 change title*: Allows to change the labels and the title of the displayed plot.

*18-25*: See section 5.5.1.

### 5.5.4 Menu 4 of 4

*1 reduced trans. emittance z*: Displays the transverse emittance without correlations with the longitudinal particle position as described in 4.13.6.

*2 reduced trans. emittance z & E*: Displays the transverse emittance without correlations with the longitudinal particle position and the particle energy as described in section 4.13.6.

*3 trans. emittance difference*: Displays the difference between standard emittance and reduced emittance in the transverse planes.

*4 trans. cor. emittance contributions x*: Displays the correlated emittance contributions as defined in Eq. (4.4).

*5 trans. cor. emittance contributions y*: Displays the correlated emittance contributions as defined in Eq. (4.4).

*6 reduced long. emittance*: Displays the longitudinal emittance minus 2<sup>nd</sup> and 3<sup>rd</sup> order correlations together with the canonical Phase Space emittance. See section 4.13.6

7 *trans. Trace Space emittance*: Displays the transverse Trace Space emittance together with the canonical Phase Space emittance. See section 4.13.4.

8 *long. Trace Space emittance*: Displays the longitudinal Trace Space emittance together with the canonical Phase Space emittance. See section 4.13.4

9 *horizontal core emittance*: Displays different levels of the horizontal core emittance. See section 4.13.5.

10 *vertical core emittance*: Displays different levels of the vertical core emittance. See section 4.13.5.

11 *long. core emittance*: Displays different levels of the longitudinal core emittance. See section 4.13.5.

12 *Emittance w. o. cross over particles or sub-ensemble emittance*: Displays the emittance without cross over particles or the emittance of a sub ensemble of particles. See sections 4.13.7 and 4.13.8.

13 *beam size w. o. cross over particles or beam size of sub-ensemble*: Displays the beam size without cross over particles or the beam size of a sub ensemble of particles. See sections 4.13.7 and 4.13.8.

14 *Charge of cross over particles or charge of sub-ensemble*: Displays the charge carried by the cross over particles or by the sub-ensemble. See sections 4.13.7 and 4.13.8.

15 *Ez on cathode*: Displays the longitudinal electric field in the center of the cathode vs. time during the emission from a cathode.

16 *charge vs. time*: Displays the development of the emitted charge vs. time during the emission from a cathode.

17 *Position v. time*: Displays the position of the head and the tail of the bunch and the average bunch position vs. time during the emission from a cathode.

18-25: See section 5.5.1.

## 5.6. The program *postpro*

The program *postpro* allows to display different phase space plots and to perform a detailed phase space analysis. *Postpro* requires as input arguments the project name, the run number and the z-position to be displayed at the start up. Within *postpro* one can step through the different z-positions at which the phase space distributions have been saved and through the different run numbers. Missing input arguments are completed by the default values:

project name: rfgun

run number: 001

z-position: last saved distribution in the run

Thus valid calls are: '*postpro*', '*postpro name*', '*postpro name,run*', '*postpro.zpos*',

*'postpro name.zpos,run'* or *'postpro name.zpos.run'*. (Here name is the project name, zpos represents a four digit number for the z-position and run represents the run number. Preceding zeros can be omitted in the run number.) If no file with the specified z-position can be found, the next available file with a higher z-position will be opened. Finally it is possible to display any distribution with the extension *'ini'*, e.g. input files generated by *generator*.

When starting the code two windows, one for displaying and one for selecting from the menu will open, even if no data exists for the specified arguments. By clicking with the left mouse button onto the circles different phase space plots can be displayed. Note, that additional text information will be displayed in the window from which *postpro* was started or in a third window in the Windows version. Here also input might be requested.

Particle distributions are plotted either with symbols or in form of a color map, depending on the settings in the win\_config file and the number of particles, respectively. With standard setting only particles with status flags  $\geq -6$  are plotted, except for 'z-plot', which will show all particles (incl. lost particles) and plots in the sub menus 'Slice Emittance' and 'Phase Space Cuts' as well as 'core emittance' plots for which only particles with status flags  $>1$  are taken into account.

For the plots with symbols a color and symbol code is used referring to the particle status as shown in Table 6.

Particle status	Status flag	color & symbol
secondary particle	$> 5$	green circle
normal particle	2,3,5	black star
marked particle	4	red star
passive particle	0, 1	green plus sign
particle at the cathode	-1 to -6	brown cross
particle lost on aperture	-12 to -25	red dot
lost particle	-26 to -30	blue circle
lost particle	$\leq -30$	blue star

Table 6: Color and symbol code for *postpro* plots.

Plots having the time as one coordinate show the emission time if the particles are not yet started (status flags -1 to -6) or a time which is calculated from the relative longitudinal particle position and the average longitudinal velocity of the bunch (status flag  $> 0$ ). A warning is given in case of a mixed distribution.

Equivalently to the redirection of the emittance calculation in *Astra* (section 4.13.7) the emittance calculation and the display conditions can be redirected to different status flags in *postpro*. A file named 'Plot\_steering.par' has to be created. The file should contain the namelist 'Steering\_parameters', in which the logical array Stat(2,-100:100) can be redefined. With the first index set to 2 only plots in the sub menus 'Slice Emittance' and 'Phase Space Cuts' as well as the 'core emittance' plots will be affected, while with the first index set to 1 all other plots except 'z-plot' will be modified. The second index numbers of the Stat array correspond to the status flags as defined in Table 2. Particles with status flags to which the corresponding Stat array entry is true will be plotted.

In the case of particle distributions with user defined particles also the parameter ion\_mass needs to be specified in the namelist 'Steering parameters' in the same way as in NEWRUN (6.1) or the *generator* (7) input deck.

In the case of mixed particle distributions it is possible to plot particles in accordance to the particle index rather than to the status flag (only in combination with Plot\_mode = 1 (see chapter 5.4). For this purpose the arrays CP\_ind\_1 to CP\_ind\_15 can be defined in the namelist 'Steering\_parameters'. CP\_ind\_1 to CP\_ind\_4 correspond to particle indices 1 to 4 (electrons, positrons, protons and hydrogen ions) while CP\_ind\_5 to CP\_ind\_14 correspond to ion\_mass(1) to ion\_mass(10). Note that mass proportional results (energy and momenta) are normalized to the charge state! For each array three numbers (between 0 and 1) can be defined corresponding to the intensity of the RGB (red, green, blue) colors. E.g. with CP\_ind\_1 = 1.0, 0.0, 0.0, CP\_ind\_2 = 0.5, 0.5, 0.5 all electrons with valid particle status will be plotted in red, while all positrons with valid particle status will be plotted in grey. Particles will not be plotted if the color setting is black (0.0, 0.0, 0.0).

### 5.6.1 Menu 1 of 2

*1 Trans. phase space:* Displays the horizontal and vertical phase space and the projection onto the horizontal and vertical space axis.

*2 Long. phase space (z):* Displays the longitudinal phase space, the projection onto the longitudinal space axis and the momentum distribution.

*3 Long. phase space (time):* The same as plot 2 but with the time as coordinate instead of the z-position.

*4 Front, Top & Side view:* Displays a view of the bunch from different directions.

*5 Front, Top & Side view vs time:* The same as plot 4 but with the time as coordinate instead of the z-position.

*6 core emittance:* Displays the transverse and longitudinal rms emittance as function of the number of particles taken into account. See section 4.13.5.

*7 slice emittance:* Opens the sub menu 'Slice Emittance'. See section 5.6.3.

*8 transverse core brightness:* Displays the transverse brightness defined as  $\frac{Q}{\epsilon_x^n \epsilon_y^n}$  as function of a radial aperture cut.

*9 core bunch length:* Displays the rms bunch length vs. charge as function of an optimal cut in longitudinal direction.

*10 z-plot:* Displays the position of all particles along the beam line.

*11 phase space manipulations:* Opens the sub menu 'Phase Space Manipulations'. See section 5.6.4.

*13 fit, save & read:* See section 5.5.1.

*14 forward:* Moves to the next higher saved beam position. At the end of the beam line *postpro* circles back to the first saved distribution.

*15 backward:* Moves to the previous saved beam position up. At the beginning of the beam line *postpro* circles back to the last saved distribution.

*16 to file:* See section 5.5.1.

*17 next run:* See section 5.5.1.

*18 previous run:* See section 5.5.1

*19 Exit:* Exits *postpro*.

### 5.6.2 Menu 2 of 2

Menu 2 allows to select parameters for particle distribution plots. The first choice determines the parameter of the abscissa, the second choice determines the parameter of the ordinate. Projections onto both axes can be added by pushing the ‘*add projections*’ button. Subtracting a linear correlation from the plotted particle distribution often allows visualizing details more clearly. As in the previous menu it is possible to move forward and backward within the data of one run, go to the next or to the previous run etc.

In order to overlay particle distribution plots it is possible to save and read particle distribution plots in the sub menu ‘*fit, save & read*’. This option is only accessible if no projections are added. When the *Plot\_mode* = 2 (or 0 with high number of particles) is activated the color scheme of the overlaid distribution is reversed in order to increase the contrast. In *Plot\_mode* = 1 (or 0 with low number of particles) the overlaid distribution is plotted in black (see chapter 5.4).

### 5.6.3 Sub menu ‘Slice Emittance’

*1 slice emittance:* Displays the emittance of longitudinal slices of the bunch.

*2 mismatch parameter:* Displays an optical mismatch parameter defined as:  
$$\varsigma_i = \frac{1}{2}[\beta_0\gamma_i - 2\alpha_0\alpha_i + \gamma_0\beta_i] \geq 1$$
, where  $\alpha, \beta$  and  $\gamma$  are the Courant-Snyder parameters, **for electrons**, of the projected phase space (index  $o$ ) and of the individual slices (index  $i$ ), respectively. See Ref. [1].

*3 slice energy spread:* Displays the energy spread of longitudinal slices of the bunch.

*4 projected emittance:* Displays projected rms slice emittance ellipses.

*5 z-projection:* A line plot showing for example:  $\frac{px}{pz}_{rms}$ ;  $x_{rms}$  and  $\frac{px}{pz}_{avr}$ ;  $x_{avr}$ . versus the longitudinal position.

*6 3D ellipses:* A 3D plot of the rms slice emittance ellipses, which can be oriented with the two slide bars below.

*7 x-px; y-py; x-py; y-px:* Toggles between different phase space projections. Acts on plot 4 - 6.

*8 w.r.t. position:* If green the bunch is cut into slices with respect to the longitudinal position.

*9 w.r.t. energy:* If green the bunch is cut into slices with respect to the bunch energy.

*10 change number of slices:* Allows to change the number of slices for the slice emittance calculation. Note, that the slices are selected such, that they contain all the same number of particles. In case of equal charge per particle all slices have hence the same statistical weight and error. On the other hand have the slices in general a different length.

*11 subtract linear correlation:* Subtracts a linear correlation from the plotted phase space ellipses. Acts on plot 4 - 6.

*12 change cor. energy:* Allows to vary the correlated energy spread of the particle distribution.

*13 forward:* See section 5.6.1.

*14 backward:* See section 5.6.1.

*15 data to file:* Prints data of the slice emittance calculation into a text file.

*16 plot to file:* Generates a post script file of the present plot.

*17 next run:* See section 5.6.1.

*18 previous run:* See section 5.6.1.

*19 Exit sub menu:* Returns to main menu.

#### **5.6.4 Sub menu 'Phase Space Manipulations'**

In the sub menu 'phase space manipulations' the particle distribution can be rotated in space to transfer it to a rotated coordinate system and different cuts on the transverse and longitudinal particle distribution can be applied.

Two classes of cuts are offered. Optimized cuts request input of an interval parameter, for example the final bunch length, to which the distribution shall be cut. The cut is applied in a way that the number of surviving particles is maximal. The second class of cuts requires the positioning of cut levels with the mouse. Note, that some cuts involve an iterative procedure, since the particle distribution will be re-matched after a cut is applied. Hence, the plots may change their appearance during the cut procedure. A thin grey frame around the plot indicates, that input with the mouse is requested. The functions of the mouse buttons are as follows:

left button: select an arrow; if selected: position arrow.

right button: release arrow; if released: quit window.

Particles which have been cut are displayed in a different color first. They will disappear from the plots only after selecting the '*accept changes*' button. All cuts can be reversed by pushing the '*reject changes*' button.

A new particle distribution may be saved for further tracking before leaving the sub menu. An exemplary application of phase space cuts is found in Ref. [8].

### **References**

- [1] P. Emma, W. Spence 'Grid Scans: A transfer map diagnostic' PAC 1991.  
[http://accelconf.web.cern.ch/AccelConf/p91/PDF/PAC1991\\_1549.PDF](http://accelconf.web.cern.ch/AccelConf/p91/PDF/PAC1991_1549.PDF)
- [8] K. Floettmann 'Preparing the decision: Conventional versus undulator based positron source' EUROTeV-Report-2005-015.  
<http://www.eurotev.org/e158/e1365/e1378/e1997/EUROTeV-Report-2005-015.pdf>

## 5.7. The program *fieldplot*

With the program *fieldplot* the electric and magnetic fields of beam line elements as well as the space charge field of saved particle distributions can be displayed. *Fieldplot* refers to the *Astra* input file, i.e. only the project name has to be specified as input argument.

When starting the code two windows, one for displaying and one for selecting from the menu will open. By clicking with the left mouse button onto the circles different plots can be displayed. Note, that additional information will be displayed in the window from which *fieldplot* was started. Here also input might be requested.

### 5.7.1 Menu 1 of 3

*1 Cavity fields:* Displays the amplitude of the longitudinal electric field of all TM mode cavity fields in the beam line. By clicking onto 'next page' the transversal electric field amplitude, the azimuthal magnetic field amplitude and the field expansion radius<sup>1</sup> (for field tables only) can be displayed.

*2 TE mode fields:* Displays the amplitude of the longitudinal magnetic field of all TE mode fields in the beam line. By clicking onto 'next page' the transversal magnetic field amplitude, the azimuthal electric field amplitude and the field expansion radius<sup>1</sup> (for field tables only) can be displayed.

*3 Dipole mode fields:* Displays the amplitude of the transverse magnetic field of all dipole mode fields in the beam line. By clicking onto 'next page' the transversal electric field amplitude, the longitudinal electric and magnetic field amplitude and the effective deflecting voltage can be displayed. For the plot it is assumed that at most two cavities are in the beam line (index 1 and 2). The phase of the first cavity is set to a phase of maximum deflection; the field is plotted as seen by the particle. The phase of the second cavity is shifted by 90 degree to adopt for travelling wave cavities. Phases and integrated field strengths are displayed on the screen.

*4 Solenoid fields:* Displays the longitudinal magnetic field and the radial field gradient of all solenoids in the beam line in one plot. By clicking onto 'next page' both components can be displayed alone and the field expansion radius<sup>1</sup> is displayed.

*5 Quadrupole fields:* Displays the horizontal and vertical field gradient of all quadrupoles in the beam line. By clicking onto 'next page' the longitudinal magnetic field and a combined plot of all components can be displayed, respectively.

*6 Dipole fields: horizontal plane:* Displays field maps of all horizontal dipoles. By clicking onto 'next page' different components are plotted.

*7 Dipole fields: vertical plane:* Displays field maps of all vertical dipoles. By clicking onto 'next page' different components are plotted

*8 Curved cathode plot:* Displays the contour of a non-planar cathode and the position of charge rings used to correct the mirror charge field, see section 4.4.5.

---

<sup>1</sup> See Appendix (chapter 8).

9 *Cathode surface field*: Displays a field map of the cavity field on the cathode surface.

10 *Space charge fields*: Opens the sub menu ‘Space Charge Fields. See section 5.7.4.

11 *include geometry*: See section 5.5.1.

12 *fit, save & read*: See section 5.5.1.

13 *ZOOM*: See section 5.5.1.

14 *next page*: Switches between different field components to be displayed.

15 *to file*: See section 5.5.1.

16 *Exit*: Exits *fieldplot*.

### 5.7.2 Menu 2 of 3

1 – 6: Displays field maps of cavity fields defined by 3D maps along various cross sections. By clicking onto ‘next page’ different components are plotted.

13 *ZOOM*: Zoom option is mouse controlled: left button to select upper left and lower right corner, right button to release zoom.

14 – 16: See section 5.7.1.

### 5.7.3 Menu 3 of 3

1 – 6: Displays field maps of laser fields along various cross sections. In addition the rms beam envelope and the focus position are displayed. By clicking onto ‘next page’ different components are plotted.

8 *Plasma fields vs. z*: Various plots of the fields as seen by a particle moving with speed of light, the plasma density and other parameters vs.  $z$ . Use ‘next page’ to toggle.

9: *Plasma fields vs. zeta*: A plot of the fields versus the co-moving parameter  $\zeta$ .

11 – 12: See section 5.7.1.

13 *ZOOM*: Zoom option for laser fields is mouse controlled: left button to select upper left and lower right corner, right button to release zoom.

14 – 16: See section 5.7.1.

### 5.7.4 Sub Menu ‘Space Charge Fields’

Sub menu for the graphical presentation of the space charge fields as calculated by *Astra*. The development of any field component along one direction at different offsets in the orthogonal direction is shown. The green hatched area in the lower part

of the plot indicates the extension of the bunch; red broken lines show the grid cells. A blue solid line indicates the position of the cathode, if defined and if the mirror charge is not taken into account. If the mirror charge contribution is taken into account the area behind the cathode is covered by a blue rectangle.

Within the sub menu it is possible to change grid parameters, scale the energy of the particle distribution and switch between different solvers (2D - 3D). The menu changes accordingly; below only the menu for the 2D solver is explained.

When started, the field components of the start distribution as defined in the input deck will be shown. (Particle distributions to be emitted from a cathode have no longitudinal extension; hence no space charge field can be displayed.) Select '*change distribution*' to load any saved particle distribution with input arguments as used for *postpro* (chapter 5.6).

*1 Er*: Displays the radial electric field component of the space charge field.

*3 Ez*: Displays the longitudinal electric field component of the space charge field.

*5 Bfi*: Displays the azimuthal magnetic field component times the velocity of light of the space charge field.

*7 Er eff*: Displays  $Er - \beta c \cdot Bfi$ .

*8 change number of lines*: Allows to change the number of lines to be displayed (default = five). Each line represents the field component at a different offset in the orthogonal direction. The offsets are equally distributed between plus/minus two times the rms-width.

*9 radial*: Field components are shown as function of the radial position.

*10 longitudinal*: Field components are shown as function of the longitudinal position.

*11 change grid*: Allows to change the number of radial and longitudinal grid cells and of the cell variation. See section 4.4.1.

*12 merge cells*: Allows to merge grid cells. See section 4.4.2.

*13 suppress grid lines*: Suppresses the display of gridlines in the plot.

*14 scale energy*: Allows to scale the energy for a given distribution.

*15 mirror charge on/off*: Switches the contribution of the mirror charge to the space charge field on or off. In general it will be necessary to specify the position of the cathode plane.

*16 velocity profile*: Displays the residual velocity components  $\beta_z$ ,  $\beta_r$  and  $\beta_\phi$  in the average rest system of the bunch. The components are averaged over the volume of the grid cells. Select several times to display the different components.

*17 charge density*: Displays the charge density averaged over the volume of the grid cells.

*18 line charge density:* Displays the line charge density. Like the charge density this plot is based on the grid parameters.

*19 3D calculation FFT solver:* Switches to a 3D calculation of the space charge field using the FFT solver.

*20 change distribution:* Allows to change the particle distribution to be displayed.

*21 forward:* See section 5.6.1.

*22 backward:* See section 5.6.1.

*23 to file:* See section 5.5.1.

*24 next run:* See section 5.5.1.

*25 previous run:* See section 5.5.1.

*26 Exit sub menu:* Returns to main menu.

## 6. Input namelists for *Astra*

### 6.1. The namelist NEWRUN

The namelist NEWRUN contains basic instructions for the tracking.

Parameter	Specification	Unit	Default Value
<b>Head</b>	Character*150		
header line for protocol.			
<b>RUN</b>	Integer		1
the RUN number is used as extension for all output files (see Table 3). It is automatically incremented if a LOOP is specified.			
<b>LOOP</b>	Logical		FALSE
see chapter 4.9.			
<b>NLoop</b>	Integer		
see chapter 4.9.			
<b>Distribution</b>	Character*150		
name of the initial particle distribution, see chapters 2 and 3.			
<b>ion_mass( )</b>	Real*8 Array	eV/c <sup>2</sup>	0.0
the mass divided by the charge state of user defined particles. Negatively charged particles are defined by a negative value of the ion_mass parameter. Particle index 5 – 14 in the input distribution file refer to ion_mass(1) – (10). See also the corresponding <i>generator</i> definitions (7). Mass proportional results (energy and momenta) are normalized to the charge state!			
<b>N_red</b>	Integer		1
if > 1 only every N_red <sup>th</sup> particle of the distribution is used. The charge of the particles is scaled accordingly.			
<b>Xoff</b>	Real*8	mm	0.0
horizontal offset of the input distribution. Active if Xoff ≠ 0.0.			
<b>Yoff</b>	Real*8	mm	0.0
vertical offset of the input distribution. Active if Yoff ≠ 0.0.			
<b>xp</b>	Real*8	rad	0.0
horizontal trajectory angle, additive to input distribution.			
<b>yp</b>	Real*8	rad	0.0
vertical trajectory angle, additive to input distribution.			
<b>Zoff</b>	Real*8	m	0.0
longitudinal offset of the input distribution. Active if Zoff ≠ 0.0.			
<b>Toff</b>	Real*8	ns	0.0
timing offset of the input distribution. Active if Toff ≠ 0.0.			
<b>Xrms</b>	Real*8	mm	-1.0
horizontal rms beam size. Scaling is active if Xrms > 0.0.			

<b><i>Yrms</i></b>	Real*8	mm	-1.0
vertical rms beam size. Scaling is active if Yrms > 0.0.			
<b><i>XYrms</i></b>	Real*8	mm	-1.0
horizontal and vertical rms beam size. The parameter XYrms has priority over the parameters Xrms and Yrms.			
<b><i>Zrms</i></b>	Real*8	mm	-1.0
rms bunch length. Scaling is active if Zrms > 0.0.			
<b><i>Trms</i></b>	Real*8	ns	-1.0
emission time of the bunch. Scaling is active if Trms > 0.0.			
<b><i>Tau</i></b>	Real*8	ns	0.0
exponential delay time of the emission. Active if Tau ≠ 0.0. Note that the delay time is random and might interfere with the quasi random nature of an input distribution.			
<b><i>cor_px</i></b>	Real*8	mrad	0.0
correlated divergence of the bunch. Scaling is active if cor_px ≠ 0.0.			
<b><i>cor_py</i></b>	Real*8	mrad	0.0
correlated divergence of the bunch. Scaling is active if cor_py ≠ 0.0.			
<b><i>Qbunch</i></b>	Real*8	nC	0.0
bunch charge. Scaling is active if Qbunch ≠ 0.0.			
<b><i>SRT_Q_Schottky</i></b>	Real*8	nC·(m/MV) <sup>1/2</sup>	0.0
variation of the bunch charge with the square root of the field on the cathode. Scaling is active if SRT_Q_Schottky ≠ 0.0.			
<b><i>Q_Schottky</i></b>	Real*8	nC·m/MV	0.0
linear variation of the bunch charge with the field on the cathode. Scaling is active if Q_Schottky ≠ 0.0.			
<b><i>debunch</i></b>	Real*8		0.0
'debunched' particles, i.e. particles with a distance to the bunch center exceeding debunch·σ <sub>z</sub> are passivated, i.e. their status will be set to 0 or 1. Debunch is defined relative to the rms bunch length, hence it should not be used close to the cathode where σ <sub>z</sub> can be zero. The procedure is active when debunch is ≠ 0.0			
<b><i>Track_All</i></b>	Logical		TRUE
if false, only the reference particle will be tracked. The ref file contains the off-axis results in this case.			
<b><i>Track_On_Axis</i></b>	Logical		FALSE
if true, the reference particle will be tracked only on axis. The ref file contains the on-axis results in this case.			
<b><i>Auto_Phase</i></b>	Logical		TRUE
if true, the RF phases will be set relative to the phase with maximum energy gain.			

<b>Phase_Scan</b>	Logical		FALSE
if true, the RF phases of the cavities will be scanned between 0 and 360 degree. Results are saved in the PScan file. The tracking between cavities will be done with the user-defined phases.			
<b>check_ref_part</b>	Logical		TRUE
if true, the run will be interrupted if the reference particle is lost during the on- and off-axis reference particle tracking.			
<b>L_rm_back</b>	Logical		FALSE
if true, particles are immediately discarded when they start to travel backwards. If false, backward traveling particles are only discarded when they pass the lower boundary Z_min. Note, that in some cases (phases) the particles can change the direction of motion several times, before hitting a boundary.			
<b>Z_min</b>	Real*8	m	
lower boundary for discarding particles. If Z_min is not specified by the user it is automatically set by the program assuming that particles are supposed to travel in positive Z-direction.			
<b>Z_Cathode</b>	Real*8	m	
position of the cathode for the calculation of the mirror charge. If Z_Cathode is not specified by the user it is automatically set by the program to the minimal particle position provided the bunch is emitted from a cathode.			
<b>H_max</b>	Real*8	ns	0.001
maximum time step for the Runge-Kutta integration.			
<b>H_min</b>	Real*8	ns	0.0
minimum time step for the Runge-Kutta integration and min. time step for the space charge calculation. During the emission process from a cathode the time step is forced to H_min. If zero H_min is set automatically based on the parameter N_min (namelist CHARGE) in accordance to Eq. (4.1).			
<b>Max_step</b>	Integer		100 000
safety termination: after Max_step Runge_Kutta steps the run is terminated.			
<b>Lmonitor</b>	Logical		FALSE
if true, the particle number and average position will be reported on every time step. For diagnostics only, slows down the calculation.			
<b>Lprompt</b>	Logical		TRUE
only for Windows PC version. If true a pause statement is included at the end of the run to avoid vanishing of the window in case of an error.			

## 6.2. The namelist OUTPUT

In the namelist OUTPUT specifications for the generation of output are defined.

Parameter	Specification	Unit	Default Value
<b>ZSTART</b>	Real*8	m	0.0
minimal z position for the generation of output, tracking may start at $z \neq$ ZSTART according to the definition of the initial particle distribution.			
<b>ZSTOP</b>	Real*8	m	0.3
tracking will stop when the bunch center passes ZSTOP.			
<b>Zemit</b>	Integer		100
the interval ZSTOP-ZSTART is divided into Zemit subintervals. At the end of each subinterval output of line-typ is generated.			
<b>Zphase</b>	Integer		1
the interval ZSTOP-ZSTART is divided into Zphase subintervals. At the end of each subinterval a complete particle distribution is saved. It is recommended to set $Zemit = n \cdot Zphase$ , $n \in \mathbb{N}$ .			
<b>Screen( )</b>	Real*8 array	m	
additional position for the generation of output.			
<b>Scr_xrot( )</b>	Real*8 array	rad	0.0
rotation angle of the screen in the x-z plane. Active if $Scr\_xrot( ) \neq 0.0$ and only in combination with Local_emit. The angles are measured relative to the z-axis, i. e. the standard position corresponds to $Scr\_xrot( ) = \pi/2$ .			
<b>Scr_yrot( )</b>	Real*8 array	rad	0.0
rotation angle of the screen in the y-z plane. Active if $Scr\_yrot( ) \neq 0.0$ and only in combination with Local_emit. The angles are measured relative to the z-axis, i. e. the standard position corresponds to $Scr\_yrot( ) = \pi/2$ .			
<b>Step_width</b>	Integer		0
output generation based on time steps rather than on positions. Output is generated every $Step\_width \cdot$ time step.			
<b>Step_max</b>	Integer		0
terminates output based on Step_width. Run may continue if $Max\_step >$ Step_max.			
<b>Lproject_emit</b>	Logical		FALSE
if true, the transverse particle positions of all particles will be projected into a common plane at the longitudinal bunch center position prior to the calculation of the emittance, spot size etc. See section 4.13.3.			
<b>Local_emit</b>	Logical		FALSE
if true, the transverse particle positions of all particles will be recorded when passing the output position plane prior to the calculation of the emittance, spot size etc. The longitudinal particle coordinates in output files are recalculated based on times and velocities and are only approximate. Hence distributions saved with this option should not be used as input distributions for further tracking! The distance between subsequent output positions has to be larger than the bunch length, or they will be skipped. See section 4.13.3.			

<b>Lmagnetized</b>	Logical		FALSE
if true, solenoid fields are neglected in the calculation of the beam emittance. See section 4.13.1.			
<b>Lsub_rot</b>	Logical		FALSE
if true Lmagnetized will be set true and the angular momentum of the bunch is subtracted for the emittance calculation based on the actual x-py and y-px correlation of the bunch rather than by the canonical momentum. See section 4.13.1.			
<b>Lsub_Larmor</b>	Logical		FALSE
if true a rotation of the transverse coordinate system induced by a solenoid will be taken into account. See section 4.13.2.			
<b>Lsub_coup</b>	Logical		FALSE
if true a rotation angle of the transverse beam spot will be corrected before the emittance is calculated. See section 4.13.2.			
<b>Rot_ang</b>	Real*8	rad	0.0
rotation angle for emittance calculation in connection with Lsub_coup. If no rotation angle is specified an optimized rotation angle will be taken. See section 4.13.2.			
<b>Lsub_cor</b>	Logical		FALSE
if true the reduced emittance is calculated in addition to the standard emittance. See section 4.13.6.			
<b>RefS</b>	Logical		FALSE
if true, output files according to Table 3 and Table 4 are generated.			
<b>EmitS</b>	Logical		FALSE
if true, output files according to Table 3 and Table 4 are generated. See section 4.13.			
<b>C_EmitS</b>	Logical		FALSE
if true, output files according to Table 3 and Table 4 are generated. See section 4.13.5.			
<b>C99_EmitS</b>	Logical		FALSE
if true, output files according to Table 3 and Table 4 are generated. See section 4.13.5.			
<b>Tr_EmitS</b>	Logical		FALSE
if true, output files according to Table 3 and Table 4 are generated. See section 4.13.4.			
<b>Sub_EmitS</b>	Logical		FALSE
if true, output files according to Table 3 and Table 4 are generated. See section 4.13.8.			
<b>Cross_start</b>	Real		0.0
start point for detecting cross over particles (Sub_EmitS = False). See section 4.13.7.			

<b>Cross_end</b>	Real		0.0
end point for detecting cross over particles (Sub_EmitS = False). See section 4.13.7.			
<b>PhaseS</b>	Logical		FALSE
if true, output files according to Table 3 and Table 4 are generated.			
<b>T_PhaseS</b>	Logical		FALSE
if true, output files according to Table 3 and Table 4 are generated.			
<b>High_res</b>	Logical		FALSE
if true, particle distributions are saved with increased accuracy. See Table 4.			
<b>Binary</b>	Logical		FALSE
if true, the particle distributions is saved in binary format.			
<b>TrackS</b>	Logical		FALSE
if true, output files according to Table 3 and Table 4 are generated.			
<b>TcheckS</b>	Logical		FALSE
if true, output files according to Table 3 and Table 4 are generated.			
<b>SigmaS</b>	Logical		FALSE
if true, output files according to Table 3 and Table 4 are generated.			
<b>CathodeS</b>	Logical		FALSE
if true, output files according to Table 3 and Table 4 are generated.			
<b>LandFS</b>	Logical		FALSE
if true, output files according to Table 3 and Table 4 are generated.			
<b>LarmorS</b>	Logical		FALSE
if true, output files according to Table 3 and Table 4 are generated.			

### 6.3. The namelist SCAN

In the namelist SCAN parameters for the scanning procedure are specified. See chapter 4.9.

Parameter	Specification	Unit	Default Value
<b>LOOP</b>	Logical		FALSE
	see chapter 4.9.		
<b>LScan</b>	Logical		FALSE
	if true a scan will be performed.		
<b>LExtend</b>	Logical		FALSE
	if true an already existing scan output file will be extended rather than overwritten.		
<b>Scan_para</b>	Character*40		
	parameter to be scanned. Valid are all parameters that are written in italic letters in the namelist tables of chapter 6.		
<b>S_min</b>	Real*8		
	minimal set point of the scanning parameter.		
<b>S_max</b>	Real*8		
	maximal set point of the scanning parameter.		
<b>S_numb</b>	Integer		
	number of scanning points.		
<b>O_min</b>	Logical		FALSE
	if true the minimum of the parameter FOM(1) is searched with decreasing interval size around the minimum.		
<b>O_max</b>	Logical		FALSE
	if true the maximum of the parameter FOM(1) is searched with decreasing interval size around the maximum.		
<b>O_match</b>	Logical		FALSE
	if true the match of the parameter FOM(1) to the match_value is searched with decreasing interval size around the optimum.		
<b>match_value</b>	Real*8		
	value to which FOM(1) has to be matched if O_match = true.		
<b>O_depth</b>	Integer		
	optimization depth if one of O_min, O_max or O_match is true. The total number of runs is about S_numb · O_depth.		

<b>L_min</b>	Logical		FALSE
	if true, the minimum value of FOM(1) in the interval S_zmin to S_zmax will be saved. The value of FOM(2)-FOM(10) will be saved at the position of the minimum of FOM(1). The position of the optimum will also be saved.		
<b>L_max</b>	Logical		FALSE
	if true, the maximum value of FOM(1) in the interval S_zmin to S_zmax will be saved. The value of FOM(2)-FOM(10) will be saved at the position of the maximum of FOM(1). The position of the optimum will also be saved.		
<b>S_zmin</b>	Real*8	m	
	minimum position for the search of an optimum of FOM(1)		
<b>S_zmax</b>	Real*8	m	
	maximum position for the search of an optimum of FOM(1)		
<b>S_dz</b>	Integer		
	the interval S_zmin to S_zmax is divided into S_dz equal intervals. At the end of each interval emittances etc. are calculated.		
<b>FOM( )</b>	Character*40 array		
	<p>specifies the output to be found in the scan file. Valid keywords are:</p> <p>bunch <b>charge</b></p> <p><b>horizontal rms emittance</b></p> <p><b>horizontal trace-space emittance</b></p> <p><b>horizontal reduced emittance z</b></p> <p><b>horizontal reduced emittance z&amp;E</b></p> <p><b>horizontal sub-ensemble emittance</b></p> <p><b>horizontal coherence length</b></p> <p><b>horizontal rms spot size</b></p> <p><b>horizontal sub-ensemble spot size</b></p> <p><b>horizontal rms beam divergence</b></p> <p><b>horizontal correlated beam divergence</b></p> <p>mean <b>horizontal beam offset</b></p> <p><b>horizontal beam offset</b> *</p> <p>mean <b>horizontal trajectory angle</b></p> <p><b>horizontal trajectory angle</b> *</p> <p><b>vertical rms emittance</b></p> <p><b>vertical trace-space emittance</b></p> <p><b>vertical reduced emittance z</b></p> <p><b>vertical reduced emittance z&amp;E</b></p> <p><b>vertical sub-ensemble emittance</b></p> <p><b>vertical coherence length</b></p> <p><b>vertical rms spot size</b></p> <p><b>vertical sub-ensemble spot size</b></p> <p><b>vertical rms beam divergence</b></p> <p><b>vertical correlated beam divergence</b></p> <p>mean <b>vertical beam offset</b></p> <p><b>vertical beam offset</b> *</p> <p>mean <b>vertical trajectory angle</b></p> <p><b>vertical trajectory angle</b> *</p> <p><b>emittance ratio</b> <math>\frac{\epsilon_y}{\epsilon_x}</math></p> <p><b>longitudinal rms emittance</b></p> <p><b>longitudinal reduced emittance minus 2nd order correlation</b></p> <p><b>longitudinal reduced emittance minus 3rd order correlation</b></p> <p>rms bunch <b>length</b></p> <p><b>mean beam energy</b></p>		

<p><b>energy</b> *</p> <p>mean beam <b>momentum</b></p> <p><b>momentum</b> *</p> <p><b>rms beam energy</b> spread</p> <p><b>correlated energy</b> spread</p> <p>horizontal core emittance 95% <b>Cx_95</b></p> <p>horizontal core emittance 90% <b>Cx_90</b></p> <p>horizontal core emittance 80% <b>Cx_80</b></p> <p>vertical core emittance 95% <b>Cy_95</b></p> <p>vertical core emittance 90% <b>Cy_90</b></p> <p>vertical core emittance 80% <b>Cy_80</b></p> <p>longitudinal core emittance 95% <b>Cz_95</b></p> <p>longitudinal core emittance 90% <b>Cz_90</b></p> <p>longitudinal core emittance 80% <b>Cz_80</b></p> <p>particle density in a sphere <b>P_dens 1</b> to <b>P_dens 5</b></p> <p>phase of cavity #1 at end of run <b>phi end</b> *</p> <p>time of flight <b>TOF</b> *</p> <p>mean time of flight <b>TOF</b></p> <p>total time <b>TOT</b> (= TOF+Toff) *</p> <p>mean total time <b>TOT</b> (= TOF+Toff)</p> <p>absolute time <b>TABS</b> (= TOF+Toff+Ref_clock) *</p> <p>mean absolute time <b>TABS</b> (= TOF+Toff+Ref_clock)</p> <p>mean <b>Larmor</b> angle</p> <p><b>Larmor</b> angle *</p> <p><b>rms Larmor</b> angle</p> <p><b>statistics: total</b> number of <b>electrons</b></p> <p><b>statistics:</b> number of <b>active</b> particles</p> <p><b>statistics:</b> number of active <b>secondary</b> electrons</p> <p><b>statistics:</b> number of <b>backward</b> traveling particles</p> <p><b>statistics:</b> number of <b>lost</b> particles on an aperture</p> <p><b>statistics:</b> number of lost particles <math>z &lt; Zmin</math></p>
---

\* output from single particle tracking (Track\_All = FALSE.)

## 6.4. The namelist MODULES

In the namelist MODULES allows to combine elements from other namelists to modules. See chapter 4.10 for an introduction.

Parameter	Specification	Unit	Default Value
<b>Loop</b>	Logical		FALSE
	see chapter 4.9.		
<b>LModule</b>	Logical		FALSE
	if false all module definitions will be ignored.		
<b>Module( , )</b>	Character*40 array		
	specifies the elements of a module.		
<b>Mod_Xoff( )</b>	Real*8 array	m	0.0
	transverse offset of a module in x.		
<b>Mod_Yoff( )</b>	Real*8 array	m	0.0
	transverse offset of a module in y.		
<b>Mod_Zoff( )</b>	Real*8 array	m	0.0
	longitudinal offset of a module.		
<b>Mod_Xrot( )</b>	Real*8 array	rad	0.0
	rotation of a module in the x-z plane, i.e. around the y-axis.		
<b>Mod_Yrot( )</b>	Real*8 array	rad	0.0
	rotation of a module in the y-z plane, i.e. around the x-axis.		
<b>Mod_Zrot( )</b>	Real*8 array	rad	0.0
	rotation of a module in the x-y plane, i.e. around the z-axis.		
<b>Mod_Zpos( )</b>	Real*8 array	m	0.0
	longitudinal position of a module. Rotations are defined with respect to this position. Note, that Mod_zpos is not affected by a shift introduced with the parameter Mod_zoff		
<b>Mod_Efield( )</b>	Real*8 array		1.0
	scaling strength for electric field of a module.		
<b>Mod_phase( )</b>	Real*8 array	degree	0.0
	phase offset of the RF fields of a module.		
<b>Mod_Bfield( )</b>	Real*8 array		1.0
	scaling strength for magnetic fields of a module.		

## 6.5. The namelist ERROR

The namelist ERROR allows adding randomly generated errors to element and bunch parameters. Errors are Gaussian distributed; the input parameter corresponds to the rms width of the distribution. A cut-off can be specified which is applied to all errors. For statistical calculations the Loop function should be used. Other than the rest of the namelists the ERROR namelist has to be specified only once in combination with the Loop option. Output parameters can be specified with the parameter FOM(1) to FOM(10) equivalently to the namelist SCAN (see chapters 4.9 and 6.3). Output other than the error file is suppressed by default when LError is set true. Auto\_phase counteracts phase errors (except for module phase errors) and should hence not be used in case of error calculations!

Parameter	Specification	Unit	Default Value
<b>Loop</b>	Logical		FALSE
see chapter 4.9.			
<b>LError</b>	Logical		FALSE
if false, no errors will be generated.			
<b>ErrorS</b>	Logical		FALSE
if true an output file will be generated. See chapter 4.12.			
<b>Log_Error</b>	Logical		FALSE
if true an additional log file will be generated which contains the actual element and bunch settings, i.e. including the variation due to the errors for each run. Note that module errors are added to the module setting and not to the individual parameter settings. See chapter 4.12.			
<b>LExtend</b>	Logical		FALSE
if true an already existing error output file will be extended rather than overwritten.			
<b>Suppress_output</b>	Logical		TRUE
if true any generation of output other than the error file is suppressed.			
<b>FOM()</b>	Character*40 array		
specifies the output to be found in the error file. Valid keywords are listed in the description of the namelist SCAN in chapter 6.3.			
<b>Err_cutoff</b>	Real*8		3.0
cut off for Gaussian distributed errors in units of sigma. Applies to all errors.			
<b>Err_Qbunch</b>	Real*8	nC	0.0
error of the bunch charge.			
<b>Err_Xoff</b>	Real*8	mm	0.0
error of the initial bunch position in x.			
<b>Err_Yoff</b>	Real*8	mm	0.0
error of the initial bunch position in y.			

<b>Err_Toff</b>	Real*8	ns	0.0
error of the initial bunch timing.			
<b>Err_Xrms</b>	Real*8	mm	0.0
error of the initial bunch size in x.			
<b>Err_Yrms</b>	Real*8	mm	0.0
error of the initial bunch size in y.			
<b>Err_XYrms</b>	Real*8	mm	0.0
error of the initial bunch size in x and y. The parameter Err_XYrms has priority over the parameters Err_Xrms and Err_Yrms.			
<b>Err_Zrms</b>	Real*8	mm	0.0
error of the initial bunch length.			
<b>Err_Trms</b>	Real*8	ns	0.0
error of the bunch emission time.			
<b>Err_A_xoff()</b>	Real*8 array	m	0.0
error of the aperture offset in x.			
<b>Err_A_yoff()</b>	Real*8 array	m	0.0
error of the aperture offset in y.			
<b>Err_A_xrot()</b>	Real*8 array	rad	0.0
error of the aperture rotation around the y-axis.			
<b>Err_A_yrot()</b>	Real*8 array	rad	0.0
error of the aperture rotation around the x-axis.			
<b>Err_A_zrot()</b>	Real*8 array	rad	0.0
error of the aperture rotation around the z-axis.			
<b>Err_C_xoff()</b>	Real*8 array	m	0.0
error of the cavity offset in x.			
<b>Err_C_yoff()</b>	Real*8 array	m	0.0
error of the cavity offset in y.			
<b>Err_C_xrot()</b>	Real*8 array	rad	0.0
error of the cavity rotation around the y-axis.			
<b>Err_C_yrot()</b>	Real*8 array	rad	0.0
error of the cavity rotation around the x-axis.			
<b>Err_C_zrot()</b>	Real*8 array	rad	0.0
error of the cavity rotation around the z-axis.			
<b>Err_phi()</b>	Real*8 array	degree	0.0
error of the cavity phase.			
<b>Err_MaxE()</b>	Real*8 array	MV/m	0.0
error of the cavity gradient.			

<b>Err_S_xoff()</b>	Real*8 array	m	0.0
error of the solenoid offset in x.			
<b>Err_S_yoff()</b>	Real*8 array	m	0.0
error of the solenoid offset in y.			
<b>Err_S_xrot()</b>	Real*8 array	rad	0.0
error of the solenoid rotation around the y-axis.			
<b>Err_S_yrot()</b>	Real*8 array	rad	0.0
error of the solenoid rotation around the x-axis.			
<b>Err_MaxB()</b>	Real*8 array	T	0.0
error of the solenoid strength.			
<b>Err_Q_xoff()</b>	Real*8 array	m	0.0
error of the quadrupole offset in x.			
<b>Err_Q_yoff()</b>	Real*8 array	m	0.0
error of the quadrupole offset in y.			
<b>Err_Q_xrot()</b>	Real*8 array	rad	0.0
error of the quadrupole rotation around the y-axis.			
<b>Err_Q_yrot()</b>	Real*8 array	rad	0.0
error of the quadrupole rotation around the x-axis.			
<b>Err_Q_zrot()</b>	Real*8 array	rad	0.0
error of the of the quadrupole rotation around the z-axis.			
<b>Err_Q_Grad()</b>	Real*8 array	T/m	0.0
error of the quadrupole gradient.			
<b>Err_Q_K()</b>	Real*8 array	m <sup>-2</sup>	0.0
error of the quadrupole strength.			
<b>Err_D_xoff()</b>	Real*8 array	m	0.0
error of the dipole offset in x.			
<b>Err_D_yoff()</b>	Real*8 array	m	0.0
error of the dipole offset in y.			
<b>Err_D_zoff()</b>	Real*8 array	m	0.0
error of the dipole offset in z.			
<b>Err_D_xrot()</b>	Real*8 array	rad	0.0
error of the dipole rotation around the y-axis.			
<b>Err_D_yrot()</b>	Real*8 array	rad	0.0
error of the dipole rotation around the x-axis.			

<b>Err_D_zrot()</b>	Real*8 array	rad	0.0
error of the dipole rotation around the z-axis.			
<b>Err_D_Strength()</b>	Real*8 array	T	0.0
error of the dipole strength.			
<b>Err_D_Radius()</b>	Real*8 array	m	0.0
error of the dipole bending radius.			
<b>Err_Mod_xoff()</b>	Real*8 array	m	0.0
error of the module offset in x.			
<b>Err_Mod_yoff()</b>	Real*8 array	m	0.0
error of the module offset in y.			
<b>Err_Mod_xrot()</b>	Real*8 array	rad	0.0
error of the module rotation around the y-axis.			
<b>Err_Mod_yrot()</b>	Real*8 array	rad	0.0
error of the module rotation around the x-axis.			
<b>Err_Mod_zrot()</b>	Real*8 array	rad	0.0
error of the module rotation around the z-axis.			
<b>Err_Mod_Efield</b>	Real*8 array		0.0
relative error of the electric field strength of a module.			
<b>Err_Mod_phase</b>	Real*8 array	degree	0.0
error of the RF phase of a module.			
<b>Err_Mod_Bfield</b>	Real*8 array		0.0
relative error of the magnetic field strength of a module.			

## 6.6. The namelist CHARGE

In the namelist CHARGE parameters for the space charge calculation are specified. See chapter 4.3.

Parameter	Specification	Unit	Default Value
<b>LOOP</b>	Logical		FALSE
	see chapter 4.9.		
<b>LSPCH</b>	Logical		FALSE
	if false, space charge fields are not taken into account.		
<b>LSPCH3D</b>	Logical		FALSE
	if true space 3D charge fields are calculated with an FFT algorithm, if false the standard calculation on a cylindrical grid is used, see chapter 4.5.		
<b>L2D_3D</b>	Logical		FALSE
	if true a transition of 2D to 3D space charge calculation is made at position $z_{trans}$ . See chapter 4.6.		
<b>Lmirror</b>	Logical		TRUE
	if true, mirror charges at the cathode are taken into account. Only for cylindrical grid algorithm, see section 4.4.4.		
<b>L_Curved_Cathode</b>	Logical		FALSE
	if true, the mirror charge will be corrected for a non-planar cathode. Only for cylindrical grid algorithm, see section 4.4.5.		
<b>Cathode_Contour</b>	Character*150 array		
	file name of the table describing the cathode contour.		
<b>R_zero</b>	Real*8		0.0
	on-axis curvature of a curved cathode.		
<b>Nrad</b>	Integer		10
	number of grid cells in radial direction up to the bunch radius. Only for cylindrical grid algorithm.		
<b>Cell_var</b>	Real*8		2.0
	variation of the cell height in radial direction. The innermost cell is cell_var times higher than the outermost cell. Only for cylindrical grid algorithm.		
<b>Nlong_in</b>	Integer		10
	maximum number of grid cells in longitudinal direction within the bunch length. During the emission process the number is reduced, according to the specification of the minimum cell length min_grid. Only for cylindrical grid algorithm.		
<b>N_min</b>	Real*8		30
	average number of particles to be emitted in one step during the emission from a cathode. N_min is needed to set H_min automatically during emission. Only for cylindrical grid algorithm.		

<b>min_grid</b>	Real*8	m	0.0
	minimum grid length during emission. If the bunch is too short the number of cells is reduced accordingly. If min_grid is zero it is set automatically according to Eq. (4.2) based on the parameter H_min. Only for cylindrical grid algorithm.		
<b>Merge_1 ... Merge_10</b>	Integer array		
	parameter to merge longitudinal cells. Only for cylindrical grid algorithm, see section 4.4.2		
<b>z_trans</b>	Real		
	longitudinal position for automatic transition of 2D to 3D space charge calculation. See chapter 4.6.		
<b>min_grid_trans</b>	Real		
	minimal longitudinal length of 2D grid cells during automatic transition of 2D to 3D space charge calculation. See chapter 4.6.		
<b>Nxf</b>	Integer		8
	number of grid cells in x-direction. Only for 3D algorithms. $N_{xf} \geq 4$		
<b>Nx0</b>	Integer		2
	number of empty boundary grid cells in x-direction on each side of the bunch. $1 \leq N_{x0} \leq \frac{N_{xf} - 2}{2}$ . Only for 3D algorithms.		
<b>Nyf</b>	Integer		8
	number of grid cells in y-direction. Only for 3D algorithms. $N_{yf} \geq 4$		
<b>Ny0</b>	Integer		2
	number of empty boundary grid cells in y-direction on each side of the bunch. $1 \leq N_{y0} \leq \frac{N_{yf} - 2}{2}$ . Only for 3D algorithms.		
<b>Nzf</b>	Integer		8
	number of grid cells in z-direction. Only for 3D algorithm. $N_{zf} \geq 4$		
<b>Nz0</b>	Integer		2
	number of empty boundary grid cells in y-direction on each side of the bunch. $1 \leq N_{z0} \leq \frac{N_{zf} - 2}{2}$ . Only for 3D algorithms.		
<b>Smooth_x</b>	Integer		0
	smoothing parameter for x-direction. Only for 3D FFT algorithm.		

<b>Smooth_y</b>	Integer		0
smoothing parameter for y-direction. Only for 3D FFT algorithm.			
<b>Smooth_z</b>	Integer		0
smoothing parameter for z-direction. Only for 3D FFT algorithm.			
<b>Max_scale</b>	Real*8		0.05
if one of the space charge scaling factors exceeds the limit $1 \pm \text{max\_scale}$ a new space charge calculation is initiated.			
<b>Max_count</b>	Integer		40
if the space charge field has been scaled max_count times a new space charge calculation is initiated.			
<b>Exp_control</b>	Real*8		0.1
specifies the maximum tolerable variation of the bunch extensions relative to the grid cell size within one time step (see section 4.4.6).			

## 6.7. The namelist APERTURE

The namelist APERTURE allows to include apertures and to define material properties for secondary electron emission. Circular apertures can be defined either by a table containing the z-position (column1 in m) and the corresponding aperture radius (column 2 in mm) in a free format or internally for the case of a simple collimating hole, a circular grid, or a cylindrical plug. Planar apertures can be defined internally only.

Parameter	Specification	Unit	Default Value
<b>LOOP</b>	Logical		FALSE
see chapter 4.9.			
<b>LApert</b>	Logical		FALSE
if true apertures will be included.			
<b>File_Aperture( )</b>	Character*150 array		
user specified file name of an aperture table or keyword. Allowed keywords are: <b>RAD</b> for a simple circular aperture, i.e. a hole or a cylindrical plug. <b>Cir</b> for a circular grid. Secondary emission does not work for a circular grid. <b>Scr_X</b> and <b>Scr_Y</b> for a single sided planar scraper in x or y, respectively. <b>Col_X</b> and <b>Col_Y</b> for a double sided planar collimator in x or y, respectively.			
<b>Ap_Z1( )</b>	Real*8 array	m	
longitudinal start position of an aperture. Only in combination with keyword input.			
<b>Ap_Z2( )</b>	Real*8 array	m	
longitudinal end position of an aperture. Only in combination with keyword input.			
<b>Ap_R( )</b>	Real*8 array	mm	
keyword <b>RAD</b> : Radius of the aperture. If Ap_R( ) is negative a cylindrical plug rather than a hole is generated. keywords <b>Scr_X</b> and <b>Scr_Y</b> : Distance of the scraper to the z-axis. If Ap_R( ) is positive particles with positions larger than Ap_R( ) are scrapped off. If Ap_R( ) is negative particles with position smaller than Ap_R( ) are scrapped off. keywords <b>Col_X</b> and <b>Col_Y</b> : Half gap of a double sided planar collimator.			
<b>Ap_GR( , )</b>	Real*8 array	mm	
radii of grid elements in combination with keyword <b>Cir</b> . The first index is the element number, the second a radius. Odd indices define the lower radius and even indices define the upper radius of a grid element. The maximum number of grid elements is 20.			
<b>A_pos( )</b>	Real*8 array	m	0.0
shifts the longitudinal aperture position. A_pos is added to the position defined in File_Aperture( ) or to Ap_Z1( ) and Ap_Z2( ), respectively.			
<b>A_xoff( )</b>	Real*8 array	m	0.0
horizontal offset of the aperture.			

<b>A_yoff()</b>	Real*8 array	m	0.0
vertical offset of the aperture.			
<b>A_xrot()</b>	Real*8 array	rad	0.0
rotation angle of the aperture in the x-z plane, i.e. around the y-axis.			
<b>A_yrot()</b>	Real*8 array	rad	0.0
rotation angle of the aperture in the y-z plane, i.e. around the x-axis.			
<b>A_zrot()</b>	Real*8 array	rad	0.0
rotation angle of the aperture in the x-y plane, i.e. around the z-axis.			
<b>SE_d0()</b>	Real*8 array		0.0
maximum secondary electron emission yield.			
<b>SE_Epm()</b>	Real*8 array	keV	10.0
kinetic electron impact energy which yields the maximum secondary electron yield.			
<b>SE_fs()</b>	Real*8 array		0.0
parameter describing the functional dependence of the secondary electron yield on the kinetic impact energy.			
<b>SE_Tau()</b>	Real*8 array	ns	0.0
exponential delay time of the emission. Active if Tau $\neq$ 0.0.			
<b>SE_Esc()</b>	Real*8 array	eV	0.0
mean kinetic energy of the secondary electrons. If the sum of the kinetic energies of all secondaries produced in one event exceeds the kinetic energy of the primary electron the kinetic energy of the secondaries is reduced accordingly.			
<b>SE_ff1()</b>	Real*8 array		0.0
factor for field enhanced secondary emission. See section 4.11.1			
<b>SE_ff2()</b>	Real*8 array	eV/m	0.0
factor for field enhanced secondary emission. See section 4.11.1			
<b>Max_Secondary</b>	Integer		500,000
maximum number of particles (primaries + secondaries) that can be held on the stack during a run. The program is aborted if the particle number exceeds Max_Secondary.			
<b>LClean_Stack</b>	Logical		.FALSE.
Option to reduce the required memory space in combination with secondary emission. If true lost particles will be taken from the stack, i.e. they don't appear anymore in saved particle distributions and in the particle statistics. The particle coordinates of lost particles are printed to a file named 'project.Lost_Part.run' before they are taken from the stack. The file structure of the Lost_Part file is equivalent to a standard particle distribution file, but all coordinates are in absolute values and not relative to a reference particle. The option TrackS cannot be used in combination with LClean_Stack.			

## 6.8. The namelist WAKE

Wake fields can be added as localized kicks which are described by tabulated values and coefficients. In order to perform convolution integrals the charge distribution is sorted into a longitudinal grid of variable grid size. Smoothing and interpolation parameters can be defined in order to optimize the result. Position and direction vectors define the location of the wake field kick and its direction.

The input of monopole or dipole wake potentials requires two column tables describing a pseudo Greens function of the wake potential in V/C, i.e. a numerical result for a charge distribution short as compared to the distribution in the actual calculation. The first line of the table consist of an integer number N and a zero. The following N lines contain the position (column 1 in m) and the corresponding longitudinal or transverse wake potential (column 2). For a detailed description see Ref. [1].

Parameter	Specification	Unit	Default Value
<b>Loop</b>	Logical		FALSE
see chapter 4.9.			
<b>LWAKE</b>	Logical		FALSE
if false all WAKE definitions will be ignored.			
<b>Wk_Type()</b>	Character*40 array		undefined
specifies the type or method of a wake field calculation. Valid keywords are <b>Monopole_Method_F</b> , <b>Dipole_Method_F</b> and <b>Taylor_Method_F</b> for wake field and <b>Monopole_Method_P</b> and <b>Dipole_Method_P</b> for wake potential input types.			
<b>Wk_filename()</b>	Character*150 array		
specifies the name of a file containing tabulated wake field or potential coefficients.			
<b>Wk_testfile()</b>	Character*150 array		
specifies the name of a file for test output. Output is only written if a file name is defined. The 3 columns of the file refer to the longitudinal position in the bunch [m], the local current [A] and the resulting longitudinal wake potential [V/C]			
<b>Wk_screen()</b>	Logical		FALSE
if true the phase space distribution will be saved right after the wake kick has been applied.			
<b>Wk_scaling</b>	Real*8		1.0
scaling factor for wake kick.			
<b>Wk_x()</b>	Real*8 array	m	0.0
transverse origin of a wake field in x.			
<b>Wk_y()</b>	Real*8 array	m	0.0
transverse origin of a wake field in y.			
<b>Wk_z()</b>	Real*8 array	m	1.0
longitudinal origin of a wake field in z.			

<b>Wk_ex()</b>	Real*8 array		0.0
x-component of the longitudinal direction vector.			
<b>Wk_ey()</b>	Real*8 array		0.0
y-component of the longitudinal direction vector.			
<b>Wk_ez()</b>	Real*8 array		1.0
z-component of the longitudinal direction vector.			
<b>Wk_hx()</b>	Real*8 array		1.0
x-component of the horizontal direction vector.			
<b>Wk_hy()</b>	Real*8 array		0.0
y-component of the horizontal direction vector.			
<b>Wk_hz()</b>	Real*8 array		0.0
z-component of the horizontal direction vector.			
<b>Wk_equi_grid()</b>	Real*8		1.0
if 1.0 an equidistant grid is set up, if 0.0 a grid with equal charge per grid cell is employed. Values between 1.0 and 0.0 result in intermediate binning based on a linear combination of the two methods.			
<b>Wk_N_bin()</b>	Integer array		10
number of bins.			
<b>Wk_ip_method()</b>	Integer array		2
interpolation method: 0 = rectangular, 1 = triangular, 2 = Gaussian.			
<b>Wk_smooth()</b>	Real*8 array		0.5
smoothing parameter for Gaussian interpolation.			
<b>Wk_sigma_min()</b>	Real*8 array		0.0
minimal sigma for Gaussian interpolation			
<b>Wk_sub()</b>	Integer array		1
sub binning parameter.			

## References

- [1] M. Dohlus et al. 'Fast Particle Tracking with Wake Fields', DESY 12-012  
<http://arxiv.org/abs/1201.5270>.

## 6.9. The namelist CAVITY

The namelist CAVITY allows the user to include, and to some extent to modify arbitrary RF, static electric and magnetic fields and fields generated by linear plasmas. The somewhat misleading name CAVITY is still kept for historical reasons.

The standard option to describe cavity fields is based on tables, which may be generated by analytical calculations, measurements or numerical codes. A field table has to contain the z-position (column 1 in m) and the corresponding longitudinal on-axis electric field amplitude (column 2 in arbitrary units) in free format. The transverse field components are calculated from the derivatives of the on-axis field; see Appendix (chapter 8). The polynomial expansion extends to 1<sup>st</sup> order or, with C\_higher\_order = True, to 3<sup>rd</sup> order. The polynomial expansion is perfect already in first order for a pure sine-like spatial wave. Deviations from a sine-like spatial field profile lead to increasing imperfections of the filed description with increasing radius. Differences of calculations done with 1<sup>st</sup> and 3<sup>rd</sup> order expansion can be used to check whether the field expansion approach is sufficient or a 3D field map is required. A smoothing procedure can be applied to suppress numerical noise by setting C\_smooth( ) = n,  $n \in \mathbb{N}$ .

**Static electric fields** To mark fields as static the name of the file containing the field table should start with the letters ‘DC’ or the frequency, Nue( ), should be set to zero.

**Static magnetic fields** The 3D field map option can be (ab)used to include static magnetic field maps. See below for details. Parameters Ex\_stat( ) and Ey\_stat( ) can be used to redirect the field scaling parameter MaxE( ) to a transverse component.

**TE modes** To mark the field of a field table as TE mode – as opposed to a standard TM mode – the file name has to start with the letters ‘TE\_’. The field table in this instance contains the position and the on-axis longitudinal magnetic field amplitude. For TE modes the parameter MaxE( ) refers to the longitudinal on-axis magnetic field component.

**Dipole modes** Dipole modes can be inserted as 3D field maps; see below.

**Traveling wave structures** Traveling wave structures can be inserted in its most general form as superposition of real and imaginary parts of the general solution; see Appendix (chapter 9). For periodic structures the description presented in Ref [1] has been incorporated. The transverse field components are derived according to a 1<sup>st</sup> order polynomial expansion. The field table has to contain the on-axis longitudinal field amplitude of at least one RF period plus the input and output coupler cells, which are treated as standing wave cells.

To the file a first line is added, containing in a free format:

$$z_1 \quad z_2 \quad n \quad m$$

where  $z_1$  and  $z_2$  are the start and end points of the traveling wave cells (i.e. the end and starting point of the input and output cell) and  $n$  and  $m$  are two integers characterizing the phase advance per cell  $\Theta = 2\pi n/m$ . Note that  $E_z(z_1) = E_z(z_2)$ ,

$$\left. \frac{\partial^i E_z}{\partial z^i} \right|_{z_1} = \left. \frac{\partial^i E_z}{\partial z^i} \right|_{z_2} \quad i = 1, 2, 3 \text{ should be fulfilled to high precision.}$$

For a backward traveling wave structure set  $n < 0$ .

The file name has to start with the letters ‘TWS’.

For a beta matched structure a wave number  $K\_wave()$  has to be specified. For a  $\beta=1$  structure the wave number is derived automatically from the frequency. The length of a periodic structure can be specified with the parameter  $C\_numb()$ , which contains the number of cells (excluding the input and output coupler cells). Note that  $C\_numb() \cdot n/m$  must be an integer.

**3D field maps** 3D field maps can be included in a most general form. The six field components  $E_x, E_y, E_z, B_x, B_y$  and  $B_z$  have to be stored in six files with a common name except for the name extension. The name of the files has to start with the letters '3D', or have '3D' at position 4 and 5 of the name; the extensions are .ex, .ey, .ez, .bx, .by and .bz. In the input deck the file name without extension has to be specified. The files start with a description of the grid, followed by the field values at each grid point. The grid does not have to be equidistant and can be different for each component except for the first and the last longitudinal grid coordinate, which has to be the same for all components. A warning is given if a particle leaves the transverse grid dimensions of a single component within the longitudinal grid boundaries at first appearance only! The program does not stop anymore as it was the case in previous versions! With  $N_x =$  number of grid knots in x,  $N_y =$  number of grid knots in y and  $N_z =$  number of grid knots in z the file looks like:

```

Nx x[1] x[2] ..... x[Nx-1] x[Nx]
Ny y[1] y[2] ..... y[Ny-1] y[Ny]
Nz z[1] z[2] ..... z[Nz-1] z[Nz]
F[ 1, 1, 1] F[ 2, 1, 1]..... F[Nx, 1, 1]
F[ 1, 2, 1] F[ 2, 2, 1]..... F[Nx, 2, 1]
:
:
:
F[ 1,Ny, 1] F[ 2,Ny, 1]..... F[Nx,Ny, 1]
F[ 1, 1, 2] F[ 2, 1, 2]..... F[Nx, 1, 2]
F[ 1, 2, 2] F[ 2, 2, 2]..... F[Nx, 2, 2]
:
:
:
F[ 1,Ny, 2] F[ 2,Ny, 2]..... F[Nx,Ny, 2]
F[ 1, 1, 3] F[ 2, 1, 3]..... F[Nx, 1, 3]
:
:
:
:
:
:
:
F[ 1,Ny,Nz] F[ 2,Ny,Nz]..... F[Nx,Ny,Nz]

```

where  $F$  is the value of the respective field component. The number format is free; the file has to contain line breaks as shown, but may contain additional line breaks as appropriate. (Note that the maximum line length in a file is a system dependent quantity.)

The maximum on axis value of the  $E_z$  component is scaled to  $MaxE()$ , for standard TM type modes, as in case of a field table, other components are scaled accordingly. For TE type modes (file name TE\_3D...)  $MaxE()$  refers to the on axis maximum of the  $B_z$  component, while for dipole modes (file names DX\_3D... or DY\_3D...)  $MaxE()$  refers to the on axis maximum of the  $B_x$  or  $B_y$  component, respectively.

In all cases it is assumed, that the ratio of electric to magnetic components is as V/m to T. A linear interpolation is applied between the grid knots. A field map can be n times periodically repeated by specifying C\_numb( ) = n. Care has to be taken, that the field values at the start and the end of the map do match in this case.

For static electric 3D fields the name of the files should start as 'DC-3D' or the frequency, Nue( ), should be set to zero. Files with magnetic field components (.bx, .by, .bz) are not required in this case. With parameters Ex\_stat( ) and Ey\_stat( ) the scaling by means of MaxE can be redirected to the specified direction.

For static magnetic 3D fields one of the logical parameters Bx\_stat( ), By\_stat( ) or Bz\_stat( ) has to be set to true. The parameter directs the field scaling parameter MaxE( ) to the respective component. Files with electric field components (.ex, .ey, .ez) are not required in this case.

If the electric field components are given on a common grid and the magnetic fields components are given on a second common grid the parameter Com\_grid = 'E,B' may be set to speed up the calculations. If all six components are given on a common grid Com\_grid = 'all' may be set.

Tracking through 3D field maps is rather time consuming. Moreover the field description is due to resolution and numerical noise problems not necessarily better than a description with a field table unless non cylindrically symmetric features are to be taken into account or field values far off-axis are required.

**Field pointers** In order to save storage place for cavities which can be described by the same field map it is possible to define a field pointer by specifying File\_Efield(j) = '3D\_Point@(i)', where *i* is the index of a cavity element specified as 3D field map and *i* < *j*. Parameters related to the grid (e.g. Com\_grid, C\_numb) are common for these cavities and are defined by index *i*. All other parameters are defined independently for each element.

**Overlaying modes or real and imaginary parts** When field tables or maps overlap longitudinally *Astra* gives a warning. The field components are added up in the overlapping region. Thus modes or real and imaginary parts of a mode can be specified as two field entries at the same location. See Appendix (chapter 9) and [9] for an application of this option.

**Time dependent fields and beam loading** An exponentially increasing or decaying field can be specified with the parameters T\_dependent( ), T\_null( ) and C\_Tau( ). The field value at the start off of the calculation is set as:

$$\vec{E} = \vec{E}_0 \left( 1 - e^{-\frac{T\_null}{C\_Tau}} \right) \quad \text{and} \quad \vec{E} = \vec{E}_0 e^{-\frac{T\_null}{C\_Tau}}, \text{ respectively.}$$

If the stored energy of the cavity is specified, beam loading is taken into account according as:

$$\vec{E} = \vec{E}_0 \sqrt{1 - \frac{E\_load}{E\_stored}} \quad \text{where } E\_stored \text{ is the stored energy at the actual}$$

gradient and *E\_load* is the energy transferred to a particle in the last time step. Overlapping cavity fields cannot be treated correctly by this option. When time dependent parameters are specified actual field values are stored in a file, see Table 3 and Table 4.

**Modifying the field profile and local perturbations** The parameter Flatness( ) allows modifications of the field profile by multiplying the longitudinal field (after the scaling to MaxE) with a linear slope. It is not applicable for TWS and 3D structures. A flatness parameter of  $\pm 0.1$  yields roughly 10% variation of field flatness. The exact variation depends on the length of the field table and should be checked with *fieldplot*. In order to approximate local asymmetries as they can be generated e.g. by input couplers a local transverse offset of the field between two positions defined by C\_zkickmin( ) and C\_zkickmax( ) can be introduced. A cosine-squared offset of amplitude C\_Xkick and C\_Ykick is simulated. An example of this option is given in Ref. [10].

**Linear plasma wakefield** Far behind the driver, the fields present in a linear plasma wake [11] are given by

$$E_z(z, r) = \frac{k_p^2 m_e c^2 a_{0\perp}(r)^2}{2e} \sqrt{\frac{\pi}{2}} \sigma_z \exp\left(-\frac{k_p^2 \sigma_z}{2}\right) \cos(k_p \zeta)$$

$$E_x(z, r) = \frac{k_p m_e c^2}{2e} \left(\frac{\partial}{\partial x} a_{0\perp}(r)^2\right) \sqrt{\frac{\pi}{2}} \sigma_z \exp\left(-\frac{k_p^2 \sigma_z}{2}\right) \sin(k_p \zeta)$$

$$E_y(z, r) = \frac{k_p m_e c^2}{2e} \left(\frac{\partial}{\partial y} a_{0\perp}(r)^2\right) \sqrt{\frac{\pi}{2}} \sigma_z \exp\left(-\frac{k_p^2 \sigma_z}{2}\right) \sin(k_p \zeta)$$

$$B_z = B_x = B_y = 0$$

with the rest mass of electrons  $m_e$ , the elementary charge  $e$  and  $c$  the velocity of light.

The wave number of the plasma  $k_p \equiv \frac{\omega_p}{c}$  is given by  $\omega_p = \left(\frac{e^2 n(z)}{\epsilon_0 m_e}\right)^{1/2}$  with the vacuum permittivity  $\epsilon_0$  and the plasma density profile  $n(z)$ .

$\sigma_z = E\_sigz$  denotes the rms length of the driver laser intensity or the beam charge density, respectively, and  $\zeta = z - v_g t$  denotes the co-moving coordinate, where  $v_g$  is the group velocity of the driver in the plasma.

The normalized vector potential of a driver of longitudinal Gaussian shape is defined

$$\text{as } a^2(\zeta, r) = a_{0\perp}(r)^2 \exp\left(-\frac{\zeta^2}{2\sigma_z^2}\right).$$

The transverse shape of the vector potential and its evolution in the longitudinal direction can be either user-defined by a 3D field map of the vector potential  $a_{0\perp}^2(x, y, z)$  by specifying the file name File\_A0( ), or it follows the free evolution as

$$a_{0\perp}^2(z, r) = E\_a0^2 \frac{E\_sig^2}{\sigma_r^2(z)} \exp\left(-\frac{r^2}{2\sigma_r^2(z)}\right), \text{ with}$$

$$\sigma_r^2(z) = E\_sig^2 + \frac{E\_eps^2 (z - E\_Z0)^2}{E\_sig^2} \quad \text{for an electron beam driver}$$

$$\sigma_r^2(z) = E\_sig^2 + \frac{E\_sig^2 (z - E\_Z0)^2}{E\_Zr^2} \quad \text{for a laser driver}$$

and the peak normalized vector potential defined as  $E\_a_0 = eA / (m_e c^2)$

A constant plasma profile with rising and falling edge can be defined using the parameters P\_Z1, P\_Z2, P\_R1, and P\_R2. Set File\_Efield( ) = 'Plasma' for this case.

The edge is modeled according to  $n(\Delta z) = n \left( 1 + \exp\left(\frac{4\Delta z}{P_R}\right) \right)^{-1}$  where  $n$  is the plasma density,  $\Delta z$  is the distance to the edge, i.e.  $\Delta z = z - P_{Z1}$  or  $\Delta z = z - P_{Z2}$  and P\_R 1 or 2 is a taper parameter.

Arbitrary plasma profiles can be defined with a two-column file which contains the longitudinal position  $z$  [m] and the plasma density  $n$  [arb. u.]. The plasma density will be scaled so that the peak value is equal to P\_n. The filename has to start with the word 'Plasma' and is specified in the input deck via the parameter File\_Efield( ). When laser wavelength E\_Lam is specified, the linear wakefield module includes slippage effects due to the laser group velocity in the plasma. Changes of the bunch phase in the wake due to changes in density are included.

### References

- [1] G. A. Loew, R. H. Miller, R. A. Early, K. L. Bane 'Computer Calculations of Traveling Wave Periodic Structure Properties', SLAC-PUB-2295, 1979.  
<http://www.slac.stanford.edu/cgi-wrap/getdoc/slac-pub-2295.pdf>
- [9] P. Piot et al. 'Steering and focusing effects in TESLA cavity due to high order mode and input coupler' PAC 2005.  
<http://accelconf.web.cern.ch/AccelConf/p05/PAPERS/WPAT083.PDF>
- [10] M. Krassilnikov, R. Cee, T. Weiland 'Impact of the RF-Gun Power Coupler on Beam Dynamics', EPAC 2002.  
<http://accelconf.web.cern.ch/AccelConf/e02/PAPERS/WEPRI077.pdf>
- [11] E. Esarey, C. B. Schroeder, W. P. Leemans, 'Physics of laser-driven plasma-based electron accelerators', Rev. of Mod. Phys., Vol 81, 2009.  
<https://doi.org/10.1103/RevModPhys.81.1229>

Parameter	Specification	Unit	Default Value
<b>LOOP</b>	Logical		FALSE
see chapter 4.9.			
<b>LEfield</b>	Logical		FALSE
if false, all cavity fields are turned off.			
<b>File_Efield()</b>	Character*150 array		
user specified file name for field tables, or maps, or key word <b>plasma</b> .			
<b>C_noscale()</b>	Logical array		FALSE
if true, the cavity field will not be scaled, but the file values will be taken as field values in MV/m (TM modes), or T (Te modes).			
<b>C_smooth()</b>	Integer array		0
controls the number of iterations of a soft, iterative procedure for smoothing field tables. Since the transverse field components are based on derivatives of the field table and can be noisy if the table is not precise, smoothing is recommended. Use fieldplot to check that the longitudinal field component remains basically unchanged and that the transverse components get smooth. Not applicable for 3D maps.			
<b>Com_grid()</b>	Character array		
either 'E,B' if the E and B components of a 3D map are given on common grids or 'all' if all six components of a 3D map are given on a common grid.			
<b>C_higher_order()</b>	Logical array		FALSE
if true, the field expansion extends to 3 <sup>rd</sup> order, if false the field expansion extends only to 1 <sup>st</sup> order. If true stronger smoothing of the field might be required. Not applicable to TWS structures.			
<b>Nue()</b>	Real*8 array	GHz	
frequency of the RF field.			
<b>K_wave()</b>	Real*8 array	m <sup>-1</sup>	
wave number of the field, only for $\beta$ matched traveling wave structures.			
<b>MaxE()</b>	Real*8 array	MV/m or T	
the absolute maximum, on-axis, longitudinal electric (TM mode) or magnetic (TE mode) field amplitude of the RF field is scaled to this value.			
<b>Ex_stat()</b>	Logical array		FALSE
redirects parameter MaxE() to the transverse electric component in x direction, for DC fields only.			
<b>Ey_stat()</b>	Logical array		FALSE
redirects parameter MaxE() to the transverse electric component in y direction, for DC fields only.			
<b>Bx_stat()</b>	Logical array		FALSE
redirects parameter MaxE() to the transverse magnetic component in x, for static magnetic fields only.			
<b>By_stat()</b>	Logical array		FALSE
redirects parameter MaxE() to the transverse magnetic component in y, for static magnetic fields only.			

<b>Bz_stat()</b>	Logical array		FALSE
redirects parameter MaxE() to the transverse magnetic component in z, for static magnetic fields only.			
<b>Flatness()</b>	Real*8 array		0.0
modifies the field flatness by multiplying the longitudinal field component with a linear slope; applied after scaling to MaxE. Not applicable for 3D and TWS structures.			
<b>Phi()</b>	Real*8 array	degree	
phase of the RF field. Phi(0) defines a global phase shift of all cavities. See section 4.30.			
<b>C_pos()</b>	Real*8 array	m	
shifts the longitudinal cavity position. C_pos is added to the position defined in File_Efield().			
<b>C_numb()</b>	Integer array		1 (3 in ASTRA Vers. 1)
number of cells excluding the input and output cell for traveling wave structures, or number of periods for 3D maps.			
<b>T_dependence()</b>	Character array		
either 'fill' or 'decay' in order to activate filling or decaying of the cavity field, respectively.			
<b>T_null()</b>	Real*8 array	ns	
for cavity filling: time between start of the filling of the cavity and start of the particle tracking; for decay: time between start of decay and start of particle tracking.			
<b>C_Tau()</b>	Real*8 array	ns	
filling time of the cavity.			
<b>E_stored()</b>	Real*8 array	J·m <sup>2</sup> /MV <sup>2</sup>	
stored field energy of the cavity. If specified beam loading is taken into account.			
<b>C_xoff()</b>	Real*8 array	m	0.0
transverse offset of the cavity in x.			
<b>C_yoff()</b>	Real*8 array	m	0.0
transverse offset of the cavity in y.			
<b>C_xrot()</b>	Real*8 array	rad	0.0
rotation angle of the cavity in the x-z plane, i.e. around the y-axis.			
<b>C_yrot()</b>	Real*8 array	rad	0.0
rotation angle of the cavity in the y-z plane, i.e. around the x-axis.			
<b>C_zrot()</b>	Real*8 array	rad	0.0
rotation angle of the cavity around the z-axis, i.e. in the x-y plane.			

<b>C_zkickmin()</b>	Real*8 array	m	
start of local field offset.			
<b>C_zkickmax()</b>	Real*8 array	m	
end of local field offset.			
<b>C_Xkick()</b>	Real*8 array	m	0.0
local transverse field offset in x.			
<b>C_Ykick()</b>	Real*8 array	m	0.0
local transverse field offset in y.			
<b>File_A0()</b>	Character*150 array		
for plasma wakefield: user specified file name for the normalized vector potential $a_{0\perp}^2(x, y, z)$ of a drive laser, file format defined like 3D field maps. If C_noscale() = False, values from File_A0 are normalized and scaled to E_a0. If no File_A0 is defined, the driver spot size evolves according to the parameters E_sig, E_Z0, and E_Zr or E_eps.			
<b>P_Z1()</b>	Real*8	m	
effective longitudinal start point of the plasma field. Used if only the key word plasma and no table is provided in File_Efield.			
<b>P_R1()</b>	Real*8	m	
ramp parameter for the entrance of the plasma field. Field calculation starts at $P\_Z1 - 2.5 \cdot P\_R1$ . Used if only the key word plasma and no table is provided in File_Efield.			
<b>P_Z2()</b>	Real*8	m	
effective longitudinal end point of a plasma field. Used if only the key word plasma and no table is provided in File_Efield.			
<b>P_R2()</b>	Real*8	m	
ramp parameter for the exit of the plasma field. Field calculation ends at $P\_Z2 + 2.5 \cdot P\_R2$ . Used if only the key word plasma and no table is provided in File_Efield.			
<b>P_n</b>	Real*8	cm <sup>-3</sup>	
peak plasma density. In the entrance and exit region the plasma density is scaled as described above, or P_n is used to scale the normalized profile defined in File_Efield().			
<b>E_a0</b>	Real*8		0.0
peak normalized vector potential $E\_a_0 = eA / (m_e c^2)$ of the generating driver laser beam or charge density.			
<b>E_Z0</b>	Real*8	m	0.0
position of the focus of the generating beam. Used if no File_A0 is defined.			
<b>E_sig</b>	Real*8	m	0.001
rms transverse beam size at the focus of the generating beam intensity. Used if no File_A0 is defined.			
<b>E_sigz</b>	Real*8	m	0.001
rms longitudinal beam size of the generating beam intensity.			

<b>E_Zr</b>	Real*8	m	0.0
Rayleigh length of the generating beam. Alternative parameter to E_eps. It is possible to specify E_Zr independently of E_sig. Used if no File_A0 is defined.			
<b>E_Eps</b>	Real*8	m	0.0
emittance of the generating beam. Alternative parameter to E_Zr. Used if no File_A0 is defined.			
<b>E_lam</b>	Real*8	m	0.0
wavelength of the driving laser. If no wavelength is specified no correction for the group velocity in the plasma is applied.			
<b>zeta</b>	Real*8	m	1.0
distance between driving laser (or electron beam) and electron beam at the plasma start. Alternative to phase, active if < 0.			

## 6.10. The namelist SOLENOID

The namelist SOLENOID allows to include arbitrary solenoid fields by means of tables, which may be generated by analytical calculations, measurements or numerical codes. The table has to contain the z-position (column1 in m) and the corresponding longitudinal on-axis magnetic field amplitude (column 2 arb. units) in a free format. The transverse field components are calculated from the derivatives of the on-axis field; see Appendix (chapter 8). The polynomial expansion extends to 1<sup>st</sup> order or, with `S_higher_order = True`, to 3<sup>rd</sup> order. A smoothing procedure can be applied to suppress numerical noise by setting `S_smooth( ) = n`,  $n \in \mathbb{N}$ .

Parameter	Specification	Unit	Default Value
<b>LOOP</b>	Logical		FALSE
see chapter 4.9.			
<b>LBfield</b>	Logical		FALSE
if false, all solenoid fields are turned off.			
<b>File_Bfield( )</b>	Character*150 array		
user specified file name.			
<b>S_noscale( )</b>	Logical		FALSE
if true, the solenoid field will not be scaled, but the file values will be taken as field values in T .			
<b>S_smooth( )</b>	Integer array		0
controls the number of iterations of a soft, iterative procedure for smoothing field tables. Since the transverse field components are based on derivatives of the field table and can be noisy if the table is not precise, smoothing is recommended. Use fieldplot to check that the longitudinal field component remains basically unchanged and that the transverse components get smooth.			
<b>S_higher_order( )</b>	Logical array		TRUE
if true, the field expansion extends to 3 <sup>rd</sup> order, if false the field expansion extends only to 1 <sup>st</sup> order. If true stronger smoothing of the field might be required.			
<b>MaxB( )</b>	Real*8 array	T	0.0
maximum field value of the solenoid field. The field is scaled to this value.			
<b>S_pos( )</b>	Real*8 array	m	0.0
shifts the longitudinal solenoid position. S_pos is added to the position defined in File_Bfield( ).			
<b>S_xoff( )</b>	Real*8 array	m	0.0
horizontal offset of the solenoid.			
<b>S_yoff( )</b>	Real*8 array	m	0.0
vertical offset of the solenoid.			

<i>S_xrot()</i>	Real*8 array	rad	0.0
rotation angle of the solenoid in the x-z plane, i.e. around the y-axis.			
<i>S_yrot()</i>	Real*8 array	rad	0.0
rotation angle of the solenoid in the y-z plane, i.e. around the x-axis.			

## 6.11. The namelist QUADRUPOLE

The namelist QUADRUPOLE allows to include quadrupole fields based on analytical expressions and field profile data.

In case of the analytic description the fringe field is tapered according to the relation

$$g(\Delta z) = g \left( 1 + \exp\left(\frac{4\Delta z}{Q\_bore}\right) \right)^{-1}$$

where  $g$  is the quadrupole gradient and  $\Delta z$  is the

distance to the quadrupole edge. The tapering is user-defined by means of the parameter  $Q\_bore$ , which might be set approximately to the diameter of the quadrupole bore. The tapered region extents on both edges over a length of  $3 \cdot Q\_bore$ . A longitudinal field component exists in the tapered region in accordance to Maxwell's law. Due to the tapering the actual field is longer than the specified effective length by  $3 \cdot Q\_bore$ . Fields of neighboring quadrupoles are superimposed if they are too close. When the length of a quadrupole is shorter than  $3 \cdot Q\_bore$  the fringe fields of both edges start to overlap. In order to reach the specified gradient a renormalization of the gradient is applied in this case and a warning is given. Strongly overlapping fringe fields lead to unphysical field profiles and a reduction of the effective magnet strength. The field profile should hence be checked with *fieldplot* in such case. When a focusing strength is specified rather than a gradient *fieldplot* assumes a beam momentum of 1 MeV/c to set a gradient for the plot.

Other field profiles can be introduced by means of a data file containing the z-position (column1 in m) and the corresponding gradient (column 2 arb. units) in a free format. ( $Q\_Type() = 'filename'$ ). The file name has to contain the string 'data' as keyword. A longitudinal field component is derived in regions of varying gradient in accordance to Maxwell's law.

**Multipole components** Multipole components can be added with the parameters  $Q\_mult\_a(i, j)$  and  $Q\_mult\_b(i, j)$ , where index  $i$  refers to the multipole coefficient and index  $j$  is the element number. The field parameterization follows closely a standard multipole expansion. With  $a_i = Q\_mult\_a(i, j)$  and  $b_i = Q\_mult\_b(i, j)$  the field components write as:

$$B_r = \sum_{i=1}^6 r^{i-2} (-a_i \cos(i \cdot \varphi) + b_i \sin(i \cdot \varphi))$$

$$B_\varphi = \sum_{i=1}^6 r^{i-2} (a_i \sin(i \cdot \varphi) + b_i \cos(i \cdot \varphi))$$

$$B_x = -Q\_grad(j) (xB_r - yB_\varphi)$$

$$B_y = -Q\_grad(j) (yB_r + xB_\varphi)$$

i.e. the coefficients are defined relative to the quadrupole gradient,  $b_i$  describes normal coefficients, while  $a_i$  describes skew coefficients and  $i=1..6$  describe dipole, quadrupole, sextupole etc. components, respectively. Note that  $Q\_grad(J)$  enters with reversed sign in order to comply to the sign convention as given below.

Multipole components are realized for standard quadrupoles and field profiles only. The fringe field of the multipole components is tapered as the main quadrupole field but the contribution of the multipole components onto the longitudinal field is ignored.

Parameter	Specification	Unit	Default Value
<b>LOOP</b>	Logical		FALSE
see chapter 4.9.			
<b>Lquad</b>	Logical		FALSE
if false, all quadrupole fields are turned off.			
<b>Q_type()</b>	Character*150 array		
besides standard quadrupoles (w. o. type specification) <b>skew</b> quadrupoles, <b>doublets</b> and <b>triplets</b> and field <b>data</b> can be specified. Doublets have the same field amplitude with reversed sign in the two magnets. For triplets the field amplitude has the same magnitude for all magnets but opposite sign of the outer magnets as compared to the inner one. The inner magnet is twice as long as the outer ones.			
<b>Q_grad()</b>	Real*8 array	T/m	
quadrupole gradient. Refers to the first quadrupole in case of doublets and triplets. A positive gradient focusses negatively charged particles traveling into positive z-direction in the x plane.			
<b>Q_K()</b>	Real*8 array	m <sup>-2</sup>	
focusing strength of the quadrupole. The gradient is set during the tracking of the reference particle in dependence of the reference particle momentum. Refers to the first quadrupole in case of doublets and triplets. A positive quadrupole strength focusses negatively charged particles traveling into positive z-direction in the x plane. If Q_K and Q_grad are specified, Q_K has a higher priority.			
<b>Q_noscale()</b>	Logical		FALSE
if true, the field profile will not be scaled, but the file values will be taken as gradients in T/m or as focusing strength in m <sup>-2</sup> .			
<b>Q_length()</b>	Real*8 array	m	
effective length of the quadrupole.			
<b>Q_smooth()</b>	Integer array		0
controls the number of iterations of a soft, iterative procedure for smoothing field profile tables.			
<b>Q_bore()</b>	Real*8 array	m	0.035
taper parameter for the quadrupole field edge.			
<b>Q_dist()</b>	Real*8 array	m	
distance between magnets in case of doublets and triplets.			
<b>Q_mult_a( , )</b>	Real*8 array		0.0
skew multipole coefficients.			
<b>Q_mult_b( , )</b>	Real*8 array		0.0
normal multipole coefficients.			
<b>Q_pos()</b>	Real*8 array	m	
longitudinal quadrupole position. Refers to the center of the magnet(s) also in case of doublets and triplets.			

<b><i>Q_xoff()</i></b>	Real*8 array	m	
horizontal offset of the quadrupole, the doublet or the triplet.			
<b><i>Q_yoff()</i></b>	Real*8 array	m	
vertical offset of the quadrupole, the doublet or the triplet.			
<b><i>Q_xrot()</i></b>	Real*8 array	rad	0.0
rotation angle of the quadrupole in the x-z plane, i.e. around the y-axis.			
<b><i>Q_yrot()</i></b>	Real*8 array	rad	0.0
rotation angle of the quadrupole in the y-z plane, i.e. around the x-axis.			
<b><i>Q_zrot()</i></b>	Real*8 array	rad	0.0
rotation angle of the quadrupole around the z-axis, i.e. in the x-y plane.			

### 6.13. The namelist DIPOLE

The namelist DIPOLE allows to include dipole fields based on analytical expressions. Dipoles are defined by two edge lines, defining the entrance and the exit face of the dipole. Each line is defined by two points in the input deck. The connecting lines of these points define the area in which the actual field calculation takes place. The shape of the area is arbitrary, except that it has to be convex.

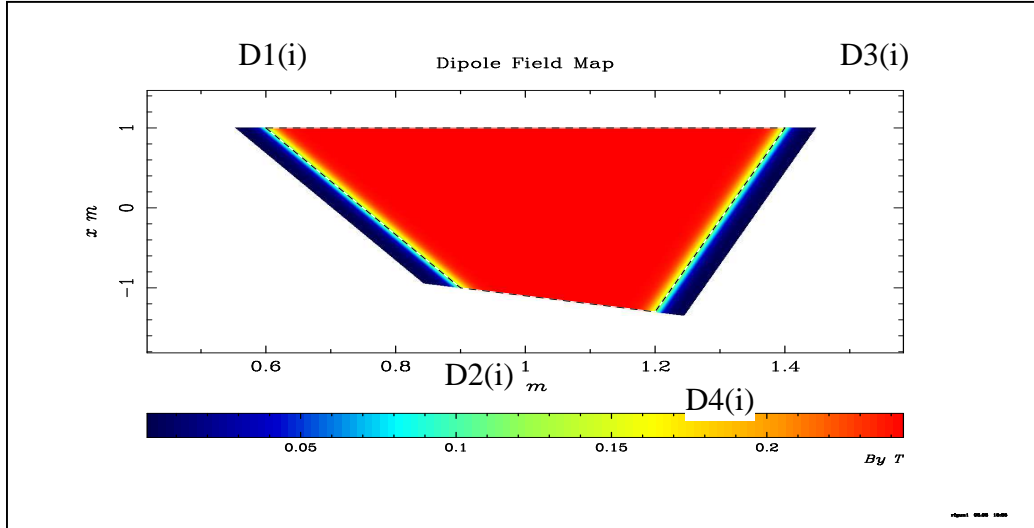


Fig. 4 Example for the definition of a dipole: The entrance and exit face of the dipole are defined by the lines  $D1(i) = (1.0, 0.6)$  to  $D2(i) = (-1.0, 0.9)$  and  $D3(i) = (1.0, 1.4)$  to  $D4(i) = (-1.3, 1.2)$ . The lines  $D1 - D2$  and  $D3 - D4$  are associated with the taper parameters  $D\_Gap(1,i)$  and  $D\_Gap(2,i)$ . The entrance and exit lines form together with the extrapolated connecting lines  $D1 - D3$  and  $D2 - D4$  the area in which the dipole field is defined. Note the order of the corner points. Exchanging  $D3$  and  $D4$  would be no valid input.

Dipoles can be defined to bend in the  $x$ - $z$  plane (horizontal) or in the  $y$ - $z$  plane (vertical). Overlapping fields are superimposed if the magnets are defined in the same bending plane. In the case of sections composed of horizontal and vertical dipoles the user has to make sure, that magnets in the two principle planes do not overlap. (Note that a dipole has an infinite extension into the direction perpendicular to the bending plane.)

The pivot point for rotations is defined by the average of the four corner points. Rotations and offsets within the bending plane are uncritical. The correct treatment of overlapping fields is, in the case of rotations out of the bending plane, however only possible, if the fields do also overlap when the magnets are not rotated out of the bending plane. A section of dipoles which are rotated by a common angle is hence uncritical. In complicated geometrical cases it is advisable to track sections wise.

The field strength is set either directly or by the bending radius. This radius is used to calculate the field strength based on the energy of the reference particle. Negative bending radii deflect electrons toward positive  $x$ -values. Fringe Fields are calculated between two parallel lines around the dipole edges. They have a  $\pm 1.5 \cdot D\_Gap$  offset from the edge. For a horizontal magnet the Field  $B_y$  decays outside of the magnet as

$$B_y(d) = B_0 \left( 1 + \exp\left(\frac{4d}{D\_Gap}\right) \right)^{-1}, \text{ where } d \text{ is the normal distance to the edge.}$$

The other field components are calculated according to Maxwell's law. The fringe fields of the same magnet are not allowed to overlap.

Parameter	Specification	Unit	Default Value
<b>LOOP</b>	Logical		FALSE
	see chapter 4.9.		
<b>LDipole</b>	Logical		FALSE
	if false all dipoles are turned off.		
<b>D_Type()</b>	Character*10 array		
	besides <b>horizontal</b> dipoles which bend in the x-plane <b>vertical</b> dipoles can be specified to bend the beam in the y-plane.		
<b>D1( , )</b>	Double Complex array	m	(0.0,0.0)
	coordinates of the first corner of a dipole. Two numbers, enclosed by brackets and separated by a comma, are to be given. The first number defines the horizontal or vertical (if D_type = 'vertical') coordinate, the second number defines the longitudinal coordinate.		
<b>D2( , )</b>	Double Complex array	m	(0.0,0.0)
	coordinates of the second corner of a dipole. Two numbers, enclosed by brackets and separated by a comma, are to be given. The first number defines the horizontal or vertical (if D_type = 'vertical') coordinate, the second number defines the longitudinal coordinate.		
<b>D3( , )</b>	Double Complex array	m	(0.0,0.0)
	coordinates of the third corner of a dipole. Two numbers, enclosed by brackets and separated by a comma, are to be given. The first number defines the horizontal or vertical (if D_type = 'vertical') coordinate, the second number defines the longitudinal coordinate.		
<b>D4( , )</b>	Double Complex array	m	(0.0,0.0)
	coordinates of the fourth corner of a dipole. Two numbers, enclosed by brackets and separated by a comma, are to be given. The first number defines the horizontal or vertical (if D_type = 'vertical') coordinate, the second number defines the longitudinal coordinate.		
<b>D_Gap( , )</b>	Real*8 array	m	0.05
	taper parameter for the dipole fringe field. The first index of the array is 1 or 2 for the first and second dipole edge, while the second index refers to the dipole number.		
<b>D_strength()</b>	Real*8 array	T	0.0
	the dipole magnet strength.		
<b>D_radius()</b>	Real*8 array	m	0.0
	if a bending radius is defined the magnet strength is set during the tracking of the reference particle in accordance to the beam energy. If D_radius and D_strength are specified, D_radius has a higher priority.		

<b><i>D_xoff()</i></b>	Real*8 array	m	0.0
transverse offset of the dipole in x.			
<b><i>D_yoff()</i></b>	Real*8 array	m	0.0
transverse offset of the dipole in y.			
<b><i>D_zoff()</i></b>	Real*8 array	m	0.0
longitudinal offset of the dipole in z.			
<b><i>D_xrot()</i></b>	Real*8 array	rad	0.0
rotation angle of the dipole in the x-z plane, i.e. around the y-axis.			
<b><i>D_yrot()</i></b>	Real*8 array	rad	0.0
rotation angle of the dipole in the y-z plane, i.e. around the x-axis.			
<b><i>D_zrot()</i></b>	Real*8 array	rad	0.0
rotation angle of the dipole around the z-axis, i.e. in the x-y plane.			

## 6.14. The namelist LASER

The namelist LASER allows to include an electromagnetic field as generated by a laser beam. ASTRA treats a laser just as a special external field, effects as e.g. Compton scattering are not included.

Besides a diffraction limited short pulse Gaussian laser model (**GLB**), a **CW** transversely Gaussian laser model has been implemented which allows to mimic different longitudinal pulse forms by means of window functions. In addition a radially polarized short pulse Gaussian laser (**RPL**) model is implemented.

Some input parameters are highly redundant, e.g. the intensity of the laser field can be specified via the pulse energy, the pulse power, the peak electric field in the focus or via the normalized vector potential. The relations used internally to convert the different quantities are summarized below.

Since a laser beam moves it has to be synchronized to the electron beam to meet the laser beam at a specified position. The interaction region is defined with parameters  $L\_Z1()$  and  $L\_Z2()$ . The laser field is only calculated when the electron bunch is in between these longitudinal positions. For the synchronization purpose parameters  $L\_zstart()$  or  $L\_tstart()$  can be set. An electron beam travelling with speed of light will meet the laser beam in the interaction region when both start at  $z = L\_zstart$  and  $t = L\_tstart$ . This applies also when the laser is rotated out of the coordinate system of the electron beam. In general one will start the electron beam at  $z = t = 0.0$  and use  $L\_zstart$  or  $L\_tstart$  to adjust for time of flight differences due to velocities differences.

Parameter  $L\_H()$  allows to reduce the time steps of ASTRA within the interaction region to cope with the short wave length of the laser field. Note that an uncertainty of  $H\_max \cdot$  electron beam velocity exists concerning the exact location at which the step width is reduced to  $L\_H()$ .  $L\_Z1()$  should hence not be chosen to tight.

The Gaussian laser beam (short pulse and cw) is by default transversely polarized with the electric field pointing into x direction. The polarization direction can be rotated with parameter  $L\_zrot()$ . Parameter  $L\_delta()$  allows to mix a second component in, which is polarized perpendicular to the first component and shifted in phase by 90 degree. Thus all sorts of elliptical and circular polarization can be realized.

The propagation direction of the laser beam can be changed with the parameters  $L\_xrot()$  or  $L\_yrot()$ . The pivot point for the rotation is center of the interaction region  $(L\_Z1() + L\_Z2())/2$ .

**Laser beam models** The relations used to describe the field of a laser beam in ASTRA follow closely the treatment by McDonald [1]. The temporal pulse shape of the fields is assumed to be of hyperbolic secant shape (= 1/hyperbolic cosine) [1].

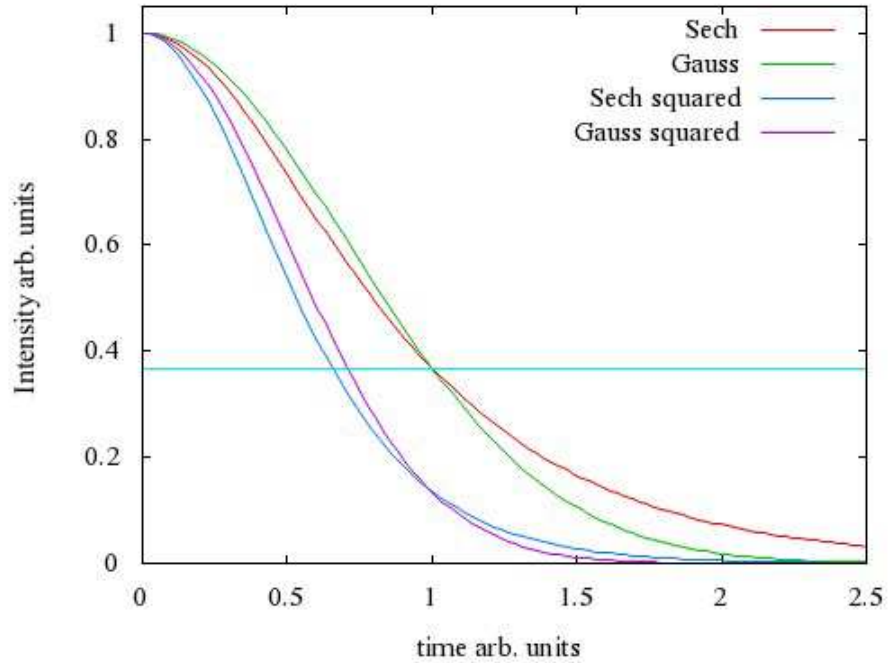


Figure 1: Comparison of Gaussian and hyperbolic secant pulse shape with equal 1/e-width and corresponding squared functions.

The pulse length relates to the 1/e-width of the field which is equal to 1.055 times the rms width for the hyperbolic secant. Since the laser intensity is proportional to the square of the laser field, the 1/e-width of the intensity is equal to 0.66 times the 1/e-width of the field.

Peak power  $P$  and laser energy  $U = \int P dt$  are related by  $P = \frac{U}{2\tau} \text{acosh}(e)$  with the 1/e pulse length  $\tau$ .

Approximations made are valid as long as  $\xi_0 = \frac{\omega\tau}{\text{acosh}(e)} > 1$ ,  $e = \exp(1) = 2.718\dots$  holds.

For the internal description the longitudinal position is measured relative to the focus position and in relation to the Rayleigh length  $Z_R = \frac{4\pi\sigma_0^2}{\lambda}$  as  $\zeta = z/Z_R$  with the rms spot size of the laser intensity at the focus  $\sigma_0$ . The transverse rms laser beam size develops as  $\sigma = \sigma_0\sqrt{1+\zeta^2}$  ( $w = w_0\sqrt{1+\zeta^2}$ ) and the beam radius  $w$  is two times the rms beam size.

**Gaussian Laser Beam** The phase for the Gaussian laser beam is given as:

$\Psi = \xi + \varphi_{CE} + \varphi_G - \frac{\zeta r^2}{w^2}$  with the Gouy phase  $\varphi_G = \text{atan } \zeta$ , the carrier envelope phase  $\varphi_{CE}$  and the phase  $\xi = \omega t - kz$ .

With an envelope function defined as  $E_{nv} = E_0 \frac{w_0}{w} e^{-\frac{r^2}{w^2}} \text{Sech} \frac{\xi}{\xi_0}$ , where  $r = \sqrt{x^2 + y^2}$  is the transverse position, the field components read as:

$$\begin{aligned} E_x &= E_{nv} \cdot \cos \Psi \\ E_y &= 0 \\ E_z &= -\frac{x}{Z_R} \frac{w_0^2}{w^2} E_{nv} (\sin \Psi + \zeta \cos \Psi) \\ B_x &= 0 \\ B_y &= E_x \\ B_z &= -\frac{y}{Z_R} \frac{w_0^2}{w^2} E_{nv} (\sin \Psi + \zeta \cos \Psi) \end{aligned}$$

The field amplitude follows from the Poynting theorem  $P = \frac{1}{\eta_0} \int_A ds \frac{\vec{E}^2}{2}$  as

$E_0 = \sqrt{\frac{\eta_0 P}{\pi \sigma_0^2}}$  with the vacuum impedance  $\eta_0$ . The normalized vector potential is given

as  $a_0 = \frac{eE_0}{m_0 c^2 k}$  with the wave number  $k = \frac{2\pi}{\lambda}$ .

For the orthogonal polarization state  $x$  and  $y$  are exchanged and an additional phase shift by  $\frac{\pi}{2}$  is introduced, i.e.  $\cos \Psi \rightarrow -\sin \Psi$  and  $\sin \Psi \rightarrow \cos \Psi$ . The components read thus as:

$$\begin{aligned} \tilde{E}_x &= 0 \\ \tilde{E}_y &= -E_{nv} \cdot \sin \Psi \\ \tilde{E}_z &= -\frac{y}{Z_R} \frac{w_0^2}{w^2} E_{nv} (\cos \Psi - \zeta \sin \Psi) \\ \tilde{B}_x &= \tilde{E}_y \\ \tilde{B}_y &= 0 \\ \tilde{B}_z &= -\frac{x}{Z_R} \frac{w_0^2}{w^2} E_{nv} (\cos \Psi - \zeta \sin \Psi) \end{aligned}$$

The two components are mixed as:

$$\begin{aligned} \hat{E}_x &= \delta E_x + (1 - \delta^2)^{1/2} \tilde{E}_y = \delta E_x \\ \hat{E}_y &= (1 - \delta^2)^{1/2} \tilde{E}_y \\ \hat{E}_z &= -\frac{E_{nv} w_0^2}{Z_R w^2} \left[ (\delta x - (1 - \delta^2)^{1/2} \zeta y) \sin \Psi + (\delta \zeta x + (1 - \delta^2)^{1/2} y) \cos \Psi \right] \end{aligned}$$

$$\begin{aligned}\hat{B}_x &= (1-\delta^2)^{1/2} \tilde{B}_x = \hat{E}_y \\ \hat{B}_y &= \delta B_y = \hat{E}_x \\ \hat{B}_z &= -\frac{E_{nv}}{Z_R} \frac{w_0^2}{w^2} \left[ (\delta y - (1-\delta^2)^{1/2} \zeta x) \sin \Psi + (\delta \zeta y + (1-\delta^2)^{1/2} x) \cos \Psi \right]\end{aligned}$$

**Radially Polarized Laser beam** The phase for the radially polarized beam is given as:  $\Psi = \xi + \varphi_{CE} + 2\varphi_G - \zeta \frac{r^2}{w^2}$  with the Gouy phase  $\varphi_G = \text{atan } \zeta$ , the carrier envelope phase  $\varphi_{CE}$  and the phase  $\xi = \omega t - kz$ .

With an envelope function defined as  $E_{nv} = E_0 \frac{w_0^2}{w^2} e^{-\frac{r^2}{w^2}} \text{Sech} \frac{\xi}{\xi_0}$ , the field components write as:

$$\begin{aligned}E_x &= \frac{x}{w_0} E_{nv} \cos \Psi \\ E_y &= \frac{y}{w_0} E_{nv} \cos \Psi \\ E_z &= \frac{w_0}{Z_R} E_{nv} \left[ \left(1 - \frac{r^2}{w^2}\right) \sin \Psi - \frac{\zeta r^2}{w^2} \cos \Psi \right] \\ B_x &= -E_y \\ B_y &= E_x \\ B_z &= 0.0\end{aligned}$$

The field amplitude follows from the Poynting relation  $P = \frac{1}{\eta_0} \int_A ds \frac{\vec{E}^2}{2}$  as

$E_0 = \sqrt{\frac{2\eta_0 P}{\pi\sigma_0^2}}$  with the vacuum impedance  $\eta_0$ . The normalized vector potential is given as  $a_0 = \frac{eE_0}{m_0 c^2 k}$  with the wave number  $k = \frac{2\pi}{\lambda}$ . Note that while  $E_0$  is a factor  $\sqrt{2}$  larger than in case of the linearly polarized beam the maximal transverse field at  $r = \frac{w}{\sqrt{2}}$  reaches only  $0.43 \cdot E_0$  and thus about 60% of the maximal field of the linearly polarized case.

## References

- [1] K. T. McDonald ‘Gaussian Laser Beams with Radial Polarization’, Princeton University 2000.  
[http://puhep1.princeton.edu/~mcdonald/examples/axicon\\_big.pdf](http://puhep1.princeton.edu/~mcdonald/examples/axicon_big.pdf)

Parameter	Specification	Unit	Default Value
<b>LOOP</b>	Logical		FALSE
see chapter 4.9.			
<b>LLaser</b>	Logical		FALSE
if false, all laser fields are turned off.			
<b>L_Type()</b>	Character*150 array		
type of laser beam. Valid keywords are: <b>CW</b> = cw Gaussian laser beam <b>GLB</b> = short pulse Gaussian Laser Beam <b>RPL</b> = short pulse Radially Polarized Laser beam			
<b>L_Z1()</b>	Real*8	m	
start position of the interaction region with the laser field.			
<b>L_Z2()</b>	Real*8	m	
end position of the interaction region with the laser field.			
<b>L_H()</b>	Real*8	ns	0.0
local time step setting, active if $\neq 0.0$ .			
<b>L_F()</b>	Real*8	m	
longitudinal position of the focus.			
<b>L_zstart()</b>	Real*8	m	0.0
longitudinal start position of the laser beam.			
<b>L_tstart()</b>	Real*8	ns	0.0
start time of the laser beam.			
<b>L_xoff()</b>	Real*8	m	0.0
transverse offset of the laser field in x.			
<b>L_yoff()</b>	Real*8	m	0.0
transverse offset of the laser field in y.			
<b>L_xrot()</b>	Real*8	rad	0.0
rotation angle of the laser field in the x-z plane, i.e. around the y-axis.			
<b>L_yrot()</b>	Real*8	rad	0.0
rotation angle of the laser field in the y-z plane, i.e. around the x-axis.			
<b>L_zrot()</b>	Real*8	rad	0.0
rotation angle of the laser field around the z-axis, i.e. in the x-y plane.			
<b>L_E0()</b>	Real*8	J	0.0
pulse energy of the laser.			
<b>L_Pow()</b>	Real*8	W	0.0
pulse power of the laser.			

<b>L_a0()</b>	Real*8		0.0
normalized vector potential of the laser in the focus.			
<b>L_Epeak()</b>	Real*8	V/m	0.0
electric field amplitude of the laser in the focus.			
<b>L_tau()</b>	Real*8	s	0.0
temporal 1/e pulse width of the laser <b>field</b> .			
<b>L_phi()</b>	Real*8	rad	0.0
carrier envelope phase.			
<b>L_lam()</b>	Real*8	m	0.0
wave length of the laser radiation.			
<b>L_sig0()</b>	Real*8	m	0.0
transverse rms size of the laser <b>intensity</b> at the focus position ( $\sigma_x = \sigma_y = \sigma$ ).			
<b>L_w0()</b>	Real*8	m	0.0
transverse size of the laser <b>intensity</b> at the focus position = $2 \cdot L\_sig0()$ . If $L\_sig0()$ and $L\_w0()$ are specified $L\_sig0()$ has priority,			
<b>L_delta()</b>	Real*8		1.0
polarization factor; $Abs(L\_delta()) \leq 1$ $L\_delta() = \pm 1.0$ linear polarization in x direction $L\_delta() = 0.0$ linear polarization in y direction $L\_delta() = 1/\sqrt{2}$ circularly polarized laser beam.			
<b>L_window()</b>	Character*150 array		
defines a window type for cw Gaussian laser beam. The window is applied over the interaction range. Valid types are: <b>Blackman</b> : a standard Blackman window <b>Tukey</b> : a Tukey window with taper parameter $L\_alpha()$			
<b>L_alpha()</b>	Real*8		1.0
Taper parameter for Tukey window; $0 < L\_alpha() \leq 1$ .			

## 7. Input namelist for *generator*

### 7.1. The namelist INPUT

Parameter	Specification	Unit	Default Value
<b>FNAME</b>	Character*150		rfgun.ini
	file name for initial particle distribution; recommended extensions are .ini or .zpos.run, respectively.		
<b>Add</b>	Logical		FALSE
	if true the input list has to be specified N_add times and N_add different distributions will be added.		
<b>N_add</b>	Integer		0
	number of distributions to be added.		
<b>Ipart</b>	Integer		100
	number of particles to be generated.		
<b>Species</b>	Character*80		Electrons
	species of particles to be generated. Valid are: <b>electrons</b> , <b>positrons</b> , <b>protons</b> <b>hydrogen</b> . The key word <b>ion</b> allows to generate particles with user defined ratio of mass to charge state. In addition to the keyword ion a number between 1 and 10 has to be specified, e.g. 'ion 1'. The number is used as index in the ion_mass specification. The parameter ion_mass needs to be specified in generator and again in the namelist NEWRUN of <i>Astra</i> . To adopt the graphics program <i>postpro</i> additional specifications in the Plot_steering.par file are optional (see chapter 5.6).		
<b>ion_mass( )</b>	Real*8 Array	eV/c <sup>2</sup>	0.0
	the mass divided by the charge state of user defined particles. The index number corresponds to the number specified together with the keyword ions in the Species definition. Negatively charged particles are defined by a negative value of the ion_mass parameter. Ion_mass(1) – (10) is mapped onto particle index 5 – 14 in the saved particle distribution file.		
<b>Probe</b>	Logical		TRUE
	if true, 6 probe particles are generated at locations: (0.5σ <sub>x</sub> , 0.5σ <sub>z</sub> ), (1.0σ <sub>x</sub> , 1.0σ <sub>z</sub> ), (1.5σ <sub>x</sub> , 1.5σ <sub>z</sub> ), (0.5σ <sub>y</sub> , -0.5σ <sub>z</sub> ), (1.0σ <sub>y</sub> , -1.0σ <sub>z</sub> ), (1.5σ <sub>y</sub> , -1.5σ <sub>z</sub> ).		
<b>Passive</b>	Logical		FALSE
	if true only passive particles will be generated.		
<b>Noise_reduc</b>	Logical		TRUE
	if true, particle coordinates are generated quasi-randomly following a Hammersley sequence.		
<b>Cathode</b>	Logical		TRUE
	if true the particles will be generated with a time spread rather than with a spread in the longitudinal position, i.e. sig_z, Lz and rz are set to zero and sig_clock, Lt and rt have to be specified. See chapter 7.2 to chapter 7.4. Status flags will be set accordingly.		
<b>R_Cathode</b>	Real*8	m	0.0
	radius in case of a curved, i.e. non planar cathode. Active if R_cathode is not zero. See section 7.5.2.		

<b>High_res</b>	Logical		FALSE
if true, the particle distribution is saved with increased accuracy. See Table 4.			
<b>Binary</b>	Logical		FALSE
if true, the particle distributions is saved in binary format.			
<b>Q_total</b>	Real*8	nC	1.0
total charge of the particles. The total charge is equally distributed on the Npart particles. ( <i>Astra</i> would allow also particles with varying macro charge in one distribution.)			
<b>Type</b>	Character*80		standard
defines the type of the distribution. Valid are <b>standard</b> and <b>ring</b> .			
<b>Rad</b>	Real*8	mm	0.0
radius of ring type distributions.			
<b>Tau</b>	Real*8	ns	0.0
exponential delay time of the emission. Active if Tau $\neq$ 0.0. The delay is added to any distribution in time, i.e. to any distribution starting at the cathode. Note that the delay time is random and might interfere with the quasi random nature of an input distribution.			
<b>Ref_zpos</b>	Real*8	m	0.0
z position of the reference particle, i.e the longitudinal bunch position.			
<b>Ref_clock</b>	Real*8	ns	0.0
initial clock value of the reference particle, can in general be set to zero.			
<b>Ref_Ekin</b>	Real*8	MeV	0.0
initial kinetic energy of the reference particle.			
<b>Dist_z</b>	Character*80		uniform
specifies the longitudinal particle distribution. For valid keywords and related parameters see chapter 7.2 to chapter 7.4.			
<b>sig_z</b>	Real*8	mm	0.0
rms value of the bunch length.			
<b>C_sig_z</b>	Real*8		0.0
cuts off a Gaussian longitudinal distribution at C_sig_z times sig_z. Active if $\neq$ 0.0.			
<b>Lz</b>	Real*8	mm	0.0
length of the bunch.			
<b>rz</b>	Real*8	mm	0.0
rising of the bunch distribution; only for plateau distribution.			
<b>sig_clock</b>	Real*8	ns	1.0D-3
rms value of the emission time, i.e. the bunch length if generated from a cathode.			

<b>C_sig_clock</b>	Real*8		0.0
cuts off a Gaussian longitudinal distribution at C_sig_clock times sig_clock. Active if $\neq 0.0$ .			
<b>Lt</b>	Real*8	ns	0.0
length of the bunch; only for plateau distribution.			
<b>rt</b>	Real*8	ns	0.0
rise time of the bunch; only for plateau distribution.			
<b>Dist_pz</b>	Character*80		uniform
specifies the longitudinal energy and momentum distribution, respectively. For valid keywords and related parameters see chapter 7.2 to chapter 7.4.			
<b>sig_Ekin</b>	Real*8	keV	0.0
rms value of the energy spread.			
<b>C_sig_Ekin</b>	Real*8		100.0
cuts off a Gaussian energy and momentum distribution at C_sig_Ekin times sig_Ekin. Active if $\neq 0.0$ .			
<b>LE</b>	Real*8	keV	0.0
width of the energy distribution.			
<b>rE</b>	Real*8	keV	0.0
rising of the energy distribution, only for plateau distribution.			
<b>emit_z</b>	Real*8	$\pi$ keV mm	0.0
longitudinal particle emittance. Can be specified instead of the energy spread. If an energy spread and an emittance is specified the energy spread has priority.			
<b>cor_Ekin</b>	Real*8	keV	0.0
correlated energy spread.			
<b>E_photon</b>	Real*8	eV	0.0
photon energy for Fermi-Dirac distribution.			
<b>phi_eff</b>	Real*8	eV	0.0
effective work function for Fermi-Dirac distribution.			
<b>Dist_x</b>	Character*80		Gaussian
specifies the transverse particle distribution in the horizontal direction. For valid keywords and related parameters see chapter 7.2 to chapter 7.4.			
<b>sig_x</b>	Real*8	mm	1.0
rms bunch size in the horizontal direction. Also the vertical bunch size if Dist_x = radial.			
<b>C_sig_x</b>	Real*8		0.0
cuts off a Gaussian horizontal distribution at C_sig_x times sig_x. Active if $\neq 0.0$ .			
<b>Lx</b>	Real*8	mm	0.0
width of the horizontal particle distribution.			
<b>rx</b>	Real*8	mm	0.0
rising of the horizontal particle distribution; only for plateau distribution.			

<b>x_off</b>	Real*8	mm	0.0
horizontal offset of the particle distribution.			
<b>Disp_x</b>	Real*8	m	0.0
horizontal dispersion; a horizontal offset is added to all particles according to: $x = x + Disp\_x \frac{\Delta P}{P}$ ; increases the calculated bunch emittance.			
<b>Dist_px</b>	Character*80		Gaussian
specifies the transverse momentum distribution in the horizontal direction. For valid keywords and related parameters see chapter 7.2 to chapter 7.4.			
<b>Nemit_x</b>	Real*8	$\pi$ mrad mm	0.0
normalized transverse emittance in the horizontal direction. Can be specified instead of a transverse momentum spread. If a momentum spread and an emittance is specified the emittance has priority. Also the normalized vertical emittance if Dist_px = radial.			
<b>sig_px</b>	Real*8	eV/c	0.0
rms value of the horizontal momentum distribution.			
<b>C_sig_px</b>	Real*8		100.0
cuts off the horizontal momentum distribution at C_sig_px times sig_px.			
<b>Lpx</b>	Real*8	eV/c	0.0
width of the horizontal momentum distribution; only for plateau distribution.			
<b>rpx</b>	Real*8	eV/c	0.0
rising of the horizontal momentum distribution; only for plateau distribution.			
<b>cor_px</b>	Real*8	mrad	0.0
correlated beam divergence in the horizontal direction = $-\frac{\alpha}{\beta[m]} x_{rms} [mm]$ . For extreme settings of cor_px the correlated beam divergence cannot be set correctly and the beam energy will be increased by <i>generator</i> . A warning will be given in this case.			
<b>Dist_y</b>	Character*80		Gaussian
specifies the transverse particle distribution in the vertical direction. For valid keywords and related parameters see chapter 7.2 to chapter 7.4.			
<b>sig_y</b>	Real*8	mm	1.0
rms bunch size in the vertical direction. Not significant if Dist_x = radial.			
<b>C_sig_y</b>	Real*8		0.0
cuts off a Gaussian vertical distribution at C_sig_y times sig_py. Active if $\neq 0.0$ .			
<b>Ly</b>	Real*8	mm	0.0
width of the vertical particle distribution.			
<b>ry</b>	Real*8	mm	0.0
rising of the vertical particle distribution; only for plateau distribution.			

<b>y_off</b>	Real*8	mm	0.0
the vertical offset of the particle distribution.			
<b>Disp_y</b>	Real*8	m	0.0
vertical dispersion; a vertical offset is added to all particles according to: $y = y + Disp\_y \frac{\Delta P}{P}$ ; increases the calculated bunch emittance.			
<b>Dist_py</b>	Character*80		Gaussian
specifies the transverse momentum distribution in the vertical direction. For valid keywords and related parameters see chapter 7.2 to chapter 7.4.			
<b>Nemit_y</b>	Real*8	$\pi$ mrad mm	0.0
normalized transverse emittance in the vertical direction. Can be specified instead of a transverse momentum spread. If a momentum spread and an emittance is specified the emittance has priority. Not significant if Dist_px = radial.			
<b>sig_py</b>	Real*8	eV/c	0.0
rms value of the horizontal momentum distribution.			
<b>C_sig_py</b>	Real*8		0.0
cuts off a Gaussian vertical momentum distribution at C_sig_py times sig_py. Active if $\neq 0.0$ .			
<b>Lpy</b>	Real*8	eV/c	0.0
width of the vertical momentum distribution; only for plateau distribution.			
<b>rpy</b>	Real*8	eV/c	0.0
rising of the vertical momentum distribution; only for plateau distribution.			
<b>cor_py</b>	Real*8	mrad	0.0
<p>correlated beam divergence in the vertical direction = <math>-\frac{\alpha}{\beta[m]} y_{rms} [mm]</math>.</p> <p>For extreme settings of cor_py the correlated beam divergence cannot be set correctly and the beam energy will be increased by <i>generator</i>. A warning will be given in this case.</p>			

## 7.2. 1D distributions

### 7.2.1 uniform distribution

#### Definition and basic relations

$$f(x) = \frac{1}{FWHM} \quad \text{for } |x| \leq \frac{FWHM}{2}$$

$$0 \quad \text{elsewhere}$$

$$\text{rms value} \quad \sigma = \frac{FWHM}{2\sqrt{3}}$$

#### Generator specifications

Dimension	Key word	Parameter <i>FWHM</i> or $\sigma$	unit
temporal <sup>1</sup>	Dist_z = 'uniform'	Lt or sig_clock	ns
longitudinal <sup>2</sup> z	Dist_z = 'uniform'	Lz or sig_z	mm
longitudinal E <sub>kin</sub>	Dist_pz = 'uniform'	LE or sig_Ekin or emit_z	keV or keVmm
transverse x	Dist_x = 'uniform'	Lx or sig_x	mm
transverse y	Dist_y = 'uniform'	Ly or sig_y	mm
transverse p <sub>x</sub>	Dist_px = 'uniform'	Lpx or sig_px or Nemit_x	eV/c or mrad mm
transverse p <sub>y</sub>	Dist_py = 'uniform'	Lpy or sig_py or Nemit_y	eV/c or mrad mm

<sup>1</sup> active if Cathode = TRUE, <sup>2</sup> active if Cathode = FALSE

### 7.2.2 plateau distribution

#### Definition and basic relations

$$f(x) = \frac{1}{L} \frac{1}{1 + \exp\left(\frac{2}{rt}(2|x| - L)\right)} \quad rt \leq \frac{L}{2}$$

Definition of  $rt$ :

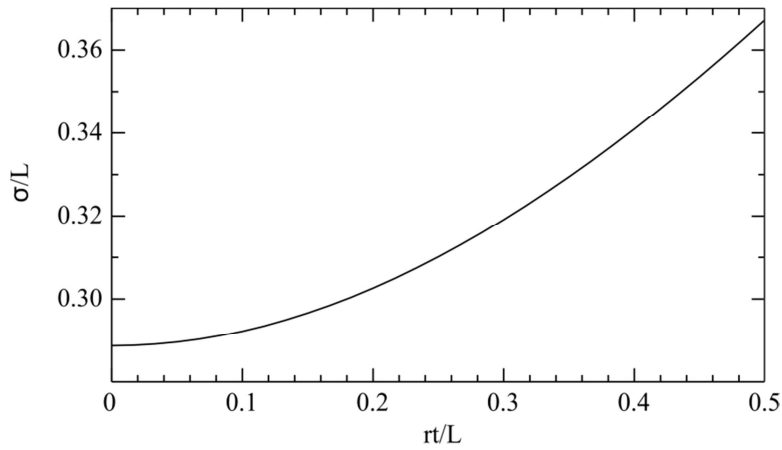
$rt$  is defined by a straight line with a slope  $A$  given by:

$$A = \frac{d}{dx} f(x) \Big|_{\pm \frac{L}{2}}$$

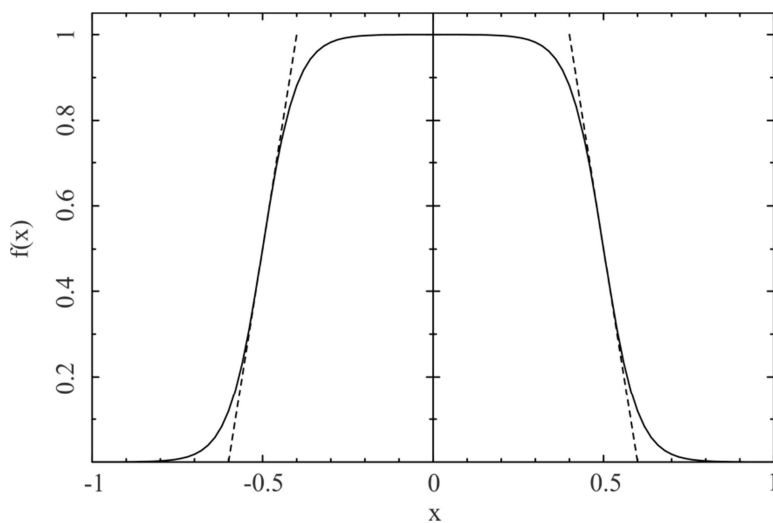
Within  $rt$  the straight line inclines from 0 to the plateau value of the distribution.

$$\text{FWHM value} \quad FWHM = L$$

$$\text{rms value} \quad \frac{L}{2\sqrt{3}} \leq \sigma \leq \frac{L}{2.8} \quad rt \leq \frac{L}{2}$$



Relation of rms value and rise time



**Example:** Plateau distribution with  $L = 1$  and  $rt = 0.2$ . Straight lines according to the definition of  $rt$ .

### Generator specifications

Dimension	Key word	Parameter $L, rt$	unit
temporal <sup>1</sup>	Dist_z = 'plateau'	Lt, rt	ns
longitudinal <sup>2</sup> z	Dist_z = 'plateau'	Lz, rz	mm
longitudinal $E_{kin}$	Dist_pz = 'plateau'	LE, rE	keV
transverse x	Dist_x = 'plateau'	Lx, rx	mm
transverse y	Dist_y = 'plateau'	Ly, ry	mm
transverse $p_x$	Dist_px = 'plateau'	Lpx, rpx	eV/c
transverse $p_y$	Dist_py = 'plateau'	Lpy, rpy	eV/c

<sup>1</sup> active if Cathode = TRUE, <sup>2</sup> active if Cathode = FALSE

### 7.2.3 inverted parabola (longitudinal)

#### Definition and basic relations

The inverted parabola distribution produces linear longitudinal space charge fields. It corresponds to the projection of a uniformly filled ellipsoid onto the z-axis.

$$f(z) = \frac{3}{4z_{\max}} \left( 1 - \frac{z^2}{z_{\max}^2} \right) \quad |z| \leq z_{\max}$$

FWHM value  $FWHM = \sqrt{2}z_{\max}$

rms value  $\sigma_z = \frac{z_{\max}}{\sqrt{5}}$

#### Generator specifications:

Dimension	Key word	Parameter $\sigma$	unit
temporal <sup>1</sup>	Dist_z = 'inverted'	sig_clock	ns
longitudinal <sup>2</sup> z	Dist_z = 'inverted'	sig_z	mm

### 7.2.4 Gaussian distribution

#### Definition and basic relations

$$f(x) = \frac{1}{\sqrt{2\pi}\sigma} \exp\left(-\frac{1}{2} \frac{x^2}{\sigma^2}\right)$$

FWHM value  $FWHM = 2\sqrt{-2\ln(0.5)} = 2.35\sigma$

#### Generator specifications:

Dimension	Key word	Parameter $\sigma$	unit
temporal <sup>1</sup>	Dist_z = 'gauss'	sig_clock	ns
longitudinal <sup>2</sup> z	Dist_z = 'gauss'	sig_z	mm
longitudinal E <sub>kin</sub>	Dist_pz = 'gauss'	sig_Ekin or emit_z	keV or keVmm
transverse x	Dist_x = 'gauss'	sig_x	mm
transverse y	Dist_y = 'gauss'	sig_y	mm
transverse p <sub>x</sub>	Dist_px = 'gauss'	sig_px or Nemit_x	eV/c or mrad mm
transverse p <sub>y</sub>	Dist_py = 'gauss'	sig_py or Nemit_y	eV/c or mrad mm

<sup>1</sup> active if Cathode = TRUE, <sup>2</sup> active if Cathode = FALSE

## 7.2.5 truncated Gaussian distribution

### Definition and basic relations

$$f(x) = \frac{1}{\sqrt{2\pi}\sigma_{inp}} \exp\left(-\frac{1}{2} \frac{x^2}{\sigma_{inp}^2}\right) \quad \text{for } |x| \leq C_{Cut}\sigma_{inp}$$

relation between  $\sigma_{inp}$  and rms value of the truncated distribution  $\sigma_{out}$

$$\frac{C_{Cut}\sigma_{inp}}{\sqrt{3}} \leq \sigma_{out} \leq \sigma_{inp}$$

Note that the cut produces a rectangular structure. Compare with the 2D-Gaussian distribution 7.3.2.

### Generator specifications

Dimension	Key word	Parameter $\sigma_{inp}$ , $C_{Cut}$	unit
temporal <sup>1</sup>	Dist_z = 'gauss'	sig_clock, C_sig_clock	ns, dim. less
longitudinal <sup>2</sup> z	Dist_z = 'gauss'	sig_z, C_sig_z	mm, dim. less
longitudinal E <sub>kin</sub>	Dist_pz = 'gauss'	sig_Ekin or emit_z, C_sig_Ekin	keV or keVmm, dim. less
transverse x	Dist_x = 'gauss'	sig_x, C_sig_x	mm, dim. less
transverse y	Dist_y = 'gauss'	sig_y, C_sig_y	mm, dim. less
transverse p <sub>x</sub>	Dist_px = 'gauss'	sig_px or Nemit_x, C_sig_px	eV/c or mrad mm, dim. less
transverse p <sub>y</sub>	Dist_py = 'gauss'	sig_py or Nemit_y, C_sig_py	eV/c or mrad mm, dim. less

<sup>1</sup> active if Cathode = TRUE, <sup>2</sup> active if Cathode = FALSE

### 7.3. 2D distributions

#### 7.3.1 radial uniform distribution

##### Definition and basic relations

$$f(x, y) = \frac{1}{\pi r^2} \quad \text{for } x^2 + y^2 \leq r^2$$

$$0 \quad \text{elsewhere}$$

The projection onto the x-axis (eqv. y-axis) is a half ellipse

$$f(x) = 2 \int_0^{y_m} f(x, y) dy = \frac{2\sqrt{r^2 - x^2}}{\pi r^2} \quad |x| \leq r$$

with the following properties:

FWHM value            FWHM =  $\sqrt{3} r$

rms value                 $\sigma = \frac{r}{2}$

##### Generator specifications

Dimension	Key word	Parameter $r$ or $\sigma$	unit
transverse x, y	Dist_x = 'radial uniform'	Lx or sig_x	mm
transverse p <sub>x</sub> , p <sub>y</sub>	Dist_px = 'radial uniform'	Lpx or sig_px or Nemit_x	eV/c or mrad mm

#### 7.3.2 (truncated) 2D-Gaussian distribution

Equivalent to distributions 7.2.4 and 7.2.5 but with  $f(y) = f(x)$ . The cut will produce a circular structure.

##### Generator specifications

Dimension	Key word	Parameter $\sigma_{inp}$ , $C_{Cut}$	unit
transverse x, y	Dist_x = '2D-Gaussian'	sig_x, C_sig_x	mm, dim. less
transverse p <sub>x</sub> , p <sub>y</sub>	Dist_px = '2D-Gaussian'	sig_px or Nemit_x, C_sig_px	eV/c or mrad mm, dim. less

## 7.4. 3D distributions

### 7.4.1 isotropic momentum distribution

#### Definition and basic relations

A distribution with isotropic emission angles into a half sphere. The following relations hold:

$$p_x^2 + p_y^2 + p_z^2 = P^2 = E_{kin}^2 + 2E_{kin}$$

rms value  $\sigma p_x = \sigma p_y = \frac{P}{\sqrt{3}}$

$$\sigma p_z = \frac{P}{2\sqrt{3}}$$

mean value  $p_{z,mean} = \frac{P}{2}$

normalized transverse emittances[1]:

$$\varepsilon_{x,y} = \sigma_{x,y} \frac{1}{\sqrt{3}} \sqrt{\frac{2E_{kin}}{m_0 c^2}}$$

#### Generator specifications

Dimension	Key word	Parameter $E_{kin}$	unit
$p_x, p_y, p_z$	Dist_pz = 'isotropic'	LE	keV

## 7.4.2 photo emission from a Fermi-Dirac distribution

### Definition and basic relations

A distribution describing the photo emission from a metallic cathode at room temperature according to ref. [2]. The random generator works only as true random generator, the noise reduction option is hence switched off, if selected in the input deck. As input parameters the effective work function  $\Phi_{eff}$ , i.e. including a possible reduction due to the Schottky effect, and the photon energy  $E_{phot}$  need to be given. The following relations hold:

$$\text{rms value} \quad \sigma p_x = \sigma p_y = \sqrt{\frac{E_{phot} - \phi_{eff}}{3m_0c^2}}$$

$$\text{mean Energy} \quad \bar{E}_{kin} = \frac{2}{3}(E_{phot} - \phi_{eff})$$

$$\text{Energy spread} \quad \sigma_{Ekin} = \frac{1}{3\sqrt{2}}(E_{phot} - \phi_{eff})$$

normalized transverse emittances:

$$\varepsilon_{x,y} = \sigma_{x,y} \sqrt{\frac{E_{phot} - \phi_{eff}}{3m_0c^2}}$$

### Generator specifications

Dimension	Key word	Parameter $\Phi_{eff}, E_{phot}$	units
$p_x, p_y, p_z$	Dist_pz = 'FD_300'	phi_eff, E_photon	eV

### 7.4.3 uniformly filled ellipsoid

#### Definition and basic relations

$$f(x, y, z) = \frac{3}{4\pi L_x L_y L_z} \quad \text{for } \frac{x^2}{L_x^2} + \frac{y^2}{L_y^2} + \frac{z^2}{L_z^2} \leq 1$$

$$0 \quad \text{elsewhere}$$

the projection onto the z-axis (equiv. x- and y-axis) is an inverted parabola:

$$f(z) = 4 \int_0^{L_x} \int_0^{L_y} f(x, y, z) dx dy = \frac{3}{4L_z} \left[ 1 - \frac{z^2}{L_z^2} \right] \quad |z| \leq L_z$$

with the following properties:

FWHM value  $\text{FWHM}_z = \sqrt{2} L_z$

rms value  $\sigma_z = \frac{L_z}{\sqrt{5}}$

#### Generator specifications

Dimension	Key word	Parameter $L_{x, y, z}$ or $\sigma_{x, y, z}$	unit
temporal <sup>1</sup>	Dist_z = 'uniform ellipsoid'	Lt or sig_clock	ns
longitudinal <sup>2</sup> z	Dist_z = 'uniform ellipsoid'	Lz or sig_z	mm
transverse x	Dist_z = 'uniform ellipsoid'	Lx or sig_x	mm
transverse y	Dist_z = 'uniform ellipsoid'	Ly or sig_y	mm

<sup>1</sup> active if Cathode = TRUE, <sup>2</sup> active if Cathode = FALSE

## **7.5. Miscellaneous options**

### **7.5.1 ring type distributions**

If Type = 'Ring' is specified any standard transverse distribution is offset by a radius specified with parameter Rad and uniformly distributed on a circle. Thus a circular charge distribution is generated. The cross section of the ring can vary from x to y depending on the setting of transverse parameters.

### **7.5.2 emission from a curved cathode**

In order to start a distribution from a curved cathode the radius of the cathode can be specified with the parameter R\_cathode. For this option photo emission is assumed, hence the longitudinal starting position and the starting time are modified according to the cathode radius. All other parameters remain unchanged.

## **References**

- [1] K. Floettmann 'Note on the thermal emittance of electrons emitted by Cesium Telluride photo cathodes' TESLA-FEL Report 1997-01.  
[http://flash.desy.de/sites/site\\_vuvfel/content/e403/e1642/e839/e829/infoboxContent830/fel1997-01.pdf](http://flash.desy.de/sites/site_vuvfel/content/e403/e1642/e839/e829/infoboxContent830/fel1997-01.pdf)
- [2] D. Dowell, J. Schmerge 'Quantum efficiency and thermal emittance of metal cathodes' PRST-AB 12,074201, 2009.  
<http://prst-ab.aps.org/pdf/PRSTAB/v12/i7/e074201>

## 8. Appendix I: Field expansion formulas

A solenoid field can be described by a polynomial expansion as:

$$B_z(r) = B_{z,0} - \frac{r^2}{4} B_z'' + \frac{r^4}{64} B_z'''' - \frac{r^6}{2304} B_z'''''' ..$$

$$B_r(r) = -\frac{r}{2} B_z' + \frac{r^3}{16} B_z''' - \frac{r^5}{384} B_z'''' ...$$

where  $B_{z,0}$  is the longitudinal on-axis magnetic field and the prime's indicate derivatives with respect to  $z$ .

In *Astra* the field expansion extends to 3<sup>rd</sup> order or is limited to the 1<sup>st</sup> order if `S_higher_order( ) = FALSE`; higher order terms tend to be noisy and are hence excluded. Since the expansion ends in both cases with an odd order the condition  $\text{div } B = 0$  is fulfilled, while the condition  $\text{rot } B = 0$  is only approximately fulfilled.

The 3<sup>rd</sup> order term contributes one percent to the radial magnetic field at a field expansion radius  $R_{3rd}$  given by:

$$R_{3rd} = \sqrt{\left| \frac{0.08 B_z'}{B_z''} \right|}$$

This quantity can be plotted with *fieldplot*.

A cylindrical symmetric TM standing wave mode can be expanded as:

$$E_z(r) = \left[ E_{z,0} - \frac{r^2}{4} \left( E_z'' + \frac{\omega^2}{c^2} E_{z,0} \right) \right] \sin(\omega t)$$

$$E_r(r) = \left[ -\frac{r}{2} E_z' + \frac{r^3}{16} \left( E_z''' + \frac{\omega^2}{c^2} E_z' \right) \right] \sin(\omega t)$$

$$B_\phi(r) = \left[ \frac{r}{2} E_{z,0} - \frac{r^3}{16} \left( E_z'' + \frac{\omega^2}{c^2} E_{z,0} \right) \right] \frac{\omega}{c^2} \cos(\omega t)$$

where  $E_{z,0}$  is the longitudinal electric field and higher order terms are ignored. A TE standing wave mode can equivalently be described by:

$$B_z(r) = \left[ B_{z,0} - \frac{r^2}{4} \left( B_z'' + \frac{\omega^2}{c^2} B_{z,0} \right) \right] \cos(\omega t)$$

$$B_r(r) = \left[ -\frac{r}{2} B_z' + \frac{r^3}{16} \left( B_z''' + \frac{\omega^2}{c^2} B_z' \right) \right] \cos(\omega t)$$

$$E_\phi(r) = \left[ \frac{r}{2} B_{z,0} - \frac{r^3}{16} \left( B_z'' + \frac{\omega^2}{c^2} B_{z,0} \right) \right] \omega \sin(\omega t)$$

In *Astra* the field expansion extends to 3<sup>rd</sup> order or is limited to the 1<sup>st</sup> order if `C_higher_order( ) = FALSE`; higher order terms tend to be noisy and are hence excluded.

The polynomial expansion is perfect already in 1<sup>st</sup> order for a pure sine-like spatial wave, since the higher order components yield zero in this case. Deviations from a pure sine-like spatial field profile lead to approximations in the condition  $\text{rot } E = -\dot{B}$  for TM modes and  $\text{rot } B = \frac{\dot{E}}{c^2}$  for TE modes.

In the case of a DC field (only TM mode) the condition  $\text{rot } E = 0$  is only approximately fulfilled equivalently to the description of solenoid fields.

The 3<sup>rd</sup> order term contributes one percent to the transverse electric or magnetic field component at a field expansion radius  $R_{3rd}$  given by:

$$R_{3rd}^{E_r} = \sqrt{\frac{|0.08 E'_z|}{\left|E_z'' + \frac{\omega^2}{c^2} E'_z\right|}} \quad R_{3rd}^{B_\phi} = \sqrt{\frac{|0.08 E_{z,0}|}{\left|E_z'' + \frac{\omega^2}{c^2} E_{z,0}\right|}}$$

for a TM mode, and:

$$R_{3rd}^{E_\phi} = \sqrt{\frac{|0.08 B_{z,0}|}{\left|B_z'' + \frac{\omega^2}{c^2} B_{z,0}\right|}} \quad R_{3rd}^{B_r} = \sqrt{\frac{|0.08 B'_z|}{\left|B_z'' + \frac{\omega^2}{c^2} B'_z\right|}}$$

for a TE mode.

These quantities can be plotted with *fieldplot*.

The derivatives of the longitudinal field component are calculated by a division of small numbers and are hence sensitive to numerical noise. The quality of a field table can be judged by means of plots of the transverse field components and especially of the quantity  $R_{3rd}$  which is notably sensitive to numerical noise. Smooth transverse fields require tables of high accuracy and not too short distance of the longitudinal base points.

An iterative procedure can be applied in order to reduce the numerical noise. A field value  $F$  (i.e.  $B_{z,0}$  or  $E_{z,0}$ ) at index  $i$  is replaced by:

$$F(i) = F(i-1) + \frac{dF}{dz} \Delta z \quad \text{with}$$

$$\frac{dF}{dz} = \frac{F(i+1) - F(i-1)}{z(i+1) - z(i-1)} \quad \text{and}$$

$$\Delta z = z(i) - z(i-1)$$

This procedure is iterated  $n$  times where  $n$  is defined by the user.

The procedure is soft, i.e. a large number of iterations might be required. Than it removes efficiently sharp, spiky structures in the transverse components but leaves the average behavior unchanged. Fig. 5 shows an example of the transverse electric field

from a particularly bad field table. After smoothing with  $C\_smooth( ) = 100$  all spikes are removed without influence onto the average behavior.

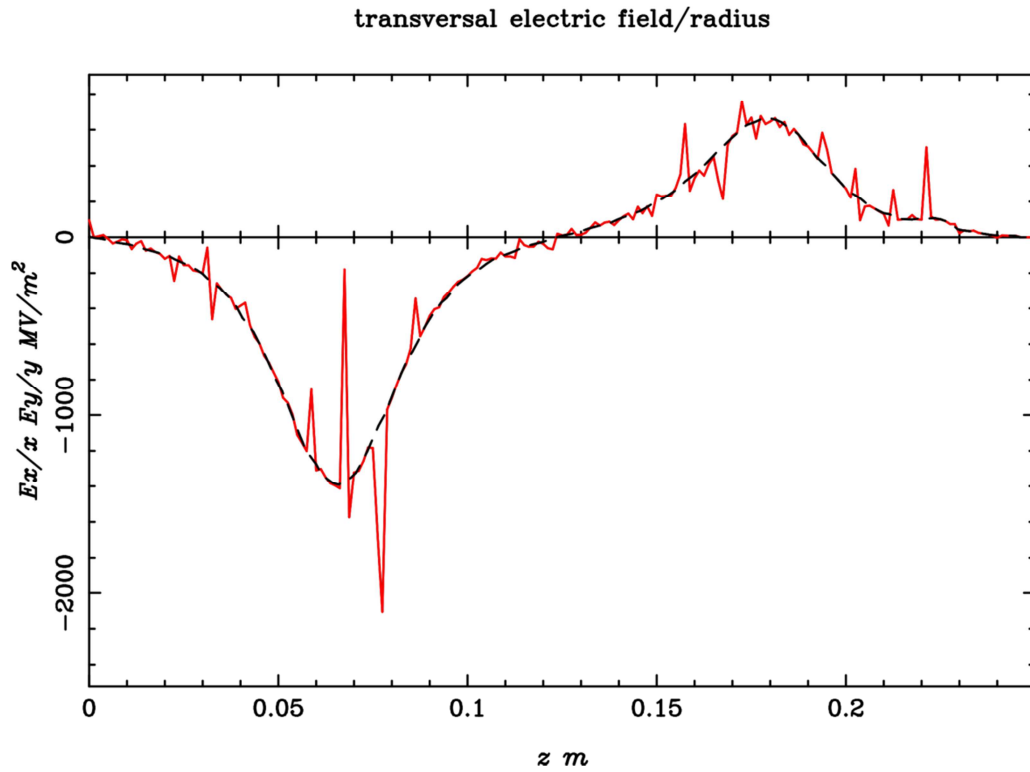


Fig. 5 Example of the transverse electric field components calculated with the field expansion formulas from an inaccurate field table. The numerical noise in the original data (red, solid line) is removed by the smoothing procedure (dashed, black line) without influence onto the average behavior.

## 9. Appendix II: Representation of a travelling wave by two standing waves

A field can be represented in complex form as:

$$V = A \cdot \exp i \left( \omega \frac{z}{c} + \alpha + \varphi \right)$$

with:  $A^2 = Re^2 + Im^2$

$$\cos \alpha = \frac{Re}{A}; \quad \sin \alpha = \frac{Im}{A}$$

$$Re = E_r, B_r$$

$$Im = E_i, B_i$$

where  $E_r$  and  $B_r$  denote the electric and magnetic component of the real part solution and  $E_i$  and  $B_i$  the corresponding imaginary part of the solution, respectively.

Assume for simplicity that  $\varphi = 0$ . Particle couple to the real part of the field  $V_r$ ,

$$\begin{aligned} V_r &= A \cdot \cos \left( \omega \frac{z}{c} + \alpha \right) \\ &= A \cdot \cos \left( \omega \frac{z}{c} \right) \cos(\alpha) - A \cdot \sin \left( \omega \frac{z}{c} \right) \sin(\alpha) \\ &= Re \cdot \cos \left( \omega \frac{z}{c} \right) - Im \cdot \sin \left( \omega \frac{z}{c} \right) \\ &= E_r \cos \left( \omega \frac{z}{c} \right) - E_i \sin \left( \omega \frac{z}{c} \right) \end{aligned}$$

$$\text{and} \quad = B_r \cos \left( \omega \frac{z}{c} \right) - B_i \sin \left( \omega \frac{z}{c} \right)$$

An equivalent representation can be formulated by superimposing a standing wave with  $\varphi = 0$  (index  $c1$ ) with a second standing wave with  $\varphi = \pi/2$  (index  $c2$ ):

$$\begin{aligned} &E_{c1} \cos \left( \omega \frac{z}{c} \right); \quad -B_{c1} \sin \left( \omega \frac{z}{c} \right) \\ &E_{c2} \cos \left( \omega \frac{z}{c} + \frac{\pi}{2} \right); \quad -B_{c2} \sin \left( \omega \frac{z}{c} + \frac{\pi}{2} \right) \\ &= -E_{c2} \sin \left( \omega \frac{z}{c} \right); \quad -B_{c2} \cos \left( \omega \frac{z}{c} \right) \end{aligned}$$

With the following identification both representations are identical:

$$E_{c1} = E_r; \quad B_{c1} = B_i$$

$$E_{c2} = E_i; \quad B_{c2} = -B_r$$

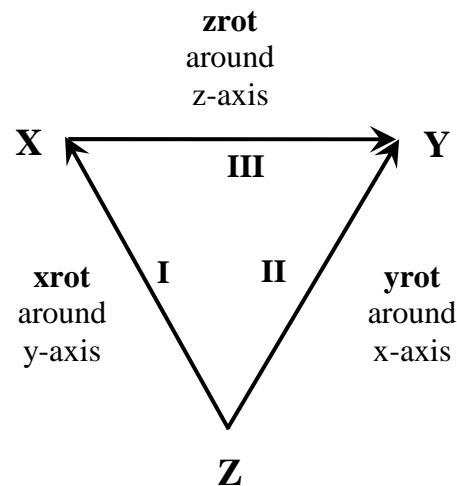
## 10. Appendix III: Rotation of Elements in *Astra*

Rotations of elements are defined by the angles ...xrot (C\_xrot, S\_xrot ...), ...yrot (C\_yrot, S\_yrot ...) and ...zrot (C\_zrot, S\_yrot ...)

The angle ...xrot defines a rotation in the x-z plane, i.e. around the y-axis of the coordinate system. The sign of the angle is positive when the element rotates from positive z to positive x.

The angle ...yrot defines a rotation in the y-z plane, i.e. around the x-axis of the coordinate system. The sign of the angle is positive when the element rotates from positive z to positive y.

The angle ...zrot defines a rotation in the x-y plane, i.e. around the z-axis of the coordinate system. The sign of the angle is positive when the element rotates from positive x to positive y.



Rotations are performed before transverse offsets are added.

The pivot point is in longitudinal direction defined by the center of the element, i.e. the mean of start and end point. Note the special case of dipoles as described in section 6.13.

Rotations are performed in the following order:

- 1<sup>st</sup> rotation around the y-axis (angle ...xrot).
- 2<sup>nd</sup> rotation around the x-axis (angle ...yrot). The angle ...yrot is defined with respect to the rotated (...xrot) element.
- 3<sup>rd</sup> rotation around the z-axis (angle ...zrot). The angle ...zrot is defined with respect to the rotated (...xrot - ...yrot) element.

The units for the rotation angles are radians.

## 11. Selected references

The following selected references are related to code comparisons and benchmarking, program developments and interesting applications, respectively. More references can be found at the end of various subsections in the document above.

- [1] S. Setzer et al. ‘FEL photoinjector simulation studies by combining MAFIA TS2 and ASTRA’, EPAC 2002.  
<http://accelconf.web.cern.ch/AccelConf/e02/PAPERS/WEPRI076.pdf>
- [3] C. Limborg et al. ‘Code comparison for simulations of photo-injectors’, PAC 2003.  
<http://www.slac.stanford.edu/pubs/slacpubs/10000/slac-pub-10735.html>
- [4] G. Geloni et al. ‘Benchmark of ASTRA with analytical solution for the longitudinal plasma oscillation problem’, FEL 2004.  
<http://accelconf.web.cern.ch/AccelConf/f04/papers/MOPOS09/MOPOS09.PDF>
- [5] K. Floettmann et al. ‘Recent improvements to the ASTRA particle tracking code’, PAC 2003.  
<http://accelconf.web.cern.ch/accelconf/p03/PAPERS/FPAG015.PDF>
- [6] G. Poeplau et al. ‘3D space charge calculations for bunches in the tracking code ASTRA’, EPAC 2006.  
<http://accelconf.web.cern.ch/AccelConf/e06/PAPERS/WEPC121.PDF>
- [7] A. Markovik et al. ‘Simulation of 3D space charge fields of bunches in a beam pipe of elliptical shape’, EPAC 2006.  
<http://accelconf.web.cern.ch/AccelConf/e06/PAPERS/WEPC120.PDF>
- [8] I. V. Bazarov, C. K. Sinclair ‘Multivariate optimization of a high brightness DC-gun photoinjector’, PRST-AB 8, 034202, 2005.  
<http://prst-ab.aps.org/oncol/PRSTAB/v8/i3/e034202>
- [9] D. Janssen et al. ‘Emittance compensation in a superconducting RF gun with a magnetic mode’ PRST-AB 7, 090702, 2004.  
<http://prst-ab.aps.org/abstract/PRSTAB/v7/i9/e090702>
- [10] R. Brinkmann et al. ‘A low emittance, flat-beam electron source for linear colliders’ PRST-AB 4, 053501, 2001.  
<http://prst-ab.aps.org/abstract/PRSTAB/v4/i5/e053501>
- [11] A. Egbert et al. ‘High-repetition rate femtosecond laser-driven hard-x-ray source’ Appl. Phys. Lett. 81, No 113, 2002.
- [12] A. Egbert et al. ‘Electron-based EUV and ultrashort hard-x-ray sources’ X-Ray Lasers 2002, AIP Conf. Proc. 614.
- [13] A. Pietzsch et al. ‘Towards time resolved core level photoelectron spectroscopy with femtosecond x-ray free-electron lasers’ New Journal of Physics 10, 2008.